MASSACHUSETTS INSTITUTE OF TECHNOLOGY
DEPARTMENT OF NUCLEAR ENGINEERING
Cambridge , Massachusetts 02139

MIT-3944-6 MITNE-117

REACTOR PHYSICS PROJECT FINAL REPORT

September 30, 1970

Contract AT (30-1)-3944
U.S. Atomic Energy Commission

MASSACHUSETTS INSTITUTE OF TECHNOLOGY
DEPARTMENT OF NUCLEAR ENGINEERING
Cambridge, Massachusetts 02139

MIT-3944-6 MITNE-117
AEC Research and Development Report
(TID-4500, 47th Edition)

REACTOR PHYSICS PROJECT FINAL REPORT

September 30, 1970

Contract AT(30-1)-3944
U.S. Atomic Energy Commission

Editors:

M. J. Driscoll
I. Kaplan
D. D. Lanning
N. C. Rasmussen

Contributors:

V. K. Agarwala
F. M. Clikeman
M. J. Driscoll
Y. Hukai
L. L. Izzo
I. Kaplan
M. S. Kazimi
D. D. Lanning
T. C. Leung
E. L. McFarland
N. C. Rasmussen
S. S. Seth
G. E. Sullivan
A. T. Supple

DISTRIBUTION

MIT-3944-6 MITNE-117

AEC Research and Development Report

UC-34 Physics

1-4. U. S. Atomic Energy Commission, Headquarters
Division of Reactor Development and Technology
Reactor Physics Branch (2 copies)
Core Design Branch (1 copy)
Water Reactor Branch (1 copy)
Washington, D. C. 20545

5. U. S. Atomic Energy Commission
Savannah River Laboratory
Attn: B. C. Rusche
Aiken, South Carolina 29801

6. AECL Chalk River Laboratory
Attn: C. Millar
Sheridan Park, Ontario, Canada

7. H. S. Potter, New York Patents Office
U. S. Atomic Energy Commission
Brookhaven Office
Upton, New York 11973

8-9. U. S. Atomic Energy Commission
Cambridge Office

ABSTRACT

This is the final report in an experimental and theoretical program to develop and apply single- and few-element methods for the determination of reactor lattice parameters.

The period covered by the report is January 1, 1968 through September 30, 1970. In addition to summarizing results for the entire contract period, this report also serves as the final annual report; thus, work completed in the period of October 1, 1969 through September 30, 1970 is dealt with in more detail than the earlier work.

Methods were developed to measure the heterogeneous parameters Γ, η and A for single fuel elements immersed in moderator in an exponential tank using foil activation measurements external to the fuel. These methods were applied to clustered fuel rods in D_2O moderator and single fuel rods in H_2O moderator, and the results were extended to and compared with data on complete multi-element lattices reported by other laboratories.

Advanced gamma spectrometric methods using Ge(Li) detectors were applied to the analysis of both prompt and fission product decay gammas for the nondestructive analysis of the fuel used in this work. The latter includes both simulated burned fuel containing plutonium and actual burned fuel irradiated to 20,000 MWD/T in the Dresden BWR.

TABLE OF CONTENTS

LIST OF FIGURES

LIST OF TABLES

1. INTRODUCTION

1.1 Foreword

This report is the third and final progress report of the Reactor Physics Project of the Massachusetts Institute of Technology (1, 2). This project was initiated January 1, 1968 with the objective of developing and applying single and few element methods for the determination of reactor physics parameters.

Earlier work at M.I.T. (3) had demonstrated the feasibility of measuring the fuel element characterization parameters used in heterogeneous reactor theory by experiments on single fuel elements. This work encouraged the hope that such an approach could provide the basis for evaluating the reactor physics characteristics of new and promising types of reactor fuel at very low cost. Previous work, however, was based on the use of in-rod foil activation experiments, which made it difficult to extend the techniques to fuel involving hard-to-handle radioactive contaminants such as plutonium and fission products. A major methods-development objective of the present work, therefore, was to determine the feasibility of carrying out all measurements in the moderator external to the fuel or on the fuel element surface.

A second major objective of this research has been to demonstrate the application of single element methods to representative fuel and moderator types. Two cases were investigated: 19- and 31-rod clusters of plutonium containing fuel rods in D_2O moderator, simulating one calandria tube of a pressure-tube-type reactor; and single rods of low enrichment UO_2 fuel in H_2O, representative of BWR and PWR fuel elements. In the latter case both unirradiated and irradiated fuel rods were employed.

Finally, the third major area of research engaged in under this project has been the application of high resolution Ge(Li) gamma-ray spectroscopy to nondestructive analysis of the fuel elements involved in the single rod experiments. Both prompt gammas and fission product

decay gammas were used in this work, and both fresh and previously irradiated fuel were investigated in demonstration applications.

1.2 Research Objectives and Results

The basic objective of the present research has been the experimental determination of those parameters of heterogeneous reactor theory which characterize the neutronic properties of a fuel element. They are:

Γ = asymptotic thermal neutron flux at the fuel element surface per thermal neutron absorbed by the element,

η = number of fast neutrons emitted by the fuel element per thermal neutron absorbed in the fuel element, and

A = number of epithermal neutron absorptions by the fuel element per unit slowing-down density.

Experiments carried out in D_2O moderator, and described in Chapter 2 of this report, have shown that all three parameters can be measured with adequate precision by foil activation experiments made external to the fuel. The parameter Γ is measured by using radial gold foil traverses in a single rod exponential experiment. The parameters η and A are measured relative to a standard element in the same experiment: η is determined from cadmium ratio measurements using gold foils in the moderator surrounding the fuel element; A is determined from the ratio of gold to molybdenum foil activities on the fuel element surface.

The experiments carried out in H_2O moderator, and described in Chapter 4, have shown that there are inherent limitations to single element measurements in H_2O which probably preclude achieving adequate accuracy directly in H_2O. However, it has also been shown that the parameters Γ and η are not sensitive to the moderator type, while A is easily corrected to account for changes in moderator. These results, coupled with the demonstration that heterogeneous calculations can be applied successfully to H_2O lattices, indicate that a viable approach in the case of H_2O systems can be devised by the use of single element experiments in D_2O or graphite.

Chapter 3 describes the results of research carried out to assay test fuel elements using high resolution Ge(Li) gamma-ray spectroscopy and both prompt and decay gamma emission. Nondestructive determination of the fissile and fertile content of fuel by this means was shown to be practicable. This work also generated new basic data on prompt capture gammas emitted by U^{238}, Th^{232}, U^{235} and Pu^{239}. In another application of gamma analysis, fuel rods previously irradiated in the Dresden BWR were studied to check on their presumed burnup history and post-burnup composition using an extension of techniques previously applied at M.I.T. for highly enriched fuel (4).

1.3 Staff

References (1) and (2) list the project staff through September 30, 1969. During the final year the project staff, including thesis students, was as follows:

M. J. Driscoll, Associate Professor of Nuclear Engineering
I. Kaplan, Professor of Nuclear Engineering
D. D. Lanning, Professor of Nuclear Engineering
N. C. Rasmussen, Professor of Nuclear Engineering
F. M. Clikeman, Associate Professor of Nuclear Engineering
A. T. Supple, Jr., Engineering Assistant
G. E. Sullivan, Technician
V. K. Agarwala, Research Assistant, S.M. student
Y. Hukai, Research Assistant, Ph.D. student (through June 1970)
L. L. Izzo, S.M. student
M. S. Kazimi, Research Assistant, S.M. student
T. C. Leung, Research Assistant, S.M. student (through Jan. 1970)
E. L. McFarland, Research Assistant, S.M. student (through June 1970)
S. S. Seth, Research Assistant, Sc.D. student (through Jan. 1970)

1.4 References

(1) Reactor Physics Project Progress Report No. 1, MIT-3944-1, MITNE-96, September 30, 1968.

(2) Reactor Physics Project Progress Report No. 2, MIT-3944-4, MITNE-111, September 30, 1969.

(3) Heavy Water Lattice Project Final Report, MIT-2344-12, MITNE-86, September 30, 1967.

(4) J. A. Sovka, "Nondestructive Analysis of Irradiated MITR Fuel by Gamma-Ray Spectroscopy," Sc.D. Thesis, Massachusetts Institute of Technology, Department of Nuclear Engineering, September 1965.

Other project publications are listed in Appendix A.

2. SINGLE-ELEMENT MEASUREMENTS IN D_2O MODERATOR

S. S. Seth

In this chapter a "single-element" method is described for the experimental determination of the nuclear fuel parameters Γ, η and A of source-sink reactor theory. This method requires the use of only one fuel element in an exponential facility; and all measurements are made outside this fuel element. The single-element method was applied to 19- and 31-rod clusters of plutonium containing fuel. The reactor physics parameters of uniform lattices composed of these clusters, calculated from the measured values of Γ, η and A, show good agreement with the results of full lattice studies of the same fuel at the Savannah River Laboratory. The proposed method should increase the efficacy of heterogeneous reactor theory and make possible the evaluation of promising reactor fuels at very low cost.

A detailed topical report, of which this chapter is a summary, has been issued on this work:

> S. S. Seth, M. J. Driscoll, I. Kaplan, T. J. Thompson and D. D. Lanning, "A Single-Element Method for Heterogeneous Nuclear Reactors," MIT-3944-3, MITNE-109, May 1970.

2.1 Introduction

The heterogeneous reactor method was first reported by Feinberg (1) and Galanin (2) in the U.S.S.R. and by Horning (3) in the U.S. Since then, several improvements have been made in the heterogeneous computations. Owing to their realistic treatment of the discrete characteristics of the core assembly, the heterogeneous calculations permit a relatively simple and accurate analysis of multicomponent lattices.

The heterogeneous reactor theory represents nuclear fuel assemblies by neutron sources and sinks, and their contribution to the

neutron density at any point is expressed by means of a suitable propagation kernel. This formulation involves the use of three parameters η, Γ and A to characterize, respectively, the fast neutron source and the thermal and epithermal neutron sinks in the fuel. These parameters are assumed to be independent of the interfuel spacing in a lattice. The three heterogeneous fuel parameters are defined as follows:

> Γ, the thermal constant, is the average value of the asymptotic thermal neutron flux in the moderator at the fuel surface, per thermal neutron per cm-sec absorbed in the fuel element. It has the dimension of inverse length.
>
> η, the fast neutron yield, is the net number of fast neutrons emerging from the fuel element per thermal neutron absorbed in the fuel.
>
> A, the epithermal absorption parameter, is the total epithermal neutron absorption per cm-sec of the fuel element per unit asymptotic neutron slowing-down density. It has the dimension of area.

A major condition for the success of the heterogeneous method is an accurate determination of the three fuel parameters Γ, η and A.

Klahr et al. (4) and Graves et al. (5) have reported success with heterogeneous calculations based on the use of the "asymptotic" flux and a "self-consistent" procedure for evaluating the fuel parameters. In the self-consistent procedure, the fuel parameters Γ and A are calculated from the experimental or analytical values of the thermal utilization (f) and the resonance escape probability (p) for a uniform lattice composed of the fuel element in question. The fast neutron yield factor, η, is normalized so that the product (ηf) is the same as would be obtained from cell calculations. The studies cited refer mainly to relatively simple lattices of single rods or tubes.

The expressions which relate Γ and A to f and p, respectively, require that the latter be known with very high accuracy. In lattices which contain complex fuel clusters with nonuniform burnup and consequent uncertain composition, reliable calculations are difficult and

unwieldy, if not impossible. The theoretical analysis has therefore to be supplemented by lattice experiments. Furthermore, it is necessary to repeat this extensive experimental and calculational effort on many lattices in order to obtain the heterogeneous parameters for each different fuel type in a reactor lattice.

2.2 A Single-Element Model

The main objective of the proposed single-element method is the direct experimental determination of the three parameters Γ, η and A of a nuclear fuel element. The term "fuel element" is used in a generic sense; thus, in the case of a tight fuel cluster, it comprises all the individual fuel rods with their cladding and the coolant within the encompassing cluster-tubing. The fuel element in question is located at the center of a cylindrical tank of heavy water moderator (Fig. 2.1). A J_o-shaped source of thermal neutrons at the lower end of the tank sets up an axial exponential flux gradient in the moderator. The single-fuel element, playing the dual role of a source of fast neutrons and a sink of thermal and resonance neutrons, superimposes its neutronic properties upon the unperturbed thermal neutron distribution. A set of four quantities is measured:

X (cm), the radial distance of the peak of the thermal neutron flux distribution in the moderator;

γ (cm^{-1}), the inverse relaxation length of the axial flux;

R, the cadmium ratio in gold at a radial distance, Y (cm), from the fuel; and

F, the ratio of the activities (per unit isotopic weight) of Au^{197} and Mo^{98} measured in cadmium-covered gold and molybdenum foils irradiated on the fuel surface.

The analytic work summarized below relates the above measurements to the three heterogeneous parameters Γ, η and A.

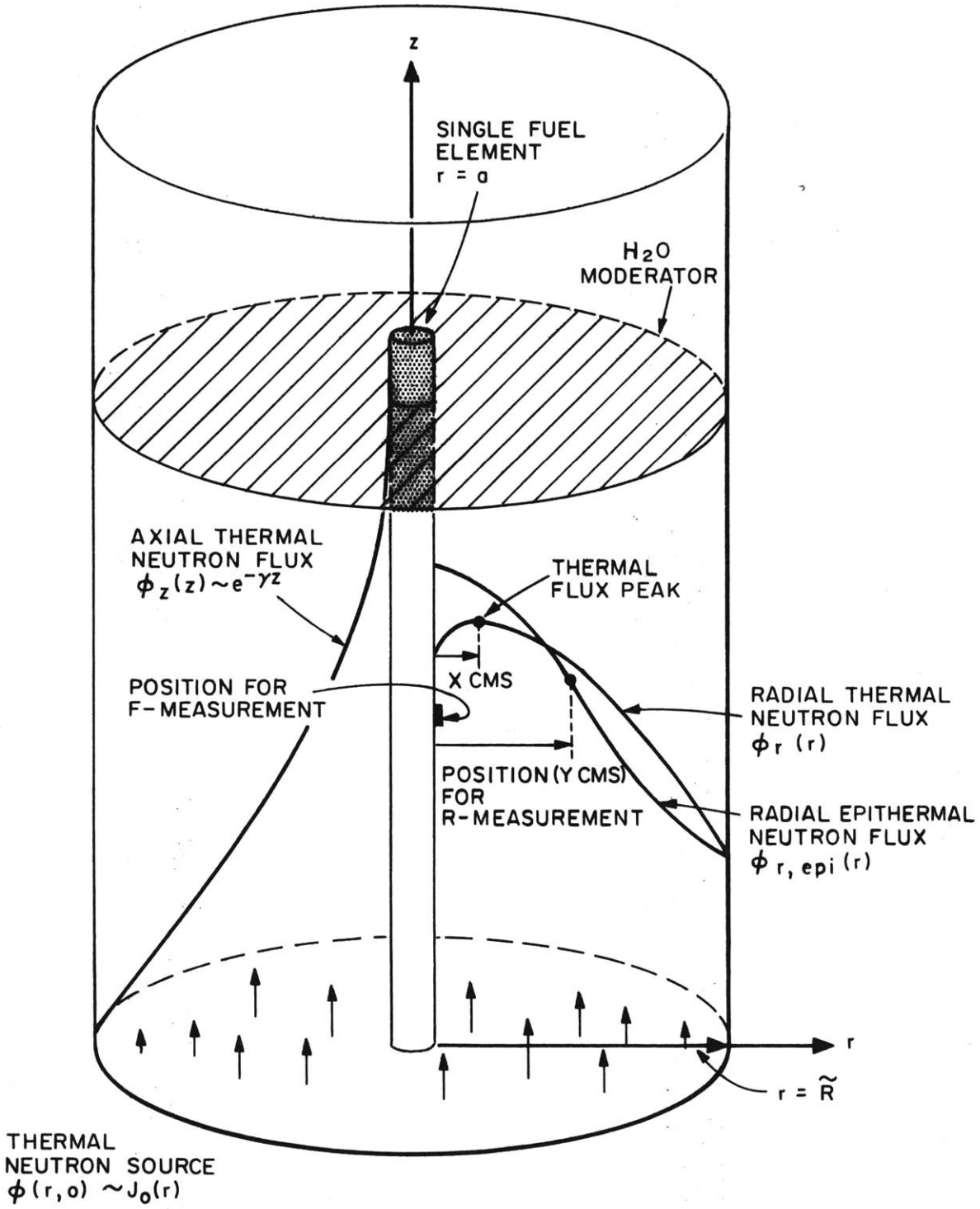

FIG. 2.1 THE SINGLE ELEMENT MODEL

2.2.1 Thermal Constant, Γ

An expression for Γ is obtained by first deriving the thermal neutron flux distribution and then using the condition that the flux passes through a maximum at the measured distance X. The balance of thermal neutrons in a unit volume of the moderator at a radial distance r from the center may be described by:

$$D\nabla_r^2\phi_r(r) + D\gamma^2\phi_r(r) - \Sigma_{am}\phi_r(r) + S_r q_r(r, \tau_{th}) = 0\,, \tag{2.1}$$

where

$\phi_r(r)$ is radial component of the thermal neutron flux at the point, r; the axial component of the flux has been assumed to vary as $e^{-\gamma z}$;

Σ_{am}, D are the macroscopic absorption cross section and the diffusion coefficient, respectively, for thermal neutrons in the moderator;

S_r is $\dfrac{\phi_r(a)}{\Gamma}\,\eta$; and (2.2)

$q_r(r, \tau_{th})$ is the radial component of the slowing-down density of thermal neutrons (age, τ_{th}) at the point r due to fast neutrons from the fuel element.

Equation 2.1 is solved with the following boundary conditions at the fuel surface (r = a) and at the "extrapolated" outer moderator boundary ($r = \tilde{R}$):

$$r = a,\quad \phi_r(a) - \Gamma\, 2\pi a D(\nabla\phi_r)_a = 0 \quad \text{(by definition of } \Gamma)\,, \tag{2.3}$$

$$r = \tilde{R},\quad \phi_r(\tilde{R}) = 0\,. \tag{2.4}$$

The use of the Green's function technique gives a closed functional representation of the solution for $\phi_r(r)$. The analytic expression for $\phi_r(r)$ can then be differentiated to meet the condition that:

$$\left[\frac{d\phi_r(r)}{dr}\right]_X = 0\,. \tag{2.5}$$

The resulting expression can be solved for Γ; the final result is

$$\Gamma = \frac{\eta\left[I_J(a,X) - \frac{J_1(\alpha X)}{Y_1(\alpha X)} I_Y(a,X)\right] - \left[J_o(\alpha a) - \frac{J_1(\alpha X)}{Y_1(\alpha X)} Y_o(\alpha a)\right]}{2\pi D\alpha a\left[J_1(\alpha a) - \frac{J_1(\alpha X)}{Y_1(\alpha X)} Y_1(\alpha a)\right]}, \quad (2.6)$$

where

$$\alpha^2 = \gamma^2 - \Sigma_{am}/D = \gamma^2 - 1/L_o^2, \quad (2.7)$$

L_o being the diffusion length of thermal neutrons in the moderator. $I_J(a,X)$, $I_Y(a,X)$ are given by

$$\begin{matrix} I_J(a,X) \\ I_Y(a,X) \end{matrix} = \int_a^X \begin{matrix} J_o(\alpha\xi) \\ Y_o(\alpha\xi) \end{matrix} q_r(\xi, \tau_{th})\, 2\pi\xi\, d\xi . \quad (2.8)$$

An expression for the slowing-down density, $q_r(r,\tau)$, is obtained by solving the basic age equation for a uniform, cylindrical source of fast neutrons, of finite radius a, in a moderator tank of finite radius $\tilde{R}$. The result is

$$q_r(r,\tau) = \sum_{n=1}^{\infty} C_n(\tau)\, J_o(\alpha_n r), \quad (2.9)$$

where

$$C_n(\tau) = \frac{2J_1(\alpha_n a)\, e^{(\gamma^2-\alpha_n)\tau}}{\pi\tilde{R}^2 \alpha_n a J_1^2(\alpha_n \tilde{R})}\left[1 - Aq_r^o(a,\tau_r)\, e^{-(\gamma^2-\alpha_n^2)\tau_r}\right], \quad (2.10)$$

and $\pm\alpha_n$, $(n = 1, 2, 3 \ldots)$ are the roots of the equation: $J_o(\alpha_n\tilde{R}) = 0$. Less than five terms of the series in Eq. 2.9 are usually sufficient for satisfactory convergence. The quantity $q_r^o(a,\tau_r)$ denotes the slowing-down density, at the fuel surface, of neutrons of effective resonance energy E_r (age, τ_r) at which all epithermal absorption in the fuel is assumed to occur; hence, the factor $Aq_r^o(a,\tau_r)$, by the definition of A, accounts for the net epithermal absorption in the source element. Substitution for q_r in Eq. 2.8 gives

$$\begin{matrix} I_J(a,X) \\ I_Y(a,X) \end{matrix} = \sum_{n=1}^{\infty} \frac{2\pi C_n}{(\alpha_n^2-\alpha^2)}\left[\alpha_n\xi J_1(\alpha_n\xi) \begin{matrix} J_o(\alpha\xi) \\ Y_o(\alpha\xi) \end{matrix} - \alpha\xi J_o(\alpha_n\xi) \begin{matrix} J_1(\alpha\xi) \\ Y_1(\alpha\xi) \end{matrix}\right]_a^X \quad (2.11)$$

2.2.2 Fast Neutron Yield, η

The epithermal neutron field in the moderator is due to the slowing down of fast neutrons produced in the single fuel element. Consequently, the ratio R of the activity in a gold foil due to epithermal neutrons (age, τ_{Au}) and that due to thermal neutrons, measured at $r = Y$, can be related to η by the age theory. This expression is

$$\frac{1}{R-1} = \frac{S_r q_r(Y, \tau_{Au})}{G \hat{\phi}_r(Y)}, \tag{2.12}$$

where G is a constant which involves the geometric and nuclear parameters of the gold foil and the slowing-down power of the moderator, $\xi\Sigma_s$. The value of G is determined by measurements on a "reference" fuel element. In the present work this reference fuel is the 1.01-inch-diameter, natural uranium rod for which the value of η is taken as 1.375. Substitution for S_r from Eq. 2.2 and rearrangement gives

$$\eta = G \frac{\Gamma \hat{\phi}_r(Y)}{q_r(Y, \tau_{Au})} \frac{1}{(R-1)}, \tag{2.13}$$

where $\hat{\phi}_r(Y)$ is $\phi_r(Y)/\phi_r(a)$; the calculation of $\hat{\phi}(Y)$ requires a few iterations between the equations for $\phi_r(Y)$ and X.

Equations 2.6 and 2.13 can be solved simultaneously for Γ and η. The coupling between Γ and η involves the third parameter A through the factor q_r; the determination of A is, however, independent of Γ and η. The method of obtaining Γ and η thus involves the use of three experimental parameters X, γ and R. In principle, two of these are sufficient, but this would require greater accuracy for the single-element experiments.

2.2.3 Epithermal Absorption Parameter, A

The absorption resonance of Au^{197} at 4.9 eV and that of Mo^{98} at 470 eV span an energy range which accounts for about 90% of the epithermal absorptions in U^{238}. Since the epithermal flux depletion in the fuel in this energy range is proportional to the value of the

epithermal absorption parameter A, it can be shown on the basis of an approximate model that the ratio, f_e, of the fluxes at 4.9 eV and 470 eV decreases linearly with the value of A. Since the epithermal flux ratio can be directly obtained from the experimental parameter F, the measurement of F therefore provides a way to infer the value of A.

A more rigorous relationship between f_e and A is obtained with the use of the computer code ANISN (6) to simulate the single-element experiment. The parameter A is varied in the range of interest by varying the absorption cross section of U^{238} in each epithermal energy group by a multiplicative factor. Values of A are calculated from the following equation:

$$A = \frac{V_f \sum_i N^i RI^i}{\xi \Sigma_s}, \qquad (2.14)$$

where

V_f is the volume of the fuel element per unit length,

N^i is the concentration in the fuel of the i^{th} nuclide, and

RI^i is the effective resonance integral of the i^{th} nuclide.

Figure 2.2 shows the relationship between the value of f_e on the fuel surface and A, obtained for homogenized clusters of 19 and 31 rods and for a natural uranium rod. The ratio f_e appears to be sufficiently sensitive to A. The differences among the curves shown in the figure appear to be due to geometric (finite size) effects.

The curves of f_e versus A are normalized such that the flux ratio f_e measured for the natural uranium rod ("reference" element) corresponds to the value of A (20.4 cm^2) calculated for this rod from Eq. 2.14. The parameter A for the test element is then obtained by first relating the measured activity ratio F to the flux ratio f_e, and then referring to the normalized characteristic curve of f_e versus A generated for the fuel element.

The epithermal absorption parameter does not appear to be significantly influenced by spectral differences, at least as shown by the restricted studies undertaken. Thus the effective age, τ_r, of epithermal absorption in U^{238} has been obtained for two cases:

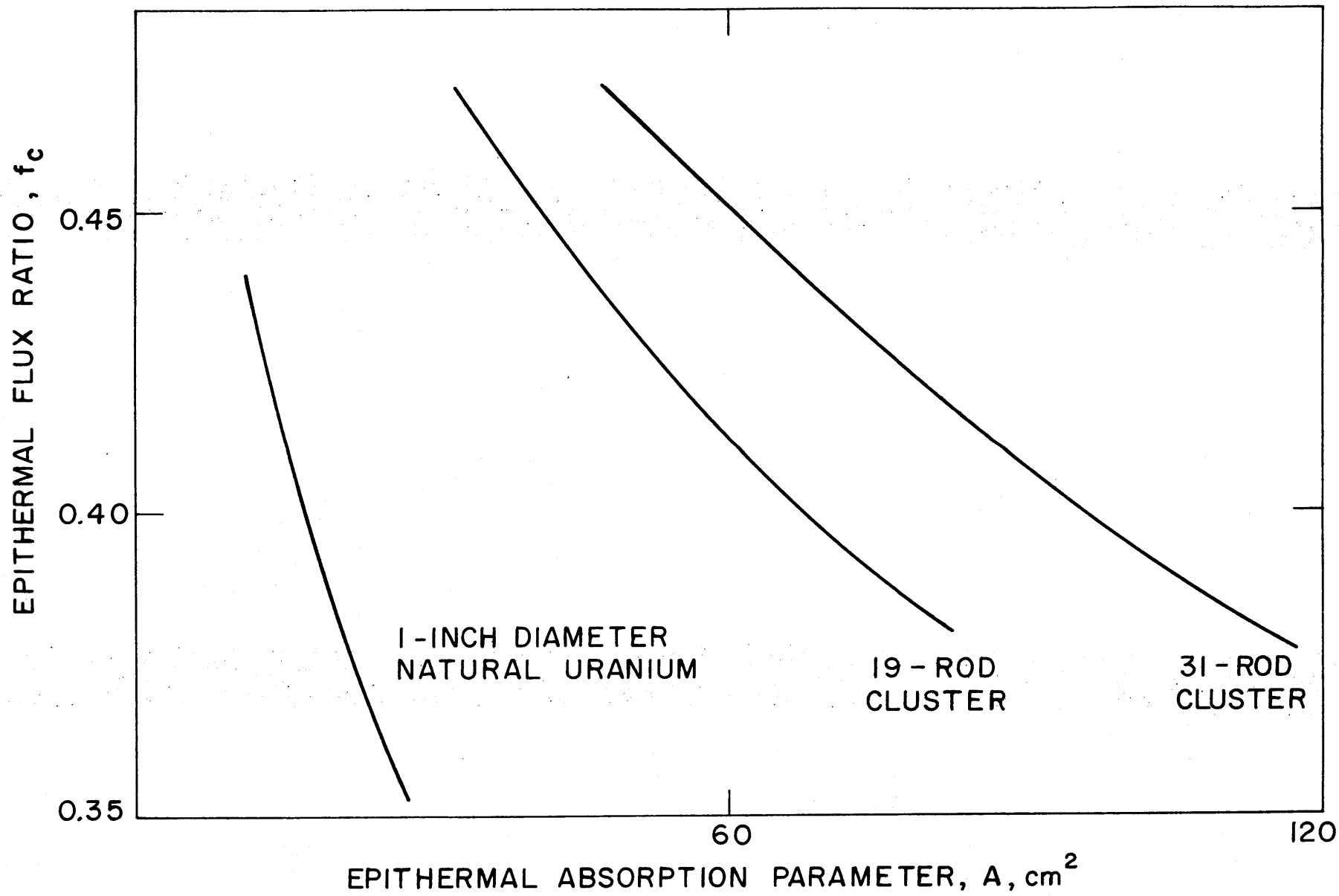

FIG. 2.2 EPITHERMAL FLUX RATIO (f_c) VERSUS EPITHERMAL ABSORPTION PARAMETER (A)

the single element isolated in the moderator ($1/\tau(u)$ spectrum) and the single element in a lattice (1/E spectrum). Calculations show an excellent agreement between the two values of τ_r. Furthermore, the variation with energy (Fig. 2.3) of the fractional U^{238} absorption in the natural uranium rod is identical for the two spectra, and about 90% of the U^{238} epithermal absorption occurs between about 5 eV and 500 eV in both cases.

2.3 Experiments

All single-element experiments have been performed in the D_2O-moderated exponential tank at the M.I.T. Reactor (Fig. 2.4). The test fuel element was located at the center of the tank. The experimental parameters X, γ, R and F were measured for a 1.01-inch-diameter, natural uranium rod ("reference" element) and for tight clusters of 19 and 31 rods typical of those used in pressure tube designs for D_2O-moderated power reactors. The UO_2-PuO_2 fuel within the clusters simulated natural uranium partially burned to 5000 MWD/ton. The geometric characteristics and the fuel composition of the clusters are given in Fig. 2.5 and Table 2.1. Uniform lattices of these clusters, cooled and moderated by heavy water, have been studied (7) at the Savannah River Laboratory (SRL). Work (8) on the same fuel with other coolants has also been carried out by the Atomic Energy of Canada Limited (AECL).

The distance X to the thermal neutron flux peak was obtained by activating gold foils, each 1/16 inch in diameter and 0.010 inch thick, positioned 1/4 inch apart on aluminum holders. The holders were suspended horizontally along radii of the moderator tank. The 411-keV gamma-ray activities of the fold foils were counted, corrected and curve-fitted. The position of the maximum of this measured activity distribution corresponds to the radial distance X. Calculations show that for the cases of present interest the difference between the measured distance X and the distance to the peak of the asymptotic thermal flux in the moderator is negligible compared to the experimental uncertainty in X. The values of X obtained for different angular orientations of the clusters show no systematic trend.

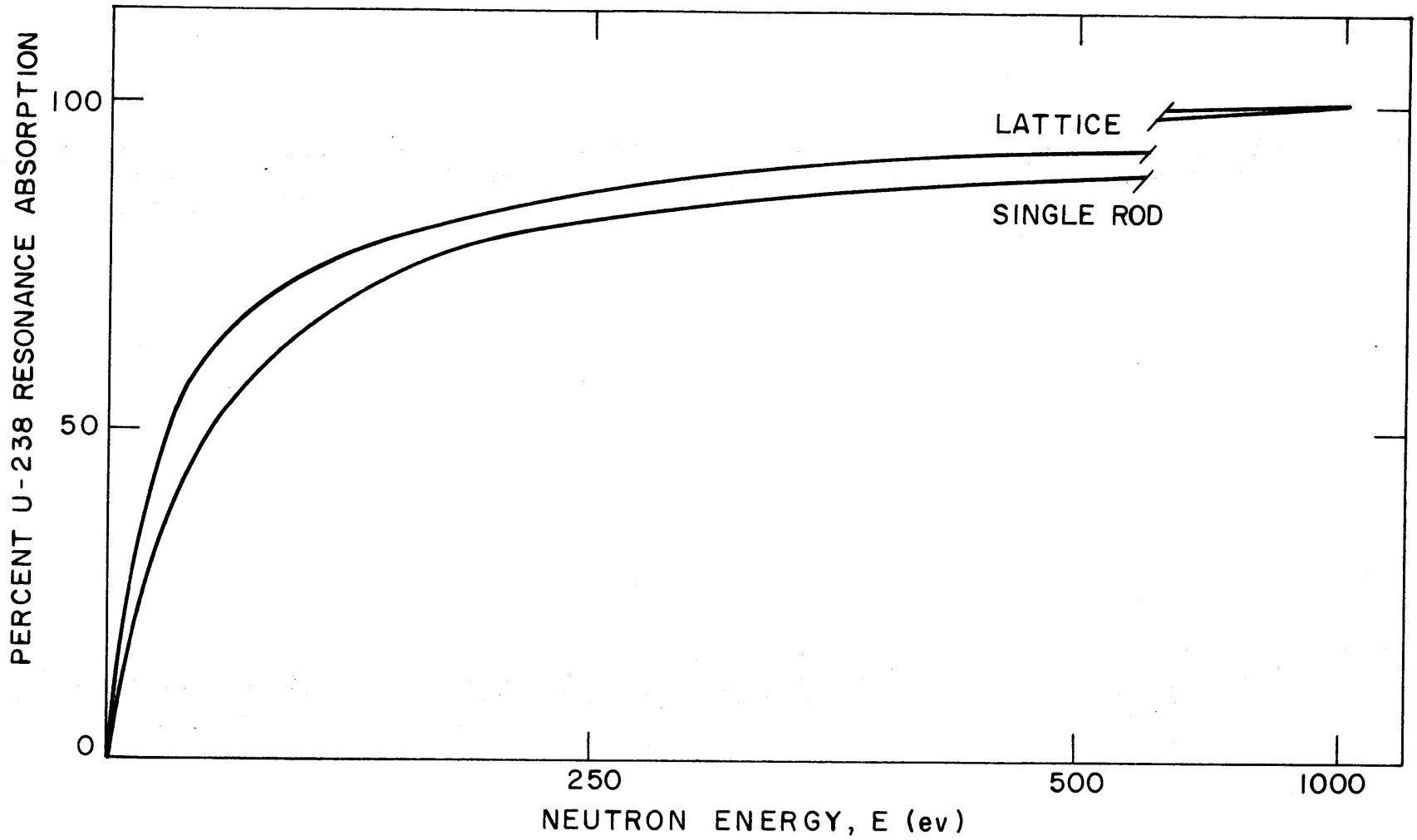

FIG. 2.3 CUMULATIVE U-238 RESONANCE ABSORPTION IN A LATTICE AND AROUND A SINGLE FUEL ELEMENT VERSUS ENERGY

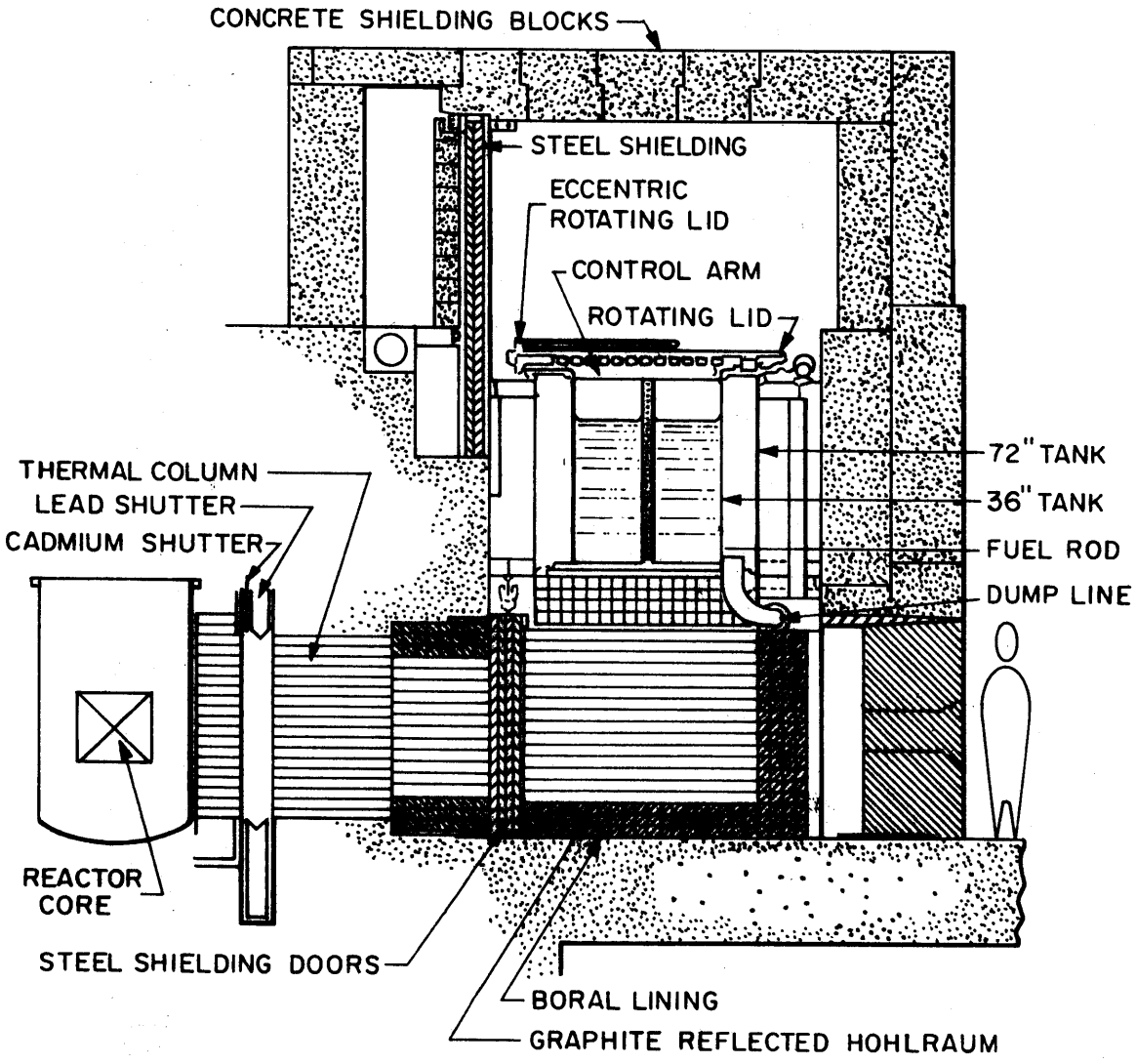

FIG. 2.4 VERTICAL SECTION OF THE SUBCRITICAL ASSEMBLY

2/3 SCALE

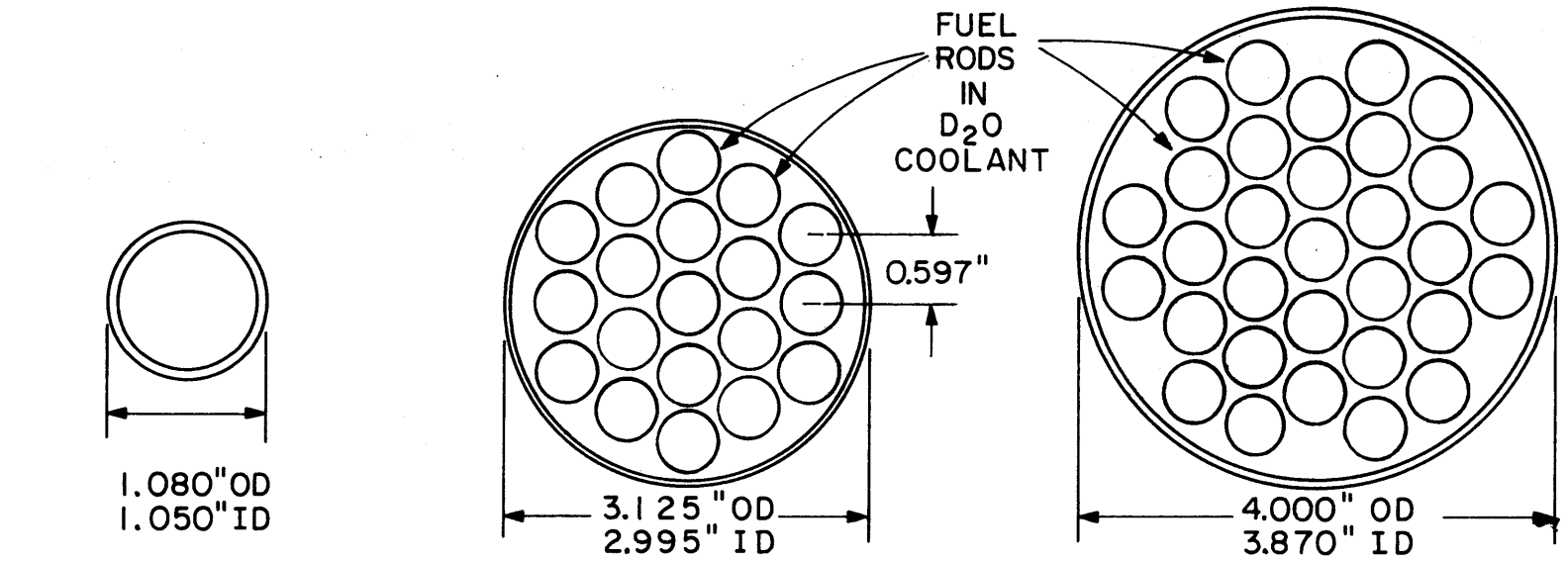

1100 Al CLADDING
(1.01-inch DIAMETER
NATURAL URANIUM)

6061 Al HOUSING TUBE
(19-ROD CLUSTER)

6061 Al HOUSING TUBE
(31-ROD CLUSTER)

FIG. 2.5 FUEL ELEMENT ARRANGEMENTS

TABLE 2.1

Isotopic Composition of Simulated Burned Fuel* Used in 19- and 31-Rod Clusters

Isotope	Wt. % of Total U + Pu
U-238	99.431
U-235	0.30
Pu-239	0.20
Pu-240	0.016
Pu-241	0.002
Pu-242	0.001

*Type B (color code: gold)
USAEC-AECL Cooperative Program (7).

The inverse relaxation length, γ, was measured by irradiating gold foils, 1/8 inch in diameter and 0.01 inch thick, spaced 2 inches apart on vertical foil holders. The distance of the holders from the center was about 22 cms. The corrected gamma-ray activities of the gold foils were fit to a sinh distribution to give γ corresponding to the best fit of the experimental data.

The gold-cadmium ratio R at a radial distance Y was directly measured by irradiating at that distance two similar gold foils, one of which was covered with cadmium. The distance Y was 21 cms for natural uranium rod and 23 cms for the two clusters. The irradiation procedure and the method for data reduction were the same as those used for the determination of γ.

The ratio F was measured by activating cadmium-covered pairs of molybdenum and dilute gold foils on the surface of the fuel element. Both foils were 1/4 inch in diameter, the molybdenum foil being 0.025 inch thick and the gold foil, 0.003 inch thick. These foils were counted for the induced activities in Au^{197} and Mo^{98}. The use of dilute gold reduces resonance self-shielding and lowers the gold activity so that the total counts and the counting times for both foils are comparable. Because of their relatively smaller activation cross section and gamma yield, the molybdenum activities (740-, 780-keV gamma rays) are low;

consequently, a well-type NaI crystal was used to provide a much larger solid angle for counting, and the background radiation was cut down to a very low level by lead shielding. Measured activities were corrected according to standard prescriptions. F is the ratio of the corrected activities of unit weights of Au^{197} and Mo^{98}.

2.3.1 Results

Average values of the experimental parameters X, γ, R and F, obtained in several independent sets of measurements for each fuel element, are tabulated in Table 2.2. These results are used with the analytic formalism described earlier to give the heterogeneous fuel parameters Γ, η and A. The final values of Γ, η and A for each single-element tested are shown in Table 2.3. The uncertainty associated with the determination of the fuel parameters is obtained by compounding the separate effects on them of the uncertainties in X, γ, R and F. The result is a composite error of about 5%, 3% and 4% in the determination of Γ, η and A, respectively.

TABLE 2.2

Values of the Experimental Parameters

Single Element Type	X (cm)	γ^2 ($cm^{-2} \times 10^6$)	R (cm)	F (cm)
Natural Uranium Rod ("Reference")	9.70 ±0.08	2488.5 ±9.2	122.18 ±2.2	361.6 ±0.5
19-Rod PuO_2-UO_2 Cluster	13.16 ±0.14	2417.6 ±6.7	77.69 ±0.44	397.15 ±10.6
31-Rod PuO_2-UO_2 Cluster	14.77 ±0.21	2388.2 ±11.6	58.41 ±0.56	389.9 ±5.0

TABLE 2.3

Heterogeneous Fuel Parameters

Fuel Type	Γ	η	A
Natural Uranium Rod ("Reference")	0.9546	1.375*	20.39*
19-Rod UO_2-PuO_2 Cluster	0.4707	1.3643	52.5
31-Rod UO_2-PuO_2 Cluster	0.3313	1.4017	81.50

*"Reference" values

2.4 Application to Uniform Lattices

The measured values of Γ, η and A are tested by using them in simple recipes for the calculation of the reactor physics parameters of uniform lattices.

2.4.1 Thermal Utilization

The thermal utilization, f_Γ, may be related to Γ on the basis of the Wigner-Seitz formalism of a unit lattice cell. This relation is

$$\frac{1}{f_\Gamma} = 1 + \Gamma \Sigma_{am} V_m + (E-1), \tag{2.15}$$

where

V_m is the volume of the moderator per unit height of the unit cell, and

(E-1) is the "excess" moderator absorption per fuel absorption (9).

The definition of f_Γ differs from that of the conventional f in that the fuel absorption in the present case includes absorption in the cladding and the coolant.

2.4.2 Fast Neutron Yield

In order to obtain the fast neutron yield factor, η_L, of the lattice, it is necessary to correct the measured value of η to include the effect of epithermal and fast fissions in the fuel due to neutrons which originate in other elements of the lattice. The result is

$$\eta_L = \eta + V_f(N\nu RI_f)^{epi} \sum_j \phi_j^{epi} + V_f(N\nu\bar{\sigma}_f)^{fast} \sum_j \phi_j^{fast} , \quad (2.16)$$

where $(N\nu RI_f)^{epi}$, $(N\nu\bar{\sigma}_f)^{fast}$ are, respectively, the number of neutrons produced per unit volume per unit flux in all the epithermal and fast fissions in the fuel; and ϕ_j^{epi} and ϕ_j^{fast} are, respectively, the contributions of the j^{th} element (distance, r_j) to the epithermal and fast neutron fluxes at the fuel element in question. With the use of the age kernel and an uncollided flux kernel to describe the propagation of epithermal and fast neutrons, respectively, it follows that

$$\phi_j^{epi} = \frac{\eta}{\xi\Sigma_s} \frac{e^{-r_j^2/4\tau_{ef}}}{4\pi\tau_{ef}} , \quad (2.17)$$

where τ_{ef} is the effective age for epithermal fissions; and

$$\phi_j^{fast} = \eta \frac{e^{-\frac{\pi}{2}\frac{r_j}{\lambda_f}}}{4r_{oj}} , \quad (2.18)$$

where λ_f is the mean free path of fast neutrons in the moderator. The summations which occur in Eq. 2.16 can be evaluated with the aid of the Euler-McLaurin sum formula. The final expressions for the two summations, to be denoted by S^{epi} and S^{fast}, respectively, are

$$S^{epi} = \frac{\eta}{\xi\Sigma_s}\left[\frac{1}{V_c} - \frac{1}{4\pi\tau_{ef}}\right] \quad (2.19)$$

and

$$S^{fast} = \eta\left[\frac{\lambda_f v}{\pi a^2} + \frac{\sqrt{3v}}{4a} + \frac{\pi}{16\lambda_f}\right] e^{-\frac{\pi\sqrt{3a}}{\lambda_f\sqrt{v}}} + \eta\frac{3\sqrt{v}}{4a} e^{-\frac{\pi a}{\lambda_f\sqrt{v}}}, \qquad (2.20)$$

where V_c is the volume per unit height of the unit cell, and v is the volume fraction of fuel.

2.4.3 Resonance Escape Probability

The resonance escape probability, p, is related to the epithermal absorption parameter, A_L, of the lattice by the equation:

$$p = 1 - A_L/V_m . \qquad (2.21)$$

The parameter A_L may be deduced from the measured value of A by correcting the latter for the Dancoff effect, the flux depletion in energy space and the spatial nonuniformity of the neutron slowing-down density across the cell. For the lattices of present interest, however, only the last effect is important. Denoting the ratio of the average epithermal flux in the fuel to that in the moderator by β, it follows that

$$A_L = A\beta . \qquad (2.22)$$

The advantage factor β is determined by solving the age equation for the epithermal neutron distribution in the lattice cell (radius, b) produced by a uniform cylindrical source (radius, a) of fast neutrons. The result is:

$$B(\tau) = \left[1 + 4\sum_{n=2}^{\infty}\frac{J_1^2(\alpha_n a)\, e^{-\alpha_n^2\tau}}{(\alpha_n a)^2 J_o^2(\alpha_n b)}\right], \qquad (2.23)$$

where α_n, (n = 2, 3, . . .) are the positive roots of $J_1(\alpha b) = 0$. The value of β which is used in Eq. 2.22 is taken to be the weighted sum of two Gaussians (characterized by τ_1 and τ_2). Thus,

$$\beta = B_1\beta(\tau_1) + B_2\beta(\tau_2), \qquad (2.24)$$

where the values (5) used for τ_1 and τ_2 are, respectively, 126.5 cm^2 and 40.5 cm^2, and those for the weighting factors B_1 and B_2 are, respectively, 0.56 and 0.44.

2.4.4 Material Buckling

The material buckling, B_m^2, is calculated from the age-diffusion theory:

$$k_\infty e^{-B_m^2 \tau_L} - (L^2 B_m^2 + 1) = 0 , \tag{2.25}$$

where k_∞ is the infinite medium multiplication factor, given by

$$k_\infty = f_\Gamma \eta_L p . \tag{2.26}$$

The diffusion length, L, for the lattice is calculated from

$$L^2 = L_o^2(1-f_\Gamma); \tag{2.27}$$

and that of the neutron age, τ_L, for the lattice is calculated from (10)

$$\tau_L = \tau_{th}\left\{1 - \frac{V_{A\ell}}{V_c} - \frac{\varepsilon_n}{2}\frac{V_f}{V_c}\right\}^{-2} , \tag{2.28}$$

where $V_{A\ell}$ is the volume of the cladding per unit fuel length, and ε_n is the ratio of the concentration of fuel atoms in the fuel element to that in natural uranium.

The uncertainty associated with the calculated value of buckling is estimated from its sensitivity to systematic variations in the experimental parameters X, γ, R and F. The composite error in B_m^2 due to all the experimental uncertainties is about 9%.

2.4.5 Comparison

Equations 2.15 through 2.28 have been used to calculate the values of B_m^2 for uniform lattices of one-inch-diameter, natural uranium rods in D_2O. The values of η and A used in the calculations are the "reference" values. The graph in Fig. 2.6 shows a comparison of the results obtained from the single-element parameters with those of experimental studies for complete lattices of the same fuel at several laboratories (11). The excellent agreement evident in this figure provides a check on the reference values used for η and A and on the single-element model.

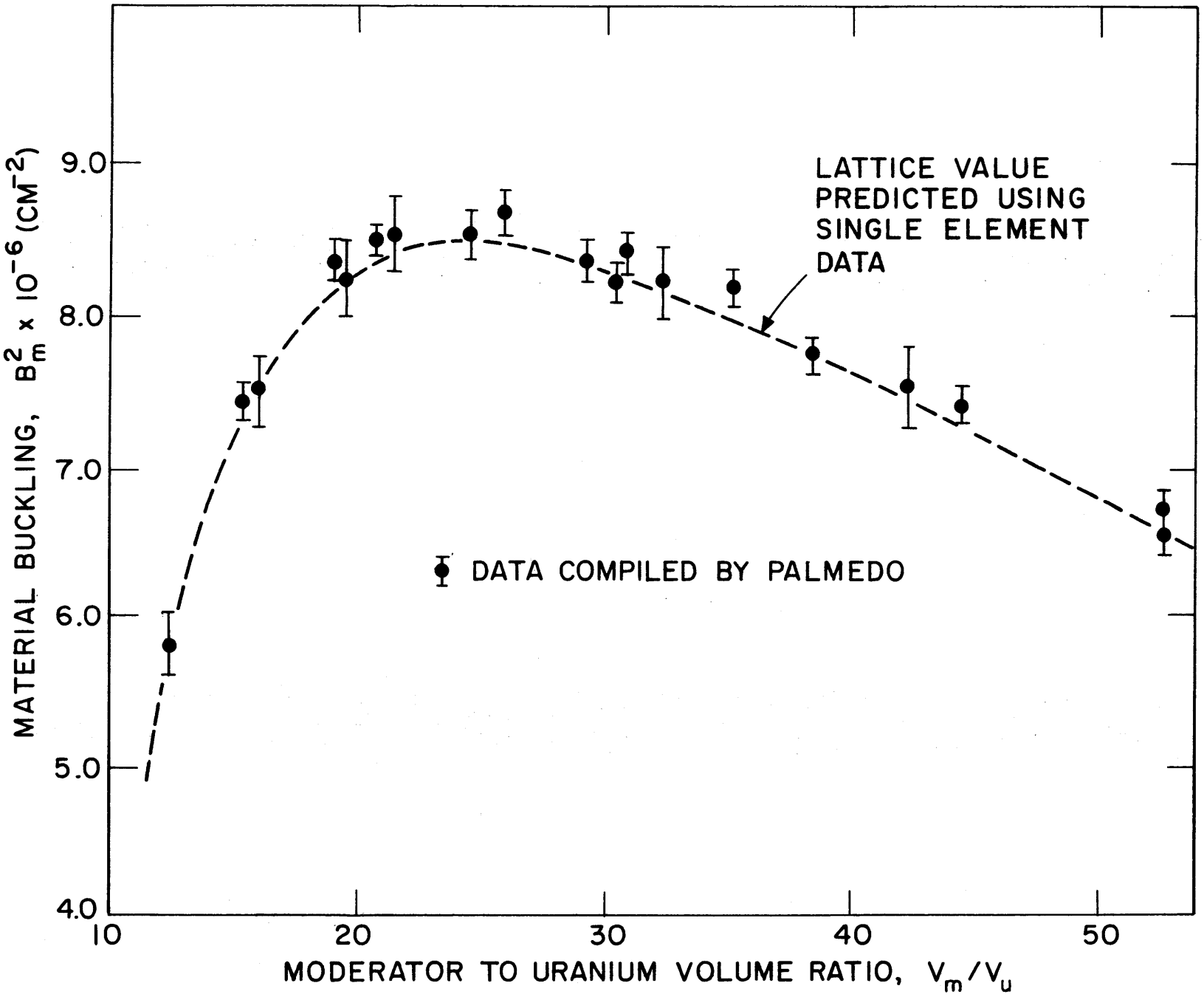

FIG. 2.6 BUCKLING OF 1.0 IN. DIAMETER, NATURAL URANIUM RODS IN D_2O

The more important test of the methods lies in their application to the tight clusters of 19 and 31 rods. Table 2.4 presents a comparison of the lattice parameters f_Γ, η_L, p and B_m^2 calculated by the single-element method with those obtained in full-lattice experiments and numerical studies at the SRL. This comparison is to be made in light of some of the differences in the definitions of the lattice parameters. The agreement between the values of buckling of MIT single-element studies and SRL experiments is very good, being in the neighborhood of 5% for two of the lattices. This compares very favorably with the general state of buckling calculations: discrepancy between theory and experiment in excess of 10% is quite common.

2.5 Conclusions

The success of the measured values of Γ, η and A in satisfactorily predicting the lattice parameters demonstrates the feasibility and adequacy of the single-element method. Since the method requires the use of only one fuel element, it is conceivable that scarce and promising fuel types can be evaluated at greatly reduced material requirements and cost. Further, all the measurements are made outside the fuel, thus circumventing the problems of contamination and hazard from the fission products or plutonium within the fuel.

TABLE 2.4

Comparison of Single Element and Lattice Results

for D_2O-Moderated and Cooled, Plutonium-Containing Fuel Clusters

Type of Result	η_L	p	f	k_∞	B_m^2 ($cm^{-2} \times 10^6$)
A. 19-ROD CLUSTER 9.33-Inch Lattice Spacing					
(1) MIT Single Element	1.385	0.8750	0.9793	1.1868	540 ± 45
(2) SRL Calculation	1.407	0.8556	0.961	1.1566	484
(3) SRL Lattice Expt.	–	–	–	–	524 ± 15
B. 31-ROD CLUSTER 9.33-Inch Lattice Spacing					
(1) MIT Single Element	1.438	0.7926	0.9863	1.1241	458 ± 43
(2) SRL Calculation	1.451	0.79	0.9621	1.1028	425
(3) SRL Lattice Expt.	–	–	–	–	501 ± 15
C. 31-ROD CLUSTER 12.12-Inch Lattice Spacing					
(1) MIT Single Element	1.412	0.8684	0.9733	1.1937	472 ± 44
(2) SRL Calculation	1.419	0.8486	0.9513	1.1458	416
(3) SRL Lattice Expt.	–	–	–	–	429 ± 20

2.6 References

(1) Feinberg, S.M., "Heterogeneous Methods for Calculating Reactors: Survey of Results and Comparison with Experiments," Proc. Intern. Conf. Peaceful Uses At. Energy, Geneva, 5, 484 (1955).

(2) Galanin, A.D., "Critical Size of Heterogeneous Reactors with Small Number of Rods," loc. cit., ref. 1, p. 477.

(3) Horning, W.A., "Small Source Model of a Thermal Pile," HW-24282 (1952).

(4) Klahr, C.N., L.B. Mendelsohn, J. Heitner, "Heterogeneous Reactor Calculation Methods," HYO-2680 (1961).

(5) Graves, W.E., F.D. Benton, R.M. Satterfield, "A Comparison of Heterogeneous Nuclear Reactor Lattice Theory and Experiment," Nucl. Sci. Eng., 31, 57 (1968).

(6) Engel, W.W., M.A. Boling, B.W. Colston, "DTF-II, A One-Dimensional, Multigroup, Neutron Transport Program," NAA-SR-10951 (1966).

(7) Baumann, N.P., J.L. Crandall et al., "Lattice Experiments with Simulated Burned-Up Fuel for D_2O Power Reactors," DP-1122 (1968).

(8) French, P.M., R. Solheim, "Experimental Bucklings of Simulated Burned-Up Natural Uranium Clusters in Heavy Water," ANS/CNA Trans. 11, No. 1 (1968).

(9) Weinberg, A.M., E.P. Wigner, "The Physical Theory of Neutron Chain Reactors," University of Chicago (1958).

(10) Dessauer, G., "Physics of Natural Uranium Lattices in Heavy Water," Proc. Intern. Conf. Peaceful Uses At. Energy, Geneva, 12, 320 (1958).

(11) Palmedo, P.F., I. Kaplan, T.J. Thompson, "Measurements of the Material Bucklings of Lattices of Natural Uranium in D_2O," NYO-9960, MITNE-13 (1962).

3. FUEL ASSAY USING Ge(Li) GAMMA-RAY SPECTROMETRY

Y. Hukai and N. C. Rasmussen

It was the object of the work reported in this chapter to study the gamma rays emitted by the products of the interaction of thermal neutrons with the nuclei of U^{238}, Th^{232}, U^{235} and Pu^{239} during and after irradiation and to explore some applications, mainly to fuel element assay. An irradiation facility and a Ge(Li) detector cryostat were constructed for this purpose.

A new method of assaying a fuel rod containing a mixture of plutonium and uranium oxide, based on the difference in the observed yield of the fission products I^{135} and Sr^{92}, has been developed.

The energies and intensities of the thermal neutron capture gamma rays for U^{238} and Th^{232} were determined. Four new lines have been found in the energy region previously unexplored for U^{238}. For Th^{232}, 66 certain lines were found, compared to 7 lines in the literature.

Many prompt gammas emitted by the highly excited fission products following the fission of U^{235} and Pu^{239} were resolved in the energy region above 1.4 MeV. For U^{235} fissions, 57 lines were found, and for Pu^{239}, 51 certain lines were recorded. The use of prompt gammas for assaying fuel rods was investigated. An accuracy of about ± 7% was obtained for the analysis of U^{238} content; ± 10% to ± 20% accuracy was obtained for U^{235} analysis in the range of 1% to 2% enrichment; and ± 35% accuracy for the analysis of 0.25% Pu-enriched rods. It has been found that Ge(Li) detectors can be operated as fast neutron detectors and used to determine the relative neutron yield. With this method, the enrichment of uranium rods can be found with an accuracy of ± 1% to ± 2% in the range from 1% to 2% enrichment.

Finally, some considerations were given to the use of prompt gamma rays for measuring the initial conversion ratio C and the neutron yield parameter η.

A detailed topical report, of which this chapter is a summary, has been issued on this work:

Y. Hukai, N.C. Rasmussen, M.J. Driscoll,
"Some Applications of Ge(Li) Gamma-Ray Spectroscopy
to Fuel Element Assay," MIT-3944-5, MITNE-113,
April 1970.

3.1 Introduction

The objective of the present work was to study the gamma rays emitted by the products of the interaction of thermal neutrons with the nuclei of U^{238}, Th^{232}, U^{235} and Pu^{239} during and after irradiation and to explore some applications concerned with Reactor Physics.

This work can be divided into four fairly independent areas:

1. A method of using delayed gamma rays for assaying Pu-containing fuel rods.
2. Study of prompt gamma rays from thermal neutron absorption by fuel elements (U^{238}, Th^{232}, U^{235} and Pu^{239}).
3. Application of prompt gamma rays for assaying fuel rods.
4. Feasibility study for an in-core gamma spectrometer operating in an exponential facility for yielding the reactor physics parameters η and C.

To conduct these studies, an irradiation facility was constructed and a high resolution Ge(Li) detector spectrometer was used.

Owing to the widespread interest in burnup measurements, the analysis of delayed gamma rays with lifetimes from a few minutes to several years has been done extensively elsewhere and was not a subject for further investigation here. Instead, an application of these gammas for the purpose of assaying fuel rods containing a mixture of plutonium and uranium was evaluated. This method is based on the difference in yield of certain short-lived fission products of U^{235} and Pu^{239}.

The study of prompt gamma rays can be divided into two categories: those not involving the fission process, which is the case for the thermal neutron capture gammas for U^{238} and Th^{232}, and those involving fission, which is the case for U^{235} and Pu^{239}. This separation is natural because the presence of prompt fission gammas and fast fission neutrons from U^{235} and Pu^{239} imposed extra problems of background reduction in obtaining resolved gamma spectra for these nuclei.

The capture gamma rays for U^{238} have been studied previously by Sheline (1) and Maier (2). The present results for U^{238} have mainly confirmed the data presented by those authors. Nevertheless, seven new lines were found, four of which are in the energy region not covered by Sheline. For Th^{232}, Groshev (3) and Burgov (4) have reported up to seven lines. In the present work, with a spectrometer of about five times better resolution, sixty-six distinct lines have been found.

For the cases of U^{235} and Pu^{239}, very little is available in the literature concerning their prompt gamma rays. Greenwood (5) has obtained the spectra of the prompt gamma rays for U^{235} and Pu^{239} using a NaI crystal, but no significant structure can be distinguished in his spectra above a few hundred keV. The present results, on the other hand, show clearly more than fifty peaks for both U^{235} and Pu^{239} spread over the energy range above 1.4 MeV in the pair spectrometer gamma spectra.

Two applications of prompt gamma rays have been studied. One is the use of prompt gammas for identification and assay of uranium fuel rods and rods containing a mixture of plutonium and uranium oxide; and the second, some considerations pertinent to the development of new techniques for measuring reactor physics parameters based on prompt gamma-ray spectroscopy. A conceptual design for a gamma spectrometer operating in the M.I.T.R. Exponential Facility is also presented.

3.2 Experimental Equipment

3.2.1 Description

The irradiation facility using the neutron beam port 4TH1 of the M.I.T. Research Reactor is composed of two parts: the front facility, closer to the reactor, followed by the rear facility using the same neutron beam.

In the present work, the experiments involving prompt gamma rays were performed using the front facility which is equipped with a spectrometer with a fixed cryostat capable of counting gamma rays in triple coincidence and Compton suppression modes of operation.

The rear irradiation facility was used in experiments involving delayed fission product gamma rays. An overall top view of the irradiation facility is shown in Fig. 3.1. The neutrons from the reactor core are scattered by a graphite plug, 3-7/8 inches in diameter and 40 inches long, placed inside the 4TH1 tangential through-port next to the reactor core; the resulting scattering source forms the neutron beam for the external irradiation facility. The thermal neutron beam coming from the reactor port can be interrupted at two distinct places preceding each of the two irradiation positions by two back-to-back boral plates of 1/4-inch thickness. A detailed description of the front facility is given by Harper in reference (6). The rear facility, although primarily designed for irradiation of fuel rods, is flexible enough for carrying out many other kinds of experiments. Basically, it has a central chamber in the form of a 10-inch square, 3 inches high, with five access ports. The fuel rod is irradiated standing vertically on the floor and may be of any reasonable height. It can be scanned continuously over a length of 21-1/2 inches.

At the front facility, the sample is inserted into the irradiation position through one of the side access ports, and the gamma rays coming from the sample are collimated via holes topped by a replaceable 6-1/2-inch-long lead segment. A segment with an opening of 3/4 inch was used throughout the present work. The shielding along the gamma-ray flight path was varied according to the requirements set for each experiment. This shielding was necessary to protect the Ge(Li) detector from either thermal or fast neutrons, or both.

Two gamma-detecting systems, both with Ge(Li) detectors, were used in this present work. One of them used a 35-cc coaxial detector with 24 cc of active volume. It was used in all the experiments involving the fission product delayed gammas and in the fission neutron yield determinations. The other, a planar hexagonal-shaped, 7-cc Ge(Li) detector with 5 cc of active volume, was used in conjunction with the pair spectrometer in all the experiments involving the prompt gammas. The use of two different detectors was dictated by availability, the nature of the experiments and the obvious convenience of having two independent systems operating alternately with one multichannel analyzer.

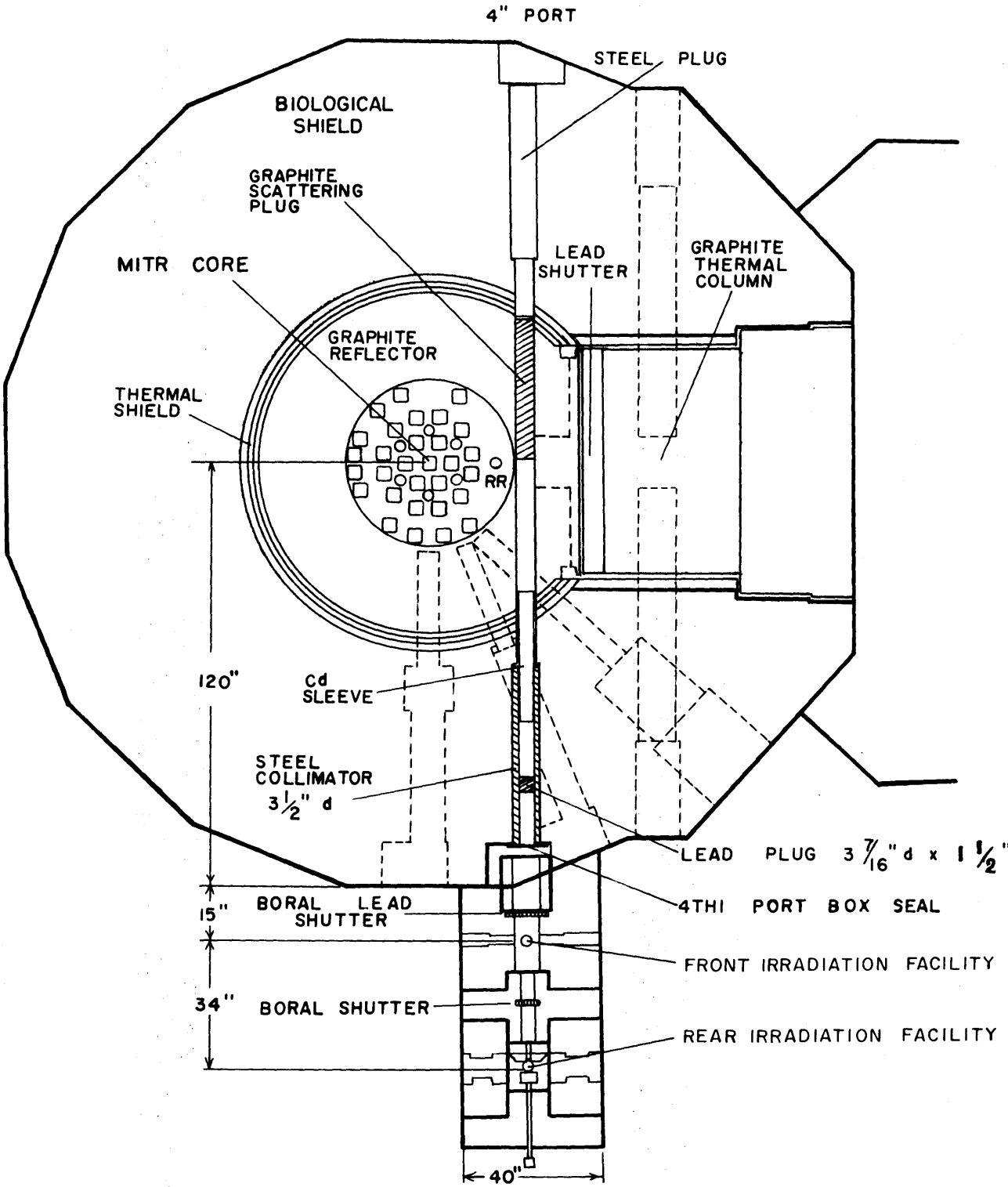

FIG. 3.1 TOP VIEW OF MITR CORE AND 4THI IRRADIATION FACILITY

For the front irradiation facility, a cryostat for the 7-cc detector was constructed. The design of this cryostat was based on a similar cryostat constructed by Miner (7). Figure 3.2 shows a general view of the cryostat and the detector.

A "chicken feeder" method for supplying LN to the cold finger was employed. A desirable characteristic of this cooling method is that the liquid level remains constant within the cryostat and maintains a stable thermal environment.

The electronics associated with the 35-cc detector was the standard arrangement for free mode operation. The signal was amplified by a Camberra Industries CI-1408c preamplifier and CI-1417 amplifier and thereafter fed into a Nuclear Data ND-161F 4096 channel analyzer.

Figures 3.3 and 3.4 show the electronic block diagrams for triple-coincidence and Compton suppression modes of operation, respectively. The details of the electronic operations are extensively described in reference (8). Basically, the components were the same as used previously by Orphan (8), but a simplified circuitry and better performance amplifier were used.

3.2.2 Operating Characteristics

During each irradiation, the incident neutron flux was monitored by using thin gold foils of 1/8-inch diameter weighing a few milligrams. These foils were calibrated against a set of gold foils irradiated for 212 hours in a flux of 4280 n/cm^2-sec known to an accuracy of $\pm$ 2% at the laboratories of the National Bureau of Standards, Washington, D. C. A typical value for the flux at the front irradiation position was 4.0×10^8 n/cm^2-sec, and 1.5×10^8 n/cm^2-sec at the rear position.

The cadmium ratio for a gold foil at the front irradiation position was measured and found to be 54. The only background line present in all the sample spectra was the 2223.3-keV line of hydrogen coming mainly from the plastic material covering the samples. The other ubiquitous line that appeared in some of the triple coincidence spectra was that at 1533.0 keV, which is the result of detecting an annihilation photon in the central crystal and at the same time satisfying the triple

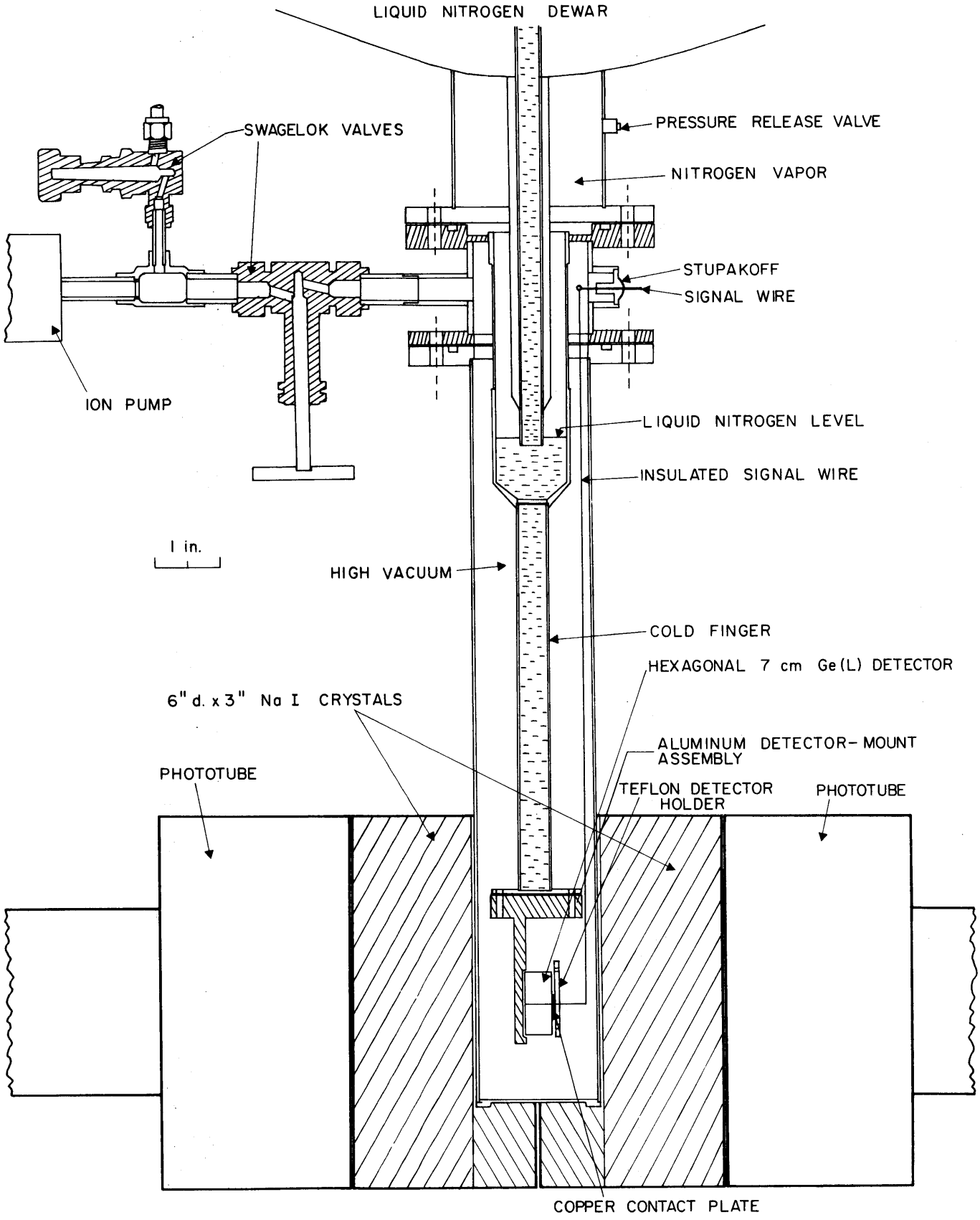

FIG. 3.2 PLAN VIEW OF THE CRYOSTAT FOR THE PAIR SPECTROMETER

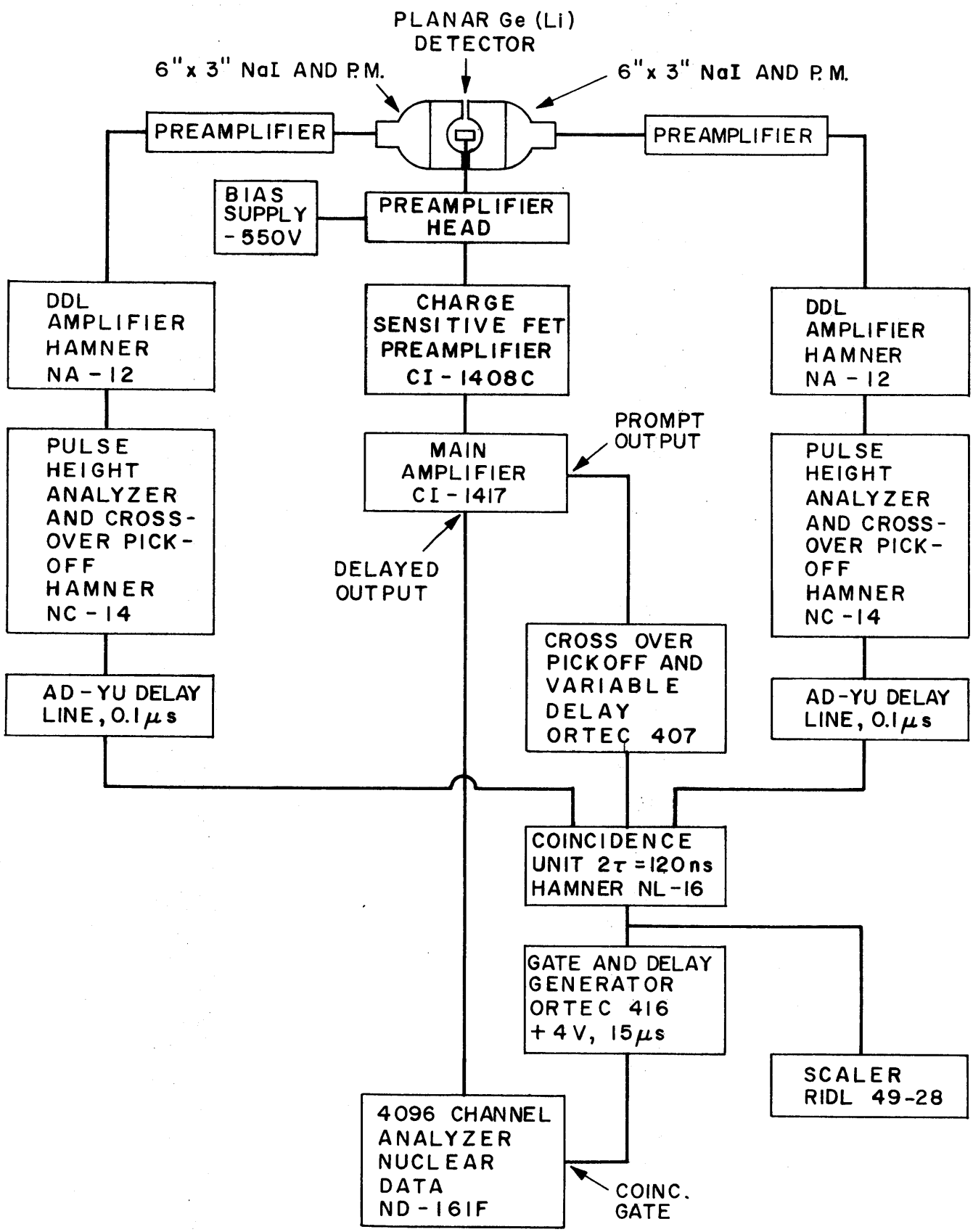

FIG. 3.3 BLOCK DIAGRAM OF ELECTRONICS FOR OPERATION IN THE TRIPLE COINCIDENCE MODE

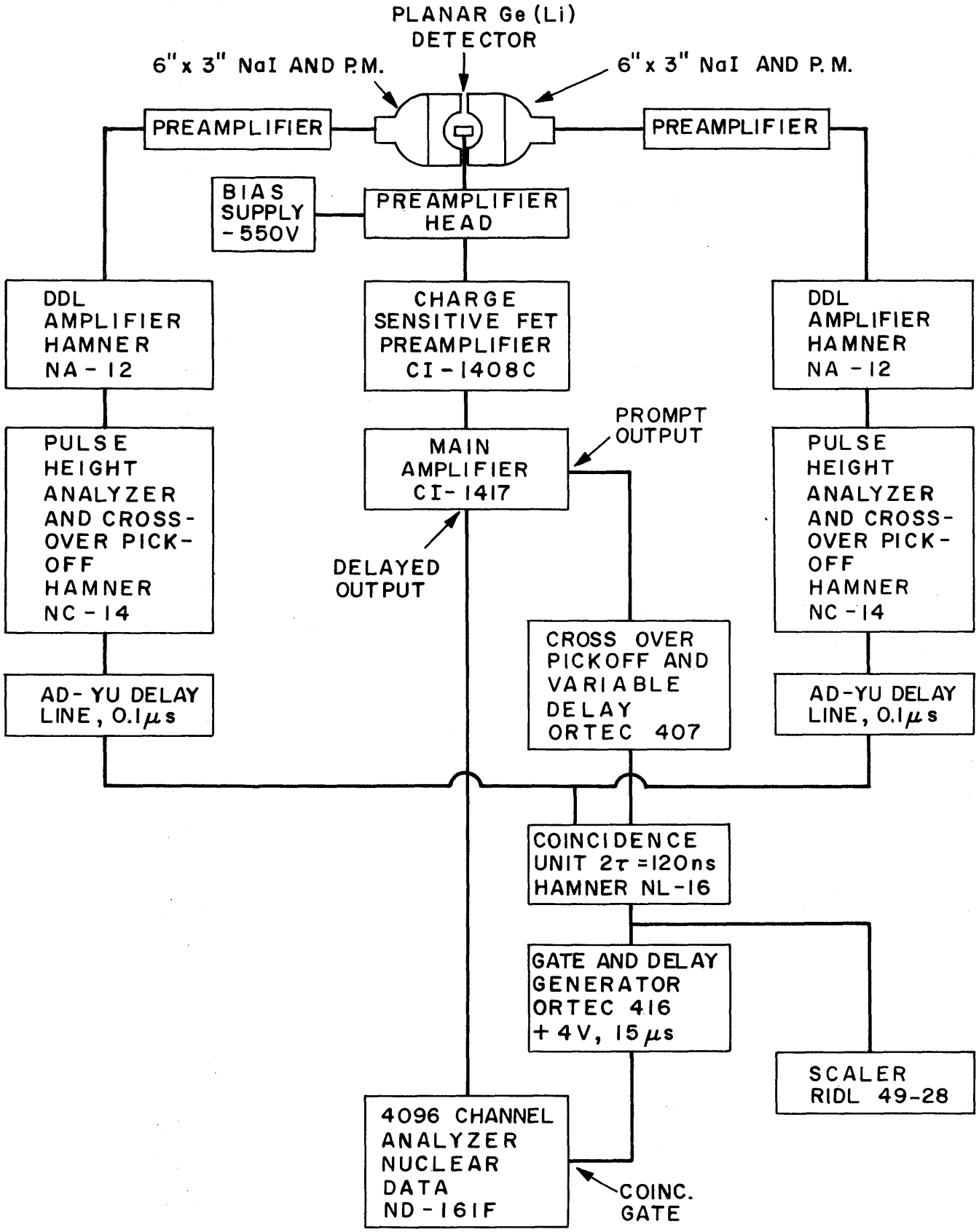

FIG. 3.4 BLOCK DIAGRAM OF ELECTRONICS FOR OPERATION IN THE COMPTON SUPPRESSION MODE

coincidence condition in the NaI detectors by accidental processes. In all the spectra taken in the Compton suppression mode, the annihilation gamma was present together with the 2223.3-keV line of hydrogen and its escape peaks.

The resolution of the system operating in the free mode varied from about 3.7 keV for 300-keV gammas up to about 5.5 keV for 2.5-MeV gammas.

A spectrum for natural iron taken in the triple coincidence mode was used in the determination of the absolute total efficiency of the system. The resolution obtained with this system was at best 2.8 keV for Co^{60} lines and 6.0 keV for 6-MeV capture gammas, for natural iron.

Two efficiency curves were experimentally obtained for the pair spectrometer. One, which includes the effect of 1.6 cm of LiF plate in the gamma beam, was used in the analysis of the samples of U^{238} and Th^{232} and is shown in Fig. 3.5. Another, which includes the effect of 4 inches of borated paraffin plus 1.6 cm of LiF and 1/4 inch of lead, was used in the analysis of the data of U^{235} and plutonium. The linearity of the electronics was checked according to the method used by Orphan (8).

The absolute efficiency curve for the Compton suppression mode of operation (Fig. 3.6) was determined by using the capture gamma rays from the $Co^{59}(n, \gamma) Co^{60}$ reaction which has 15 strong lines of well-known intensity well spread over the energy range from 162 keV to 1.836 MeV. The resolution obtained in the Compton suppression system was about 3.0 keV.

3.3 Nondestructive Assay of Plutonium-Uranium Fuel Rod Using Fission Products

Forsyth and Ronquist (9) have studied the possibility of using the ratio of activities of Ru^{103} (half-life = 9 days) and La^{140} as a measure of the relative fission rate in U^{235} and Pu^{239} based on the difference in the yield of those two fission products for U^{235} fission compared to Pu^{239} fission. Their study suggested the possibility of using short-lived fission products, with half-life of a few hours, for assaying fuel

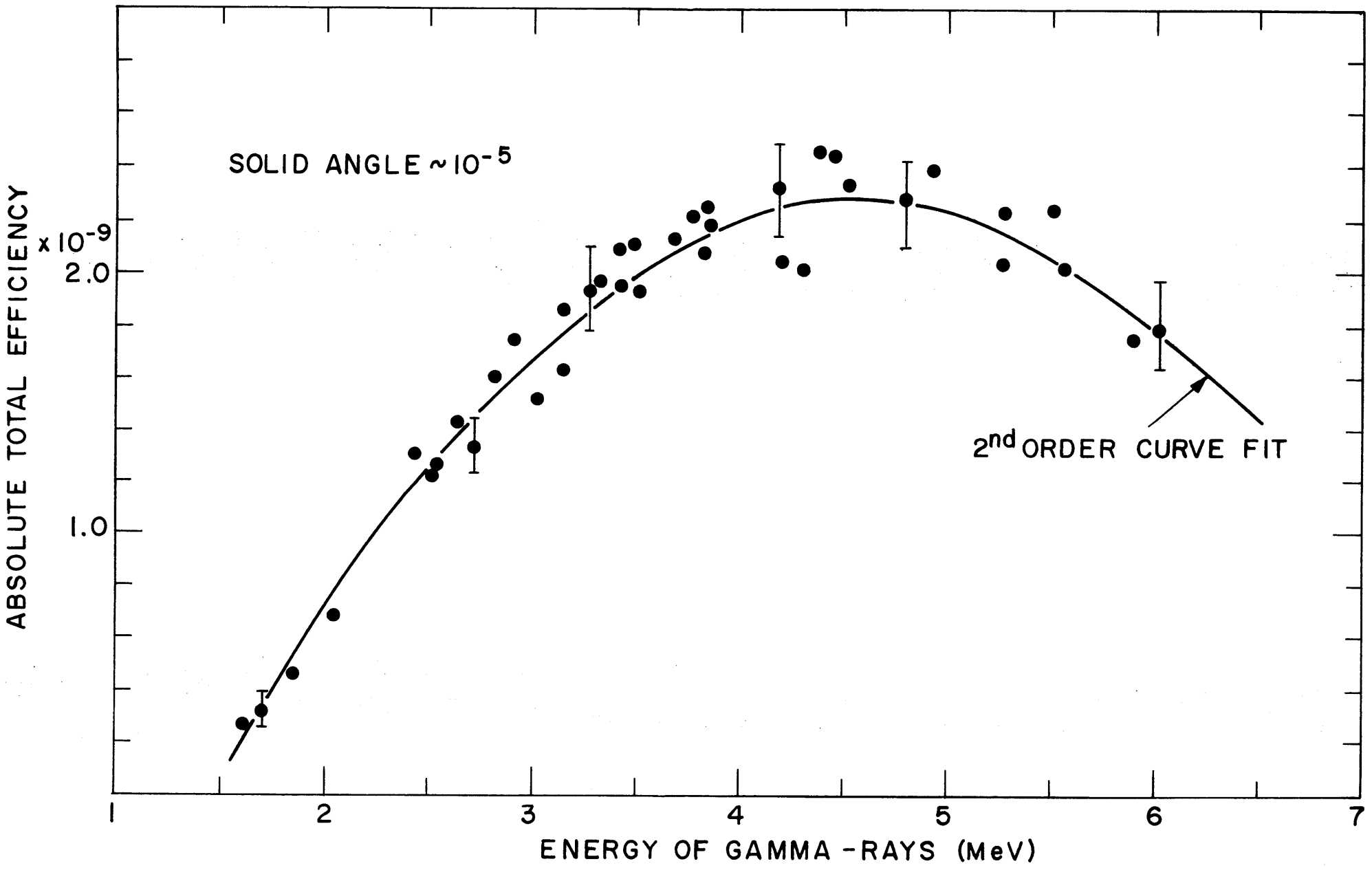

FIG. 3.5 TOTAL EFFICIENCY OF TRIPLE COINCIDENCE MODE WITH LiF PLATE IN THE GAMMA BEAM

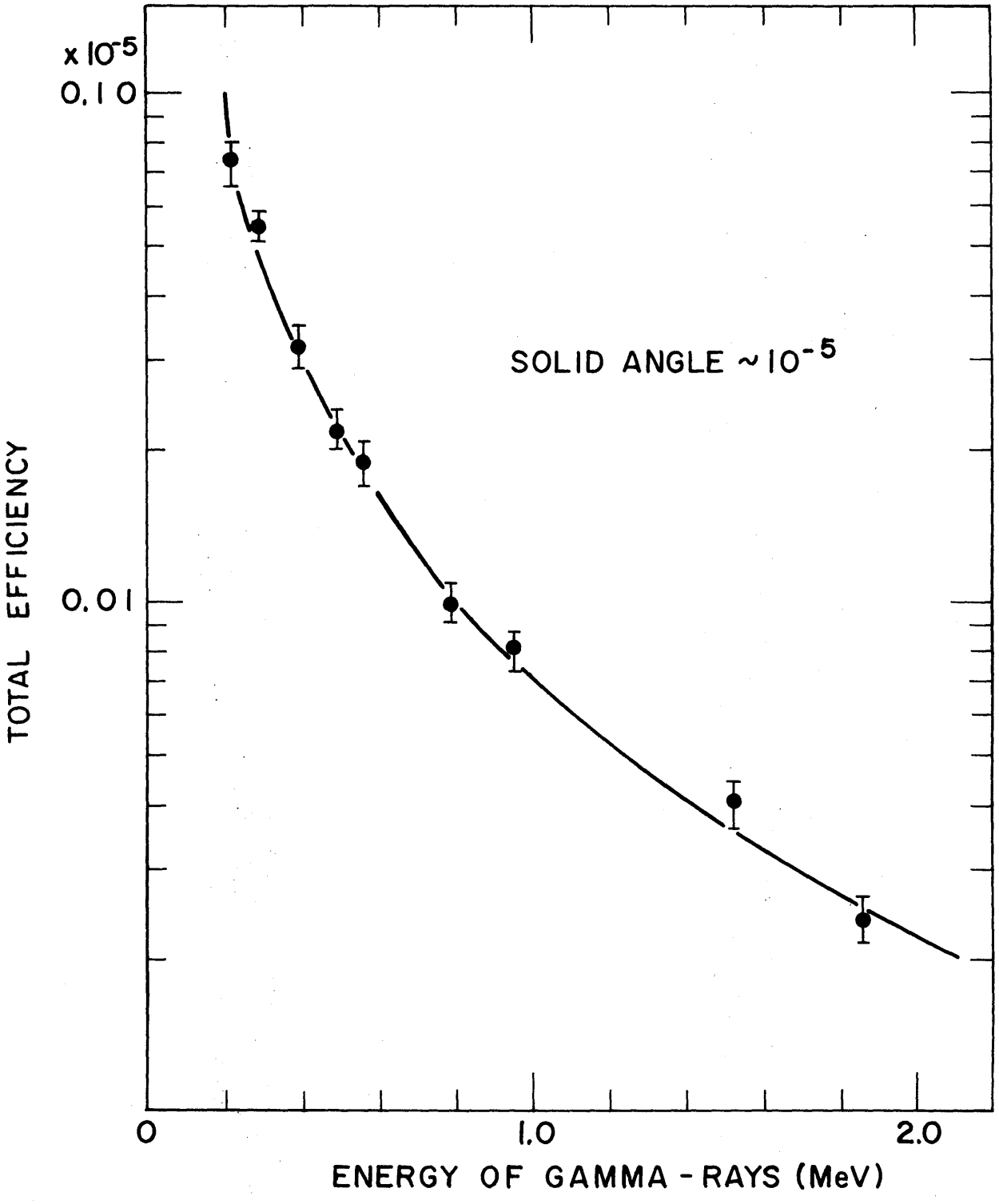

FIG. 3.6 ABSOLUTE TOTAL EFFICIENCY OF COMPTON SUPPRESSION MODE OF OPERATION

of uranium and plutonium oxide with total enrichment not very different from the calibrating rod but with the composition of U^{235} and Pu^{239} unknown. Assume, for simplicity, that both rods are made up of pellets of the same size.

Suppose two prominent peaks can be selected from the spectrum of the fission product decay gamma rays coming from two distinct short-lived fission products (numbers 1 and 2) present in the spectrum of both fuel rods.

The activity of one of the fission products, as given by the area of the gamma lines for the standard rod, is expressed in the form of Eq. 3.1 by the relation:

$$A^{1s} = N_5^s \sigma_5 \phi^s F_5^1 \epsilon^1 , \tag{3.2}$$

where the superscript 1 indicates fission product number 1, s denotes standard, and the subscript 5 represents U^{235}. The detector efficiency for the energy of peak number 1 is given by ϵ^1.

The activity of the same fission product in the unknown rod, using the same gamma ray, is expressed by the equation,

$$A^{1x} = N_5^x \sigma_5 \phi^x F_5^1 \epsilon^1 + N_9^x \sigma_9 \phi^x F_9^1 \epsilon^1 , \tag{3.3}$$

where the superscript x denotes the unknown rod containing U^{235} and Pu^{239}, and the subscript 9 represents Pu^{239}. The function F_9^1 differs from F_5^1 because, although the decay constants, irradiation time and decay time are the same for both U^{235} and Pu^{239} composing the same fuel rod, the yields of the fission product under consideration and its precursors are different.

Dividing Eq. 3.3 by Eq. 3.2 and noticing that both rods were irradiated and cooled for the same period of time,

$$\frac{A^{1x}}{A^{1s}} = \frac{N_5^x}{N_5^s} \frac{\phi^x}{\phi^s} + \frac{N_9^x}{N_5^s} \frac{\phi^x}{\phi^s} \frac{\sigma_9 F_9^1}{\sigma_5 F_5^1} . \tag{3.4}$$

For fission product number 2, we have a similar relation:

$$\frac{A^{2x}}{A^{2s}} = \frac{N_5^x}{N_5^s} \frac{\phi^x}{\phi^s} + \frac{N_9^x}{N_5^s} \frac{\phi^x}{\phi^s} \frac{\sigma_9 F_9^2}{\sigma_5 F_5^2} . \tag{3.5}$$

rods containing a mixture of uranium and plutonium. The method investigated in the present work uses a pair of fission products (Sr^{92} and I^{135}), one of which has a higher yield for Pu^{239} fission than for U^{235} fission and the other a lower yield. It required the use of a standard rod containing only uranium and a set of two calibrating foils, one containing only U^{235} and the other only Pu^{239}, as fissile elements.

3.3.1 Theory

A typical chain of short-lived fission products that is visible in the gamma spectrum of an irradiated fissile material (15 hours irradiation) is presented by the mass chain 92 that leads to stable Zr^{92}:

$$3.0\,\text{sec}\ Kr^{92} \rightarrow 5.3\,\text{sec}\ Rb^{92} \rightarrow 2.7\,\text{hr}\ Sr^{92} \rightarrow 3.6\,\text{hr}\ Y^{92} \rightarrow \text{stable}\ Zr^{92}.$$

Each of the components, besides being genetically related, is produced directly by fission. The decay of the activity of each component of this chain can be given in the following form:

$$A = N\sigma\phi F\ , \tag{3.1}$$

where

N = number of atoms of fissile element under irradiation,

σ = fission cross section,

ϕ = neutron flux,

F = a function of the yield and decay constants of the fission product under consideration and its precursors, the irradiation time and the decay time.

Suppose two fuel rods have been irradiated for the same period of time with the same geometry of irradiation and then, after equal cooling time, counted over the same period of time with the identical geometrical arrangement of fuel rods, collimators and detector. Suppose one of the fuel rods contains uranium oxide enriched in U^{235} as its only fissile element in a well-known quantity and it can therefore serve as the standard rod. Another fuel rod contains a mixture

Now, from the experiment, the ratios A^x/A^s are given by the ratio of the areas under the peaks for the standard and the unknown rod spectra. The ratio of the neutron flux, ϕ^x/ϕ^s, is given by the flux monitor foils. Thus, Eqs. 3.4 and 3.5 are two equations with four unknowns for which two of the unknowns are the ratios $R_1 = \sigma_9 F_9^1/\sigma_5 F_5^1$ and $R_2 = \sigma_9 F_9^2/\sigma_5 F_5^2$, which can be obtained by an independent experiment. These ratios are obtained by using two calibrating foils, one containing only plutonium and the other containing only uranium, which are irradiated, cooled and counted for the same amounts of time as the unknown and standard rods. Thus, by solving the above set of equations, the following equations are obtained:

$$\frac{N_9^x}{N_5^s} = \frac{\phi^s}{\phi^x} \frac{\dfrac{A^{1x}}{A^{1s}} - \dfrac{A^{2x}}{A^{2s}}}{R_1 - R_2}, \tag{3.6}$$

$$\frac{N_5^x}{N_5^s} = \frac{\phi^s}{\phi^x} \frac{R_1 \dfrac{A^{2x}}{A^{2s}} - R_2 \dfrac{A^{1x}}{A^{1s}}}{R_1 - R_2}. \tag{3.7}$$

Once these ratios are known, the enrichment in weight percent due to fissile plutonium and uranium can be calculated, assuming as known the enrichment of the standard rod and the densities of both unknown and standard rods.

3.3.2 Experimental Procedure and Results

The calibrating foils used for determining the ratios R_1 and R_2 were:

(a) metallic uranium foil 0.0052 inch thick, with 0.2259 g/cm^2 of U^{235} in the 93.2% enriched foil, encased in a 3-inch-diameter, aluminum leakproof cladding, 0.015 inch thick;

(b) metallic foil of plutonium, 91% Pu^{239}, 8% Pu^{240}, and 1% Pu^{241}, alloyed with 1% aluminum, with fissile foil density of 0.274 g/cm^2 and thickness of 0.006 inch, clad in aluminum 0.020 inch thick.

The uniformity of distribution of fissile material in the foils was checked by a monochromatic neutron transmission experiment. Both these foils were irradiated and counted in exactly the same geometry.

The standard rod was made up of 1.30% enriched uranium oxide pellets of 0.500-inch diameter. The "unknown" rod was a simulated burned fuel from the USAEC-AECL Cooperative Program (10). In fact, two rods of slightly different composition were used. Both were composed of uranium-plutonium oxide pellets of average density (10.41 g/cm^3) and the same dimensions as those of the standard rod. Their compositions are shown in Table 3.1. All the rods and the foils were irradiated for 15 hours, cooled for 130 minutes, and thereafter counted for 160 minutes livetime.

TABLE 3.1

Isotopic Composition of the Pu-Containing Fuel Rods

Fuel Type	Isotopic Weight Percent of Total Uranium and Plutonium				
	U-235	Pu-239	Pu-240	Pu-241	Pu-242
A-Red*	0.30	0.24	0.062	0.009	0.001
B-Gold*	0.30	0.25	0.016	0.002	0.001

*The colors, red and gold, refer to the paint on top of each rod for identification purposes.

The ratios of the areas under the peaks, as given in Eqs. 3.6 and 3.7, had to be corrected due to two principal effects: (1) the dead time of the electronics which was higher for the standard rod containing more fissile material than for the unknown rods (the dead time also varies with time); (2) the difference in the neutron flux inside the rods due to different attenuation.

These corrections were studied extensively and programmed into the computer code FUEL ASSAY which was written to perform the calculation of enrichment.

I^{135} and Sr^{92} were chosen as the pair of fission products involved in the ratios given by Eqs. 3.6 and 3.7. Figure 3.7 illustrates the difference in the observable gamma yield of the peaks of Sr relative to

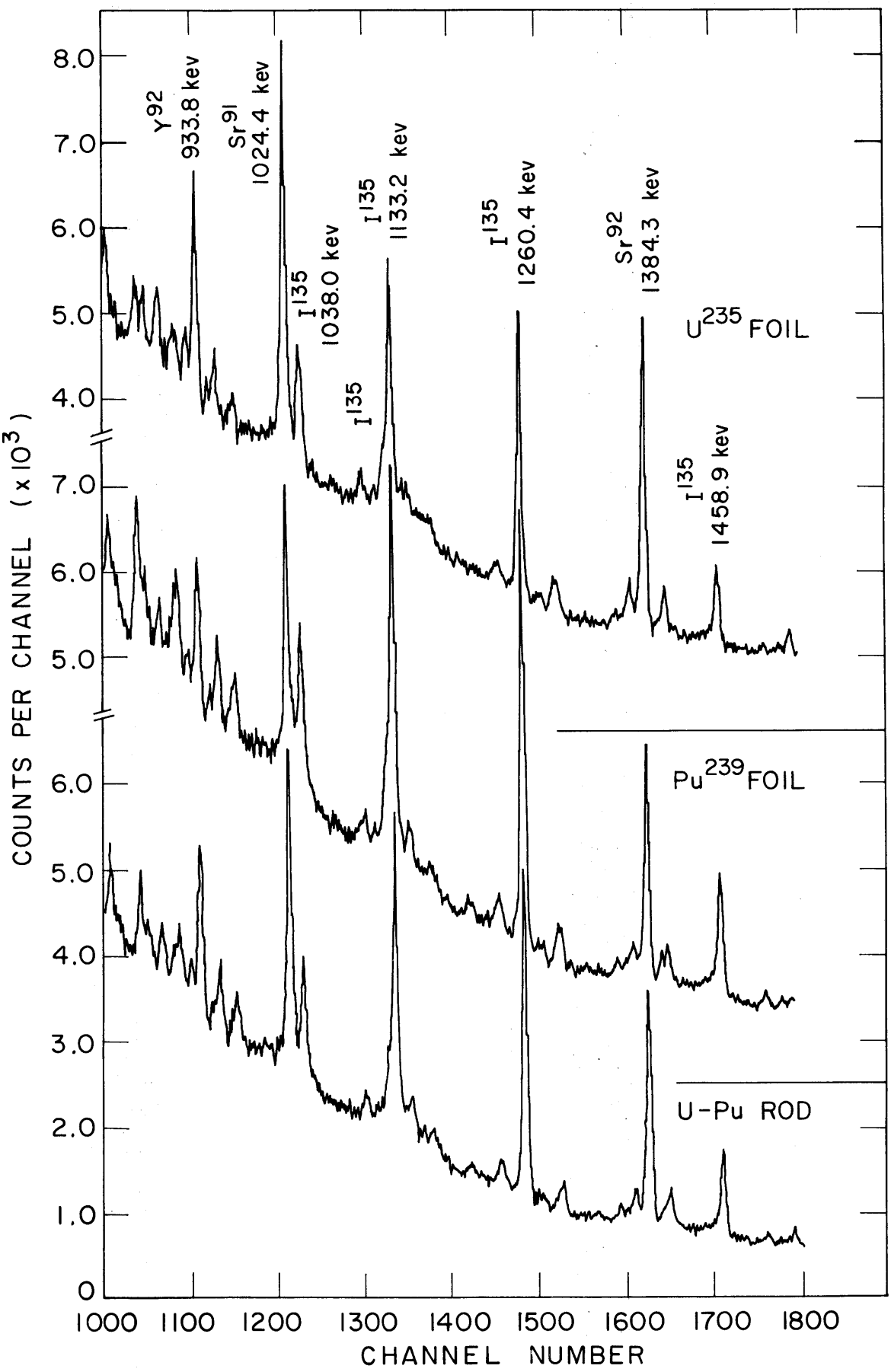

FIG. 3.7 DETAIL OF THE SPECTRA OF FISSION PRODUCTS FOR THE U-FOIL, Pu-FOIL AND MIXED ROD B-GOLD

the I peaks. Table 3.2 gives the final results of the analysis of mixed rods, Types B-Gold and A-Red.

TABLE 3.2

Final Results for the Analysis of Mixed Rods

Measured Values	B-Gold Fuel	A-Red Fuel
N_9^x/N_5^s *	0.193 ± 0.015	0.178 ± 0.017
N_5^x/N_5^s	0.254 ± 0.016	0.270 ± 0.027
E_9^x **	0.249 ± 0.019	0.230 ± 0.022
E_5^x	0.322 ± 0.016	0.343 ± 0.034

Fabricator Data	B-Gold Fuel	A-Red Fuel
E_9^x ***	0.252	0.249
E_5^x	0.30	0.30

*Ratio of the number of atoms between the unknown and the standard rods.

**Pu weight percent enrichment.

***Weight percent enrichment of $Pu^{239} + Pu^{241}$.

It was concluded that, with the present method, it is possible to determine the U^{235} and Pu^{239} content in a mixed rod with an accuracy ranging from ± 5% to ± 10%. The main source of error is the statistical error from the counting of the gammas. The accuracy of the method could be increased by using a pair of fission products with a more dramatic yield difference, such as Ru^{103} and La^{140}, but in this case a cooling time of a few days would be necessary as well as a long irradiation time. With the present method an analysis can be performed in one day's work.

3.4 The Capture Gammas for U^{238} and Th^{232}

For U^{238} the sample consisted of small metal sheet scraps of depleted uranium with 170 ppm of U^{235} contamination. The sample weighed 45.237 grams and it was tightly sealed in a cylindrical polyethylene vial, 2 inches long and 1 inch in diameter. To insure that no contribution from fission gammas was present in the spectra, an additional sample of 19 grams of depleted uranium having only 18 ppm of U^{235} was also irradiated and the spectral results were compared. No significant differences were noticed.

For Th^{232} the sample consisted of thorium oxide powder of 99.8% purity, weighing 115.36 grams and contained in a polyethylene vial similar to that for U^{238}.

All the samples were irradiated in the sample holder in exactly the same position. The plan view of the geometry for irradiation and counting is shown in Fig. 3.8. The irradiation time for each sample was between 20 and 25 hours for the triple coincidence mode of operation for studying high energy gammas (above 1.5 MeV) and 3 hours for the Compton suppression mode for studying low energy gammas (130 keV to 2.5 MeV).

The energies and intensities of the gammas were determined. The results are shown in Tables 3.3 and 3.4. Some of the spectra are shown in Figs. 3.9 and 3.10. The data were analyzed by the computer code GAMANL.

3.5 The Prompt Gammas from U^{235} and Pu^{239}

The spectrum of gamma rays that comes from the absorption of thermal neutrons by the fissile nuclei U^{235} and Pu^{239} has contributions from the following three processes:

(a) the prompt gamma rays from the thermal neutron capture process ($U^{235}(n, \gamma)U^{236}$),

(b) the prompt fission gamma rays,

(c) the delayed gamma rays emitted by the decay of the fission fragments of earlier fissions in the sample.

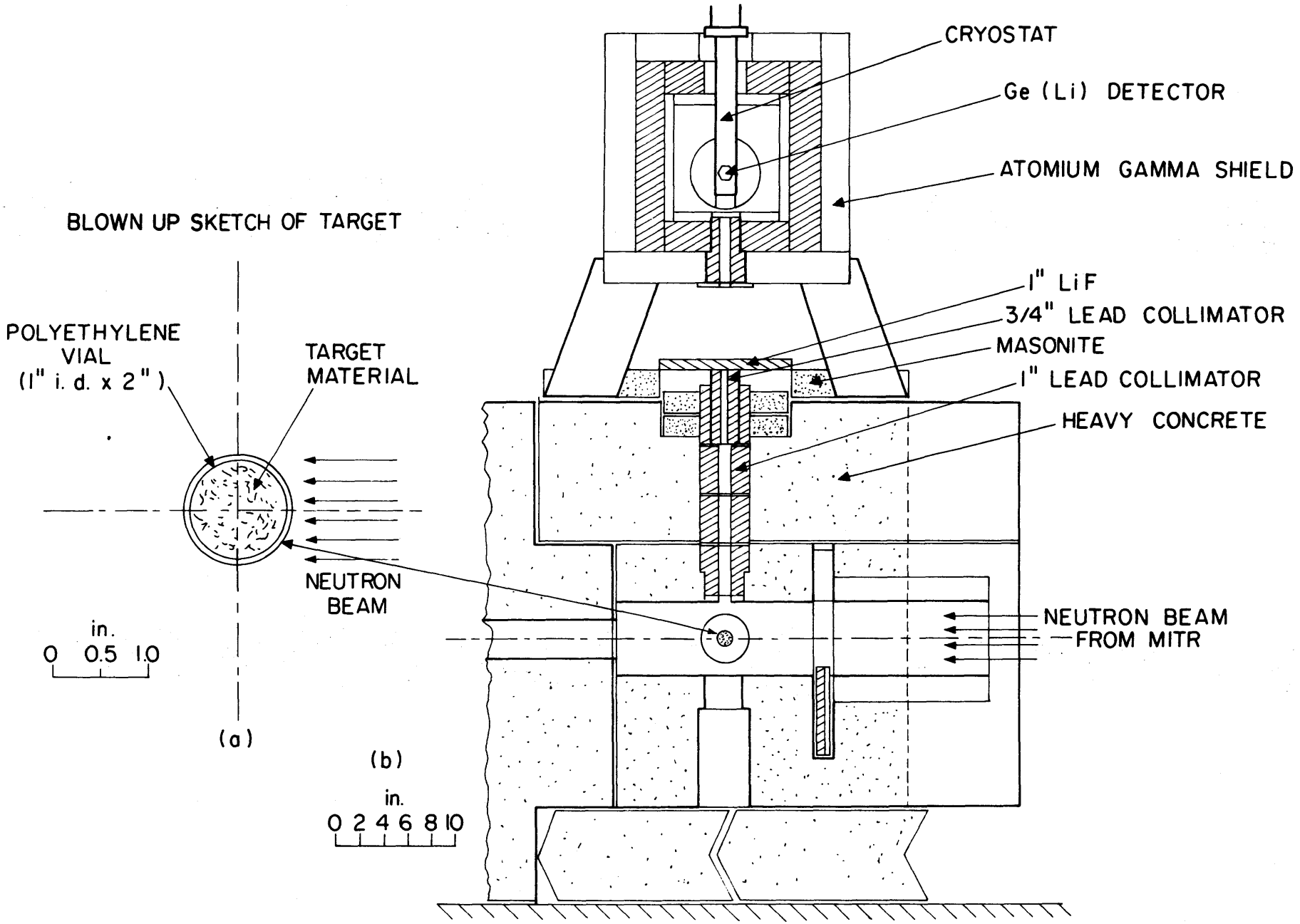

FIG. 3.8 GEOMETRY FOR IRRADIATION AND COUNTING SAMPLES OF U^{238} AND Th^{232}

TABLE 3.3

The Energy and Intensity of the Capture Gamma Rays for U^{238}

Line No.	This Work		Maier (2)		Sheline et al. (1)	
	Energy* (keV)	Intensity** (No./100 captures)	Energy (keV)	Intensity (No./100 captures)	Energy (keV)	Intensity (No./100 captures)
1	133.6		133.799	2.3		
2	251	3.2	250.08	2.8		
			341.65	2.6		
3	497.6	0.6			498	0.7
4	521.6	1.67	522.00	2.6	522	2.8
			536.2	1.8	537	4.3
5	539.3	2.31	540.7	3.5	542	1.9
6	552.5	6.54	552.8	6.5	552	10.5
7	562.4	1.10	562.8	0.5	561	1.3
8	580.7	1.40	581.3	1.4	580	2.4
9	592.9	1.82	592.9	2.0	592.4	4.8
			603.9	2.2	601	2.0
					609	1.2
10	611.6	2.73	612.0	3.0	612	8.0
11	628.7	0.5	629.7	1.6	629	2.3
12	637.6	0.4			638	1.8
					658	0.6
			669.7	1.5		
13	683.7	1.19			683	1.1
			687.5	1.5	690	2.4
					698	0.9
					713	0.7
					722	0.7
					750	0.7
					770	0.6
			780	1.5		
					788	0.8
					797	0.7

*The standard deviation for energy determination is ± 1 keV.
**The accuracy for the intensity was estimated as ± 15% for the lines for which the intensity is higher than 1.00 photons/100 captures and better than ± 30% for the others.

TABLE 3.3 (continued)

Line No.	This Work		Sheline et al. (1)	
	Energy* (keV)	Intensity** (No./100 captures)	Energy (keV)	Intensity (No./100 captures)
14	2959.7	0.85		
15	3000.4	0.90		
16	3114.6	0.95		
			3186	0.24
17	3197.4	0.98	3201	0.22
			3208	0.65
18	3220.1	0.98		
			3229	0.63
19	3233.4	0.45		
			3242	0.38
20	3295.6	0.35	3293	0.20
			3304	0.48
21	3311.5	0.35		
			3318	0.45
			3406	0.20
			3446	0.41
			3532	0.14
			3540	0.23
22	3565.2	0.32	3567	0.22
23	3583.0	3.04	3584	2.5
24	3612.6	1.20	3612	0.84
25	3641.1	0.93	3639	0.68
			3653	0.63
26	3729.0	0.85		
27	3739.6	0.30	3739	0.23
			3818	0.12
28	3844.6	0.50	3843	0.56
			3873	0.13

TABLE 3.3 (concluded)

Line No.	This Work		Sheline et al. (1)	
	Energy (keV)	Intensity (No./100 captures)	Energy (keV)	Intensity (No./100 captures)
29	3982.3	1.87	3982	1.5
30	3991.0	1.81	3991	1.5
			4052	0.5
31	4059.7	12.1	4059.4	11.0
32	4090.2	0.15	4090	0.22
33	4105.2	0.20	4117	0.08
34	4610.2	0.25	4610	0.21
35	4659.8	0.37	4659	0.22

TABLE 3.4

The Energy and Intensity of the Capture Gamma Rays for Th^{232}

Line No.	This Work		Burgov et al. (4)	
	Energy* (keV)	Intensity** (No./100 captures)	Energy (MeV)	Intensity (No./100 captures)
1	264.2	0.11		
2	319.2	0.21		
3	326.0	0.12		
4	336.6	0.25		
5	472.5	0.72		
6	522.6	0.39		
7	540.0	0.32		
8	566.6	0.99		
9	577.9	0.33 (semiresolved doublet)		
10	584.7			
11	626.6	0.18		
12	665.3	0.26		
13	681.3	0.22		
14	2127.8	(unresolved triplet)		
15	2294.9	0.38		
16	2314.9	0.26		
17	2334.9	0.25		
18	2447.0	0.33		
19	2503.9	0.13		
20	2525.6	0.24		
21	2544.8	0.29 (semi-resolved doublet)	2.60(5)	5.6
22	2702.8	0.23		
23	2712.9	0.21		

*The standard deviation for energy determination is ± 1 keV.

**The accuracy for the intensity was estimated as ± 20% for the lines for which the intensity is higher than 0.50 photons/100 captures and better than ± 35% for the others.

TABLE 3.4 (continued)

Line No.	This Work		Groshev et al. (3)		Burgov et al. (4)	
	Energy (keV)	Intensity (No./100 captures)	Energy (MeV)	Intensity (No./100 captures)	Energy (MeV)	Intensity (No./100 captures)
24	2719.1	0.21			2.76(5)	4.2
25	2823.3	0.25				
26	2861.0	0.36				
27	3005.0	0.12				
28	3027.9	0.15				
29	3129.8	0.12				
30	3147.4	0.33			3.15(5)	1.6
31	3175.4	0.17				
32	3186.3	0.18				
33	3197.0	0.33				
34	3227.4	0.13				
35	3230.9	0.15				
36	3288.5	0.19				
37	3326.3	0.15				
38	3342.0	0.27				
39	3372.1	0.08				
40	3376.8	0.17				
41	3396.5	0.26				
42	3436.2	0.29				
43	3447.7	0.23	3.45(3)	0.6		
44	3461.5	0.07				
45	3473.5	0.71				
46	3508.7	0.22				
47	3527.3	0.31	3.53(2)	1.1	3.55(5)	3.4
48	3590.3	0.08				
49	3603.0	0.17				
50	3615.7	0.05				

TABLE 3.4 (concluded)

	This Work		Groshev et al. (3)		Burgov et al. (4)	
Line No.	Energy (keV)	Intensity (No./100 captures)	Energy (MeV)	Intensity (No./100 captures)	Energy (MeV)	Intensity (No./100 captures)
51	3633.6	0.08				
52	3682.5	0.09				
53	3725.1	0.11			3.71(5)	0.4
54	3740.2	0.12				
55	3752.9	0.12	3.75(3)	0.4		
56	3801.8	0.09				
57	3860.6	0.10				
58	3946.3	0.33	3.94(3)	0.5		
59	3959.0	0.05				
60	4004.5	0.14				
61	4072.6	0.12				
62	4201.5	0.14				
63	4244.7	0.13	4.25(3)	0.3		
64	4448.0	0.06				
65	4486.2	0.03				
66	4749.3	0.05				
			4.92(3)	0.3		
					5.11	0.2

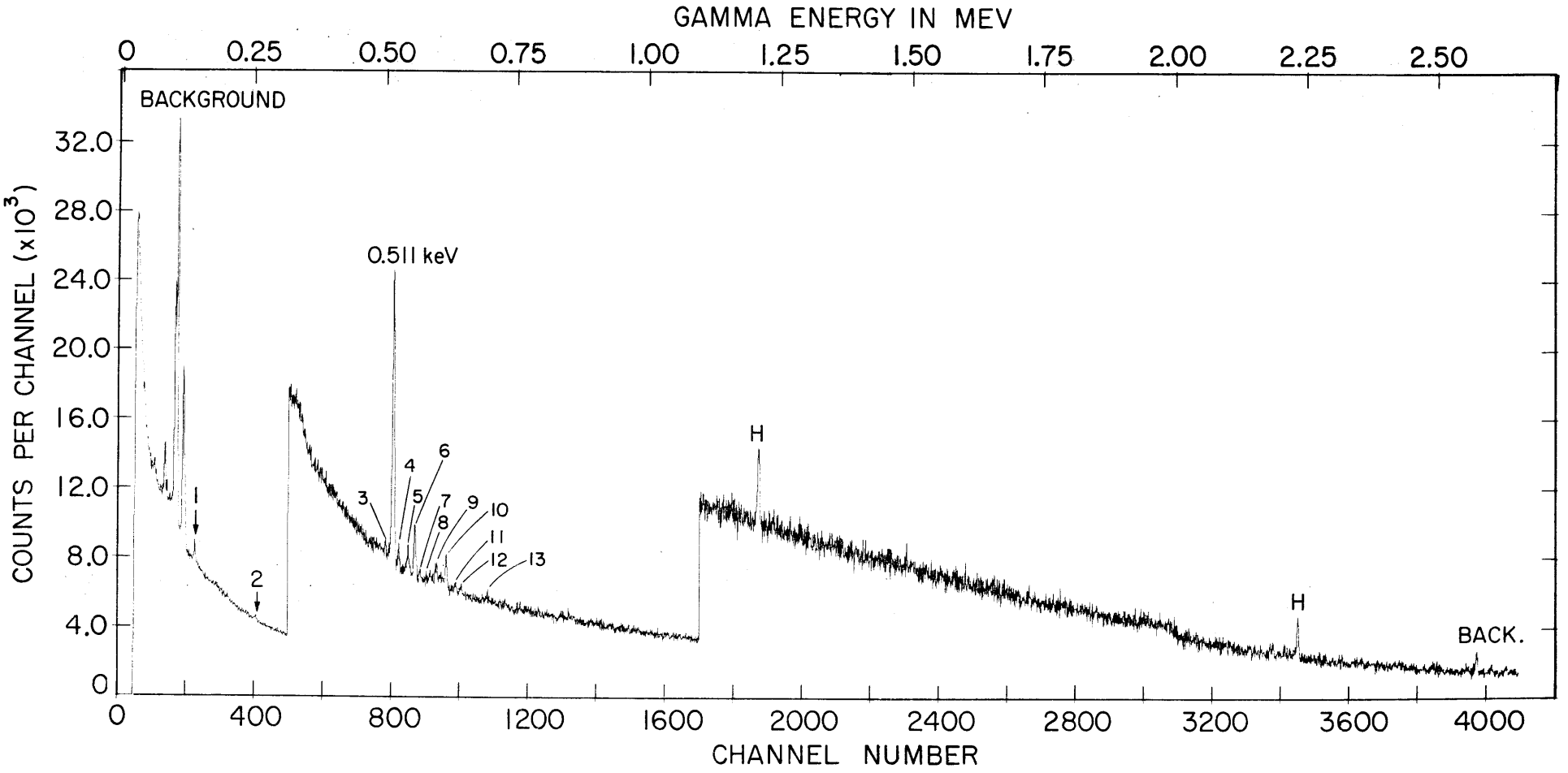

FIG. 3.9 THE LOW ENERGY CAPTURE GAMMA-RAYS FOR U^{238} TAKEN IN COMPTON SUPPRESSION MODE

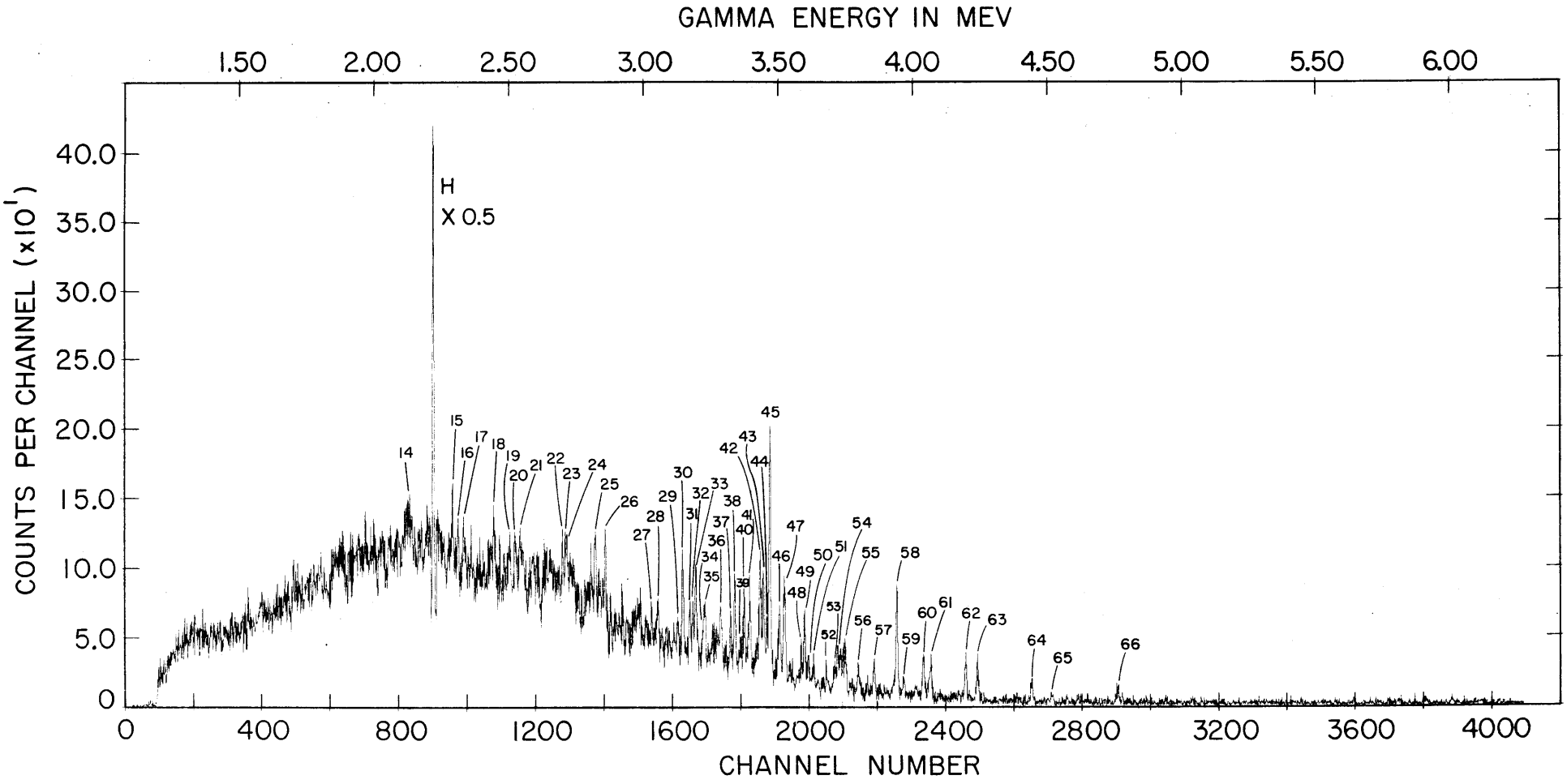

FIG. 3.10 THE HIGH ENERGY CAPTURE GAMMA-RAYS FOR Th^{232} TAKEN IN TRIPLE COINCIDENCE MODE

The fission process is the predominant reaction, with 85.1% compared to 14.9% of captures for U^{235} and 73% compared to 27% of captures for Pu^{239}. Studies done by Maienschein (11) indicate that from every fission of U^{235} about 7.4 photons are emitted promptly in the energy range from 0.3 MeV to 10 MeV. The total energy emitted is (7.2 ± 0.8) MeV/fission. Comparison of these data with the intensity of the capture gamma rays, which generally are less than a few percent per capture, indicates that the prompt fission gammas are expected to be overwhelmingly predominant over the capture gamma rays.

The samples of uranium and plutonium were the same as described previously in the method of assaying fuel rods using delayed gammas.

A plan view of the geometry for irradiation is shown in Fig. 3.11. It proved necessary to insert a fast neutron scatterer in the gamma beam: 4-inches-thick borated paraffin with 5% boron in weight. A preliminary experiment to determine the fraction of fission neutrons attenuated as a function of the thickness of borated paraffin was performed, and for a 4-inch thickness only 12% of the unscattered beam is transmitted, while only about 50% of the gammas are attenuated.

The prompt spectra taken in the Compton suppression mode did not yield any significant peaks other than those of the background due to Ge and Fe. Thus, only the data taken in the triple coincidence mode were considered.

Figures 3.12 and 3.13 show the plots of the spectrum for uranium and plutonium, respectively. Table 3.5 shows the results of the data analysis.

3.6 The Assay of Fuel Rods Using Prompt Gamma Rays

An extensive evaluation of the potential of neutron capture gamma rays in elemental analysis using germanium detectors has been published recently by Hamawi (12).

In this section the use of prompt fission gammas, together with capture gamma rays, for the analysis of fuel rods is described. Also, measurement of the fission neutron yield as detected through the Ge^{72} inelastic scattering conversion electrons is shown to be a powerful means to analyze uranium fuel rods.

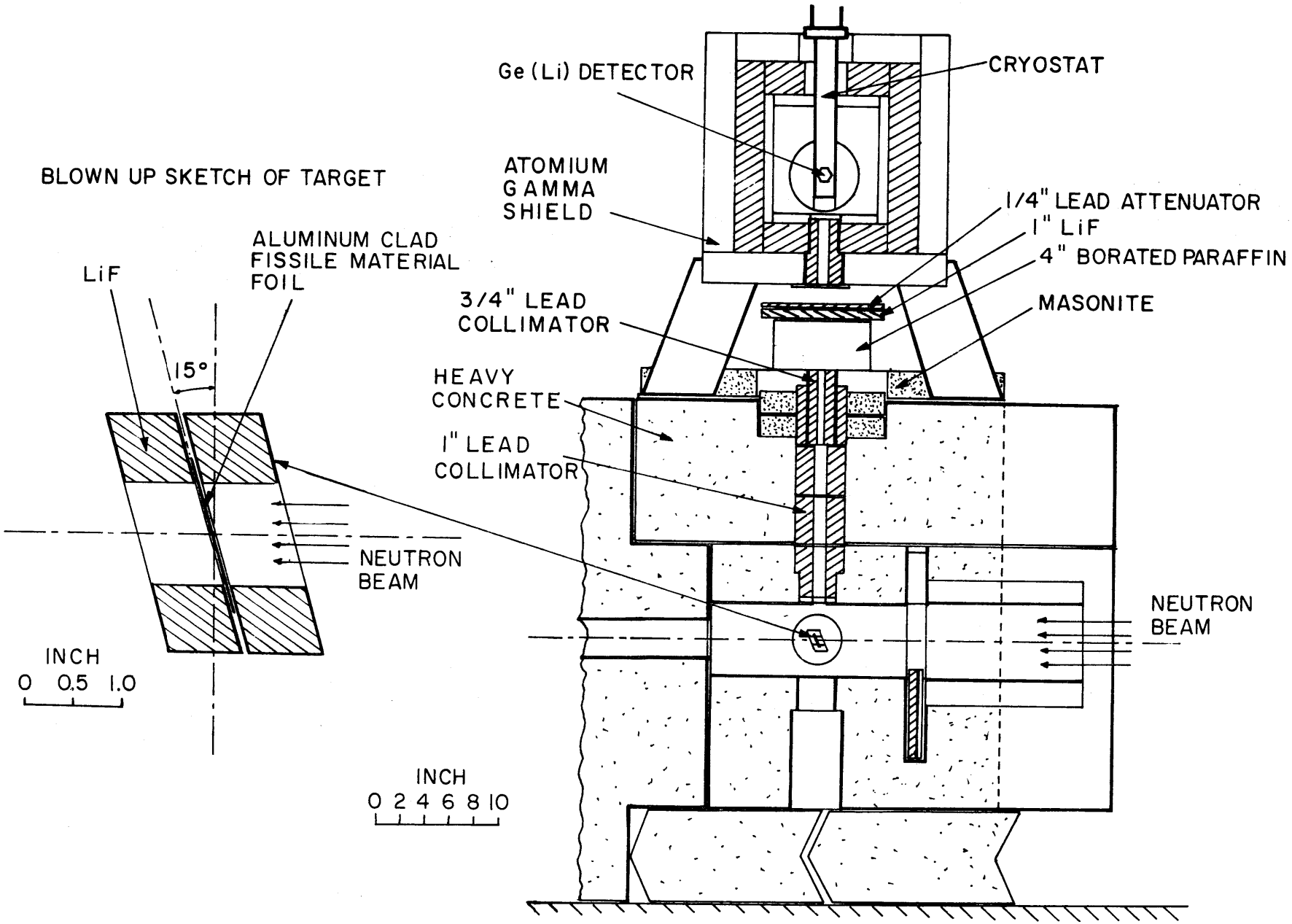

FIG. 3.11 GEOMETRY FOR IRRADIATION AND COUNTING SAMPLES OF U^{235} AND Pu^{239}

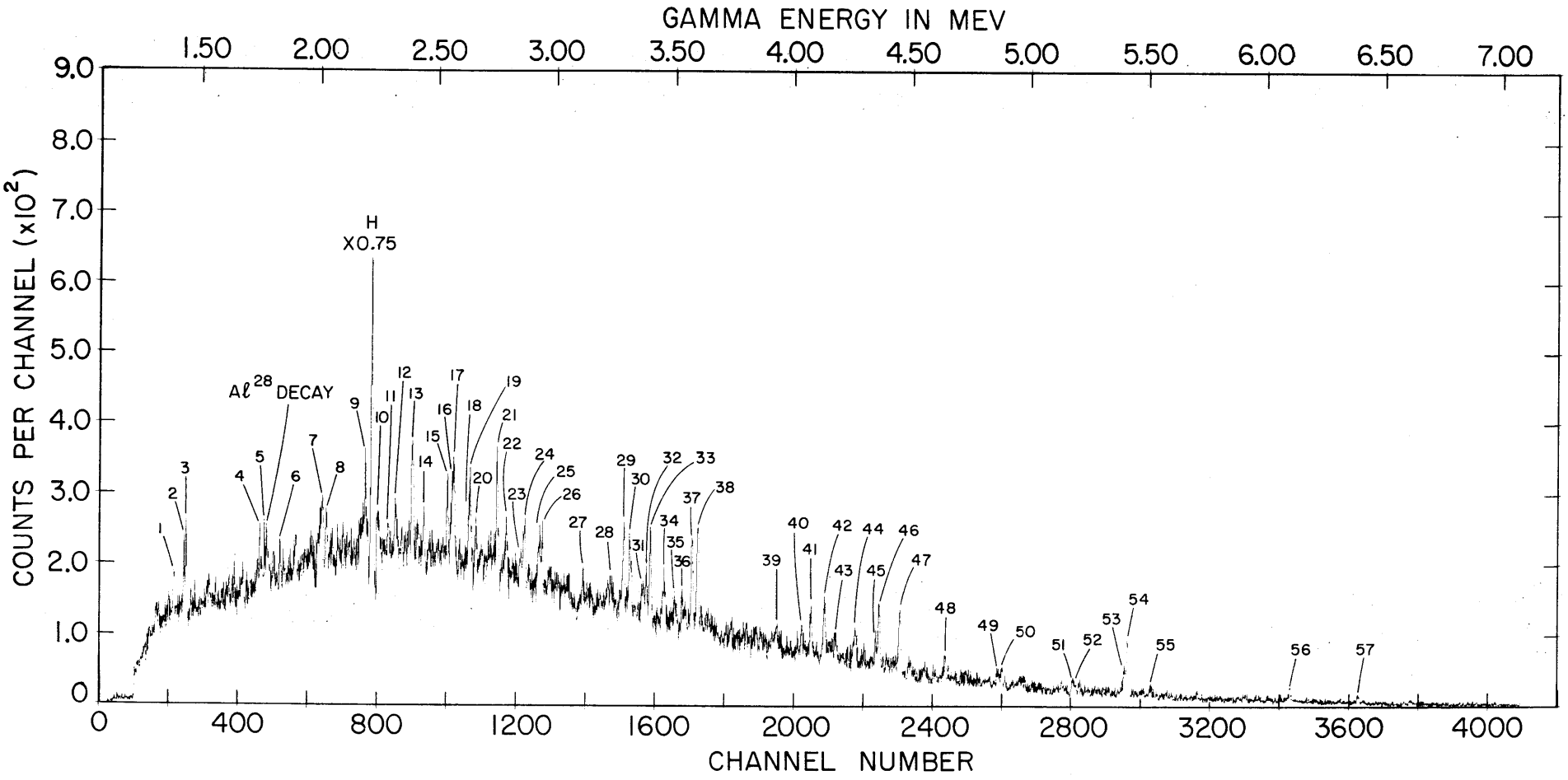

FIG. 3.12 THE PROMPT GAMMA-RAYS FOR U^{235} TAKEN IN TRIPLE COINCIDENCE MODE

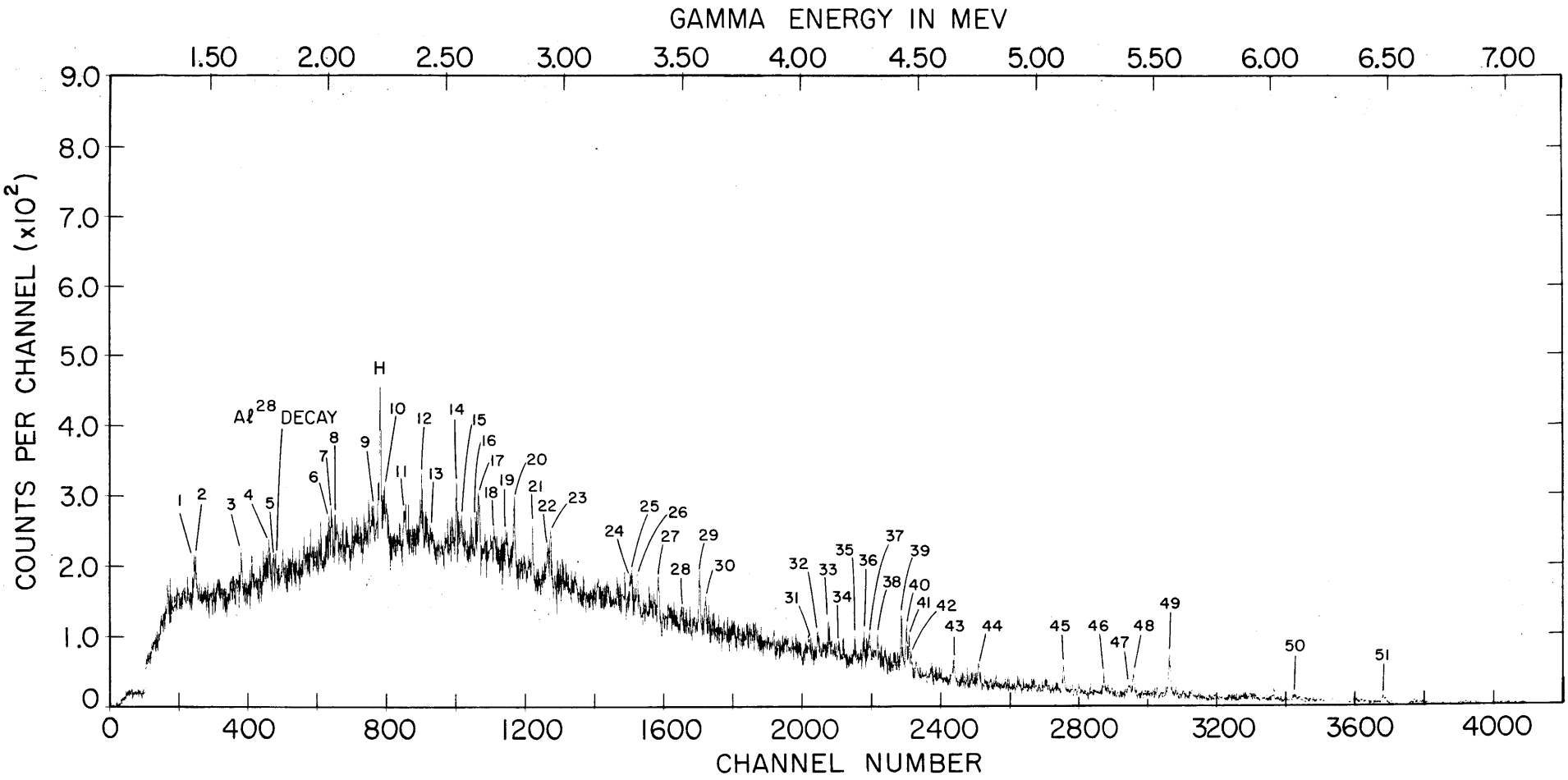

FIG. 3.13 THE PROMPT GAMMA-RAYS FOR PLUTONIUM TAKEN IN TRIPLE COINCIDENCE MODE

TABLE 3.5

The Energy and Intensity of Prompt Gamma Rays for U^{235} and Plutonium

U^{235}			Plutonium		
Line No.	Energy* (keV)	Intensity** (No./100 fissions)	Energy* (keV)	Intensity** (No./100 fissions)	Line No.
1	1383.9	–	inconclusive		
2	1427.7	–	1428.8		1
3	1435.4	–	1435.2		2
	inconclusive		1632.1		3
4	1750.9	1.80	1750.0	1.20	4
5	1769.2	1.46	1767.7	0.86	5
6	1835.1	1.57	inconclusive		
7		unresolved	2006.4	0.52	6
8	2016.0	1.34	2015.5	0.72	7
9	2032.2	1.15	2031.4	0.66	8
10	2196.3	1.15		unresolved	9
11	2252.4	0.33		unresolved	10
12	2294.1	0.29	definite no		
13	2322.6	0.52	2321.9	0.51	11
14	2394.3	1.63	2395.5	0.66	12
15	2443.1	0.70	2443.0	unresolved	13
16	2544.1	1.00	2544.3	0.61	14
17	2565.2	0.59	2565.2	0.20	15
18	2568.4	0.81	inconclusive		
19	2634.9	0.52	unresolved		16
20	2638.6	1.03	2638.0	0.62	17
21	2662.7	0.40		unresolved	18

*The standard deviation for energy determination is ± 1 keV.

**The accuracy for intensity determination is better than ± 30%. The live numbers correspond to the numbers shown in Figs. 3.12 and 3.13 for U^{235} and Pu^{239}, respectively.

TABLE 3.5 (continued)

U^{235}			Plutonium		
Line No.	Energy (keV)	Intensity (No./100 fissions)	Energy (keV)	Intensity (No./100 fissions)	Line No.
22	2753.4	1.35	2753.6	0.28	19
23	2791.7	0.41	2789.8	0.59	20
24	2853.3	0.21	inconclusive		
25	2868.8	0.61	2867.6	0.39	21
26	2933.1	0.36	2931.8	0.31	22
27	2942.9	0.37	2943.9	0.46	23
28	3115.9	0.30	inconclusive		
29	3231.3	0.30	inconclusive		
	inconclusive		3281.8	0.26	24
30	3288.1	0.80	3288.6	0.31	25
31	3312.3	0.61	3310.8	0.34	26
32	3370.8	0.27	inconclusive		
33	3383.4	0.33	inconclusive		
34	3400.4	0.80	3401.3	0.38	27
35	3458.3	0.41	inconclusive		
36	3502.6	0.18	3501.6	0.17	28
37	3532.8	0.24	inconclusive		
38	3575.2	0.78	3575.2	0.36	29
39	3600.0	0.88	3601.4	0.23	30
40	3934.1	0.20	inconclusive		
41	4040.3	0.24	4040.3	0.16	31
42	4079.0	0.38	4078.3	0.14	32
	definite no		4123.0	0.18	33
43	4135.7	0.43	definite no		
44	4184.1	0.20	4184.5	0.10	34
	inconclusive		4233.6	0.14	35
45	4263.1	0.29	definite no		

TABLE 3.5 (concluded)

U^{235}			Plutonium		
Line No.	Energy (keV)	Intensity (No./100 fissions)	Energy (keV)	Intensity (No./100 fissions)	Line No.
	inconclusive		4272.7	0.18	36
	inconclusive		4295.2	0.22	37
	inconclusive		4329.9	0.16	38
46	4351.2	0.20	inconclusive		
47	4364.9	0.46	definite no		
	definite no		4430.0	0.37	39
48	4453.5	0.54	4452.0	0.32	40
	definite no		4462.0	0.27	41
	definite no		4470.7	0.13	42
49	4646.9	0.17	inconclusive		
	definite no		4651.9	0.14	43
	definite no		4757.5	0.17	44
50	4885.7	0.10	inconclusive		
	definite no		5119.5	0.22	45
51	5185.7	0.11	inconclusive		
52	5188.4	0.08	inconclusive		
	definite no		5291.2	0.15	46
53	5405.2	0.24	5405.2	0.08	47
54	5418.2	0.52	5416.5	0.18	48
55	5520.8	0.13	inconclusive		
	definite no		5570.5	0.40	49
56	6102.0	0.13	6102.0	0.05	50
57	6389.0	0.12	inconclusive		
	definite no		6480.0	0.10	51

3.6.1 Prompt Activation Analysis of Uranium Fuel Rods

Figure 3.14 shows the plan view of the geometry for irradiation of the fuel rods. Table 3.6 describes the five types of fuel rods irradiated. The 1.61% enriched fuel rod was taken as a standard against which the other rods are compared. Figure 3.15 shows the spectrum of the 1.61% enriched fuel rod. The data were analyzed by GAMANL and the areas under the peaks for each nucleus, U^{235} and U^{238}, were added up to give better counting statistics. The results of the analysis of U^{238} content are shown in Table 3.7. Figure 3.16 gives the results for the calibration line used for the U^{235} analysis.

TABLE 3.6

Uranium Oxide Fuel Rods Used in Enrichment Experiment

Enrichment Weight Percent	Pellet Diameter (Inch)	Cladding** Thickness (Inch)	Density (g/cc)	Cladding External Diameter (Inch)
0.711*	0.500	0.031	5.185	9/16
1.0999	0.446	0.025	10.11	1/2
1.30	0.500	0.030	10.11	9/16
1.61	0.500	0.030	10.11	9/16
1.999	0.446	0.025	10.11	1/2

*Made by compressing natural uranium oxide powder in aluminum tubing.

**Aluminum 1100 series.

TABLE 3.7

Results of the Analysis of U^{238} Content

Rod	N^x/N^s	
	Experimental	Calculated*
2.0%	0.770 ± 0.068	0.793
1.3%	0.977 ± 0.074	1.003
1.1%	0.816 ± 0.060	0.800
0.711%	0.526 ± 0.052	0.518

*Calculated from the data given by the fuel supplier, General Electric Company, except for the natural uranium rod which was made by the author.

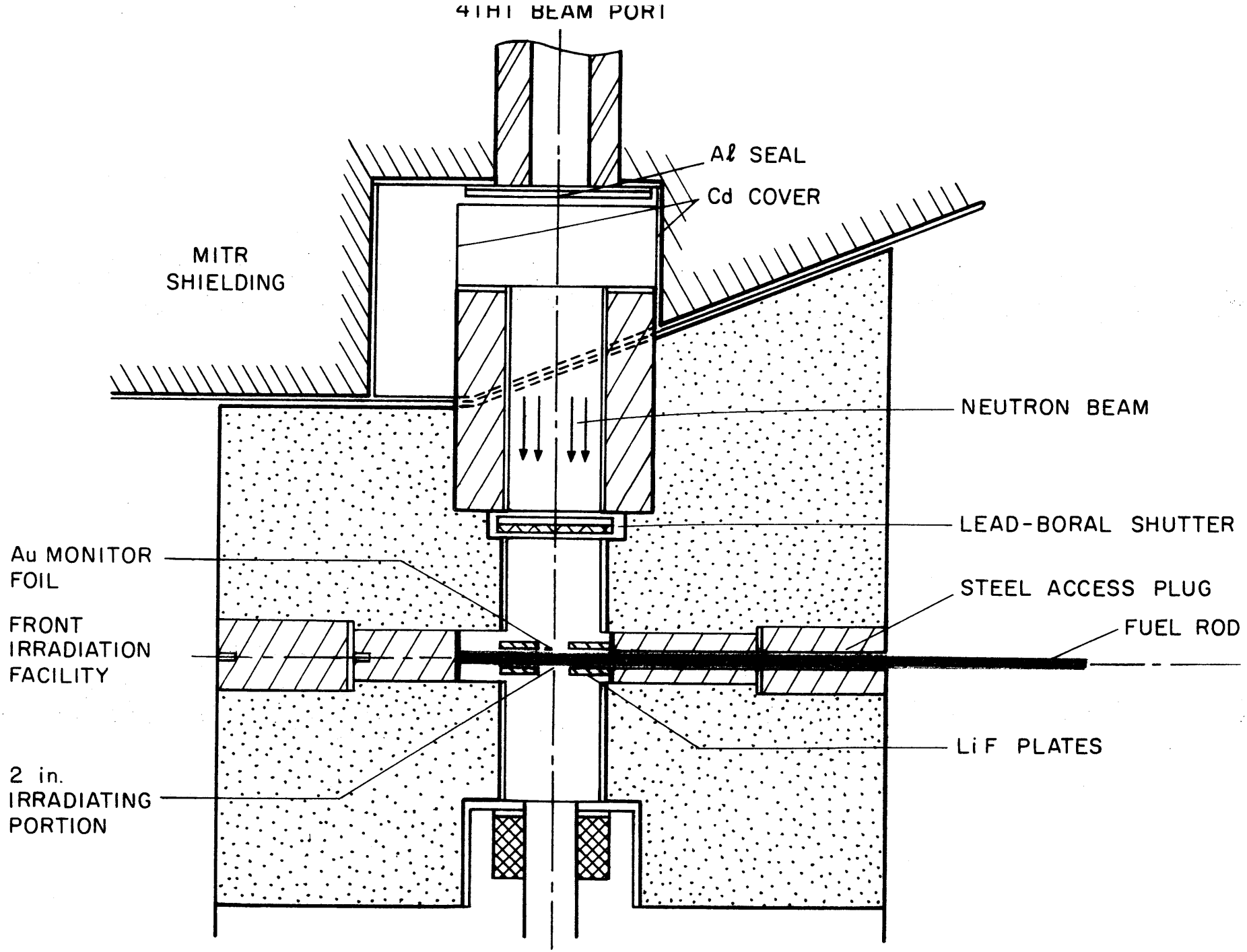

FIG. 3.14 THE GEOMETRY FOR IRRADIATION OF FUEL RODS AT THE FRONT FACILITY

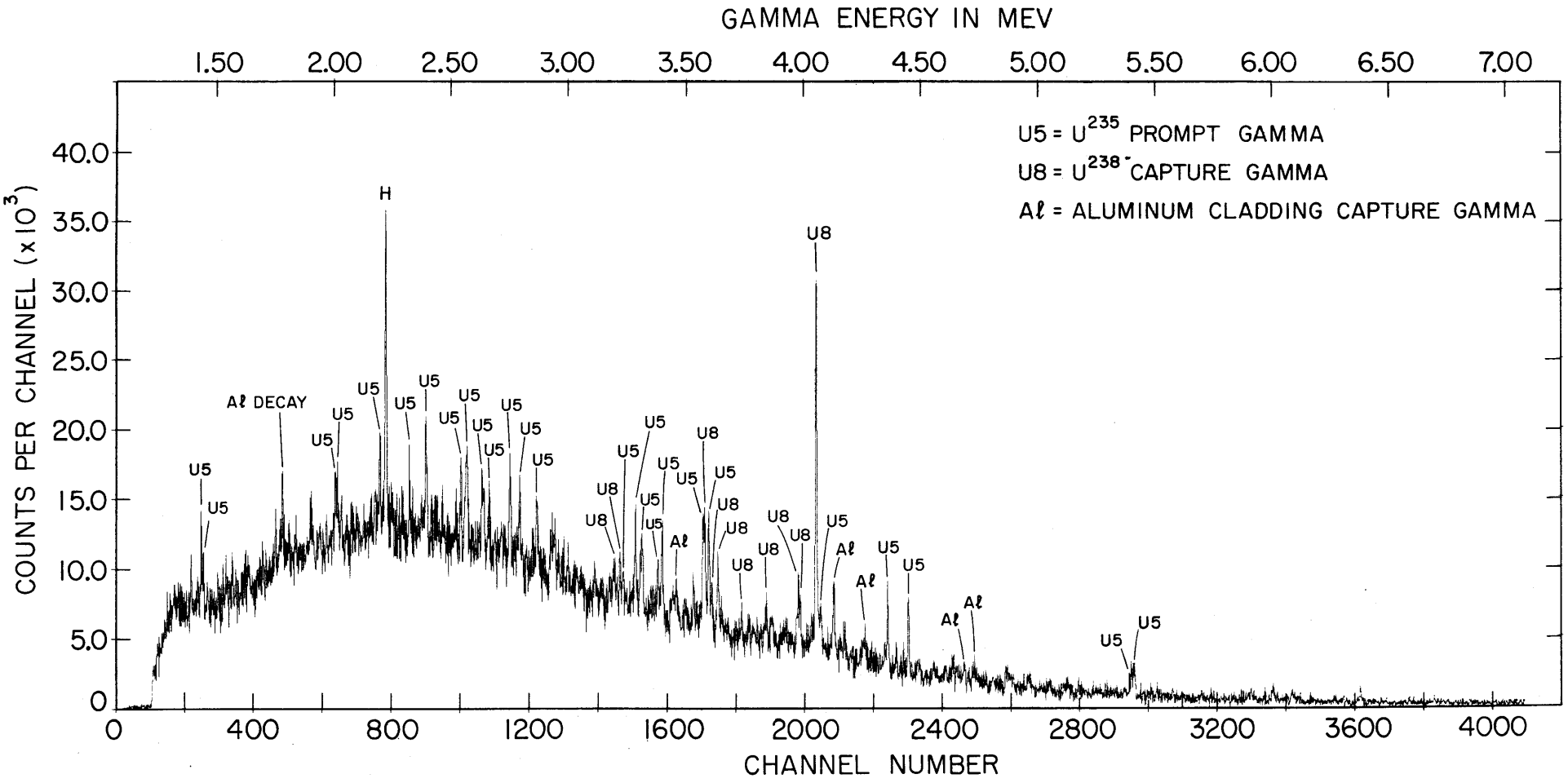

FIG. 3.15 THE GAMMA SPECTRUM OF A URANIUM OXIDE 1.61% ENRICHED ROD TAKEN IN TRIPLE COINCIDENCE MODE

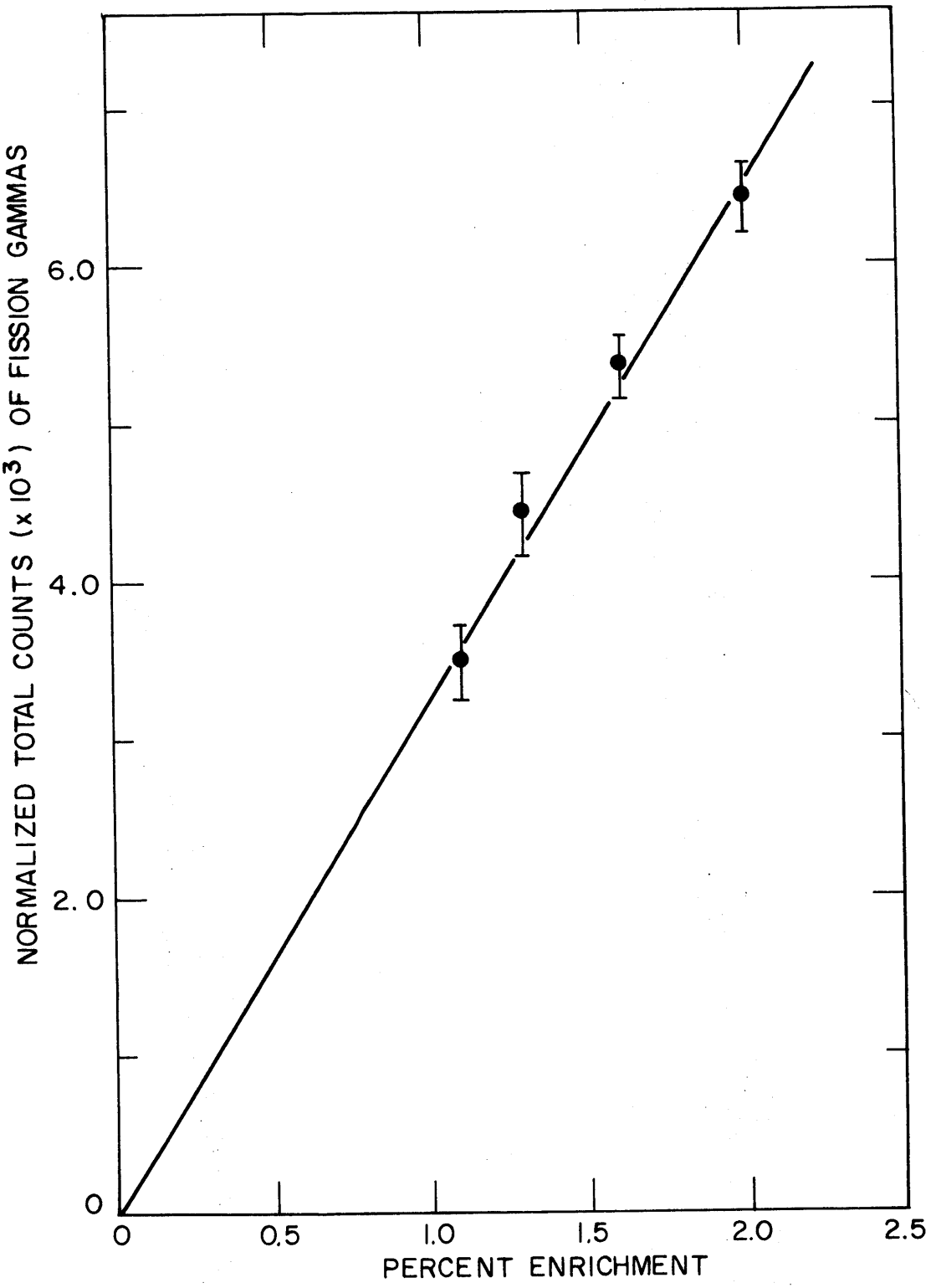

FIG. 3.16 THE VARIATION OF FISSION GAMMA COUNTS WITH FUEL ROD ENRICHMENT

3.6.2 The Prompt Activation Analysis of Pu-U Rods

For the purpose of investigating the possibility of assaying fuel rods of mixed fissile composition by using the prompt gammas, a fuel rod of the type B-Gold was irradiated with the same experimental arrangement as the uranium rods described in the previous section. Figure 3.17 shows the resulting gamma spectrum.

Theoretically, there are several different ways of treating the problem of analyzing the content of the fissile elements starting from the spectral data shown in Fig. 3.17.

In order to separate the contribution of U^{235} from that of plutonium, at least one piece of information must be extracted from the spectrum which is a characteristic of only one of them. Considering the statistics of counting, the best choice for this differential characteristic was the total area under the five peaks due only to plutonium, although this total number of counts is still low. The prompt fission gamma data for the calibrating foils, one containing only uranium and the other plutonium, and also the data for a standard uranium rod of 1.61% enrichment were used.

The results of this analysis are shown in Table 3.8.

TABLE 3.8

Experimental Results of the Analysis of a Plutonium-Uranium Rod, Type B-Gold

Weight Percent Ratio	Experimental Result	Calculated Result
W_5/W_9	1.346 ± 0.287	1.190
W_5/W_8	$(0.314 \pm 0.096) \times 10^{-2}$	0.301×10^{-2}
W_9/W_8	$(0.233 \pm 0.087) \times 10^{-2}$	0.253×10^{-2}

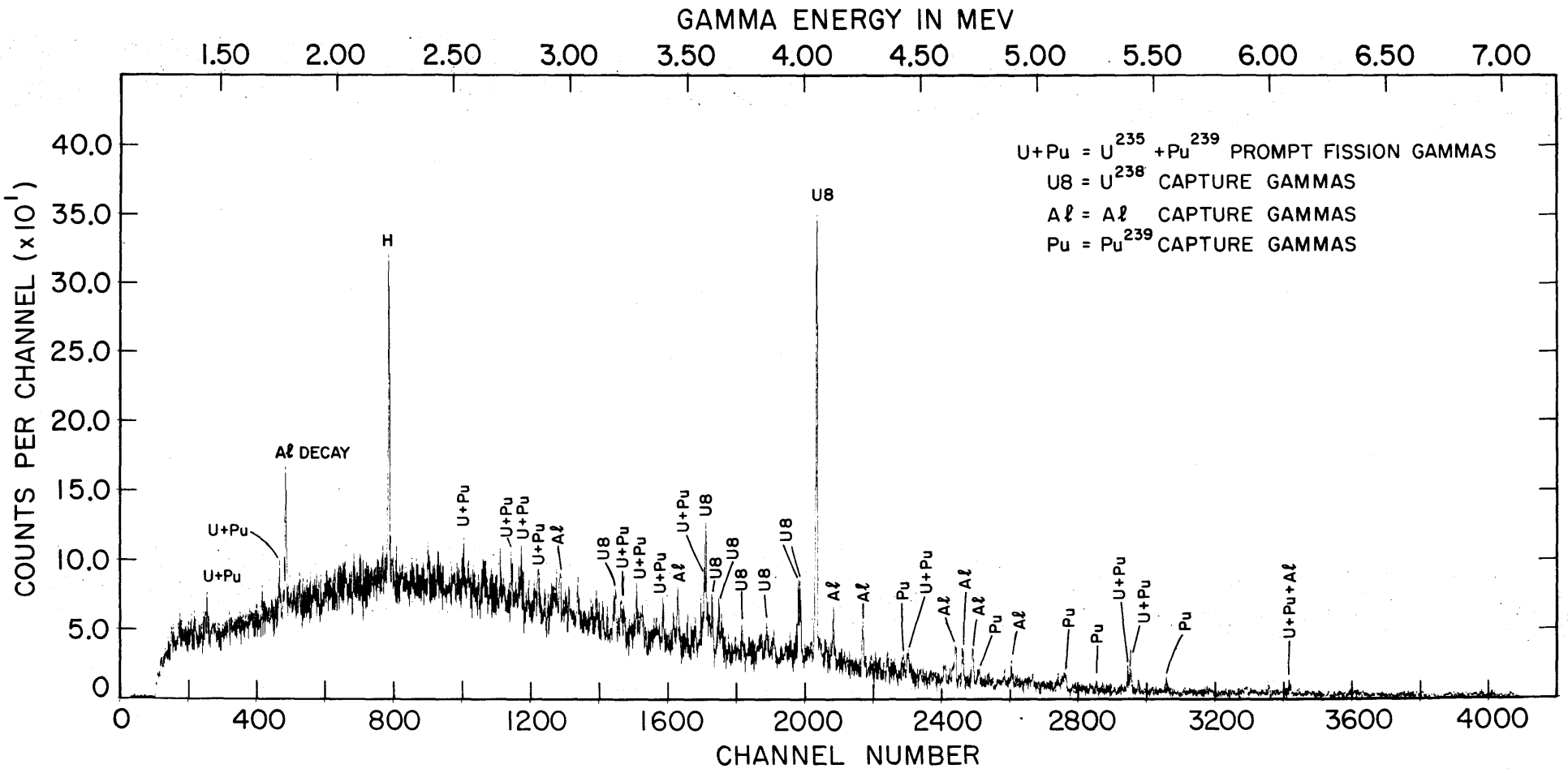

FIG. 3.17 THE GAMMA SPECTRUM OF PLUTONIUM-URANIUM ROD, TYPE B-GOLD, TAKEN IN TRIPLE COINCIDENCE MODE

3.6.3 Analysis of Fuel Rods Using the Fission Neutron Yield

Fission neutrons are potentially good indicators for analysis of fissile material. The main problem for the detection of the fission neutrons is the need to discriminate against the source neutrons that induce the fission and against the background gammas. Both of these functions of discriminating against the gamma background and the source neutrons can be performed by a single Ge(Li) detector operating in the free mode and acting now as a fast neutron detector.

This method is based on the inelastic scattering of fission neutrons by Ge^{72} in the crystal: the fission neutrons striking the 27.3% abundant Ge^{72} isotope inside the germanium detector excite it to a level at 693 keV which then de-excites to the ground state by emitting internal conversion electrons which lose their energy inside the germanium detector and appear in the prompt gamma spectrum as a prominent peak.

The intensity of this inelastic transition is proportional to the fission neutron yield because this transition occurs only through inelastic scattering. There is no Ge^{71} in the natural state to allow contribution from thermal neutron capture to the intensity of that transition.

Figure 3.18 shows the linear relation between the enrichment and the number of counts, which can be used for determining the enrichment of uranium fuel rods.

3.7 Other Measurements

In this section are presented some considerations pertinent to the development of new techniques for measuring reactor physics parameters based on high resolution gamma-ray spectroscopy of fuel elements. The classical method of inserting activation foils in between the fuel pellets of fuel elements for measuring the reactor physics parameters of lattices composed of fresh fuel elements is well established and widely used. However, the use of the same techniques for burned fuel would involve cutting into the fuel and would obviously present severe problems such as the release of fission products and plutonium from the burned fuel during the cutting process. Thus, any method that

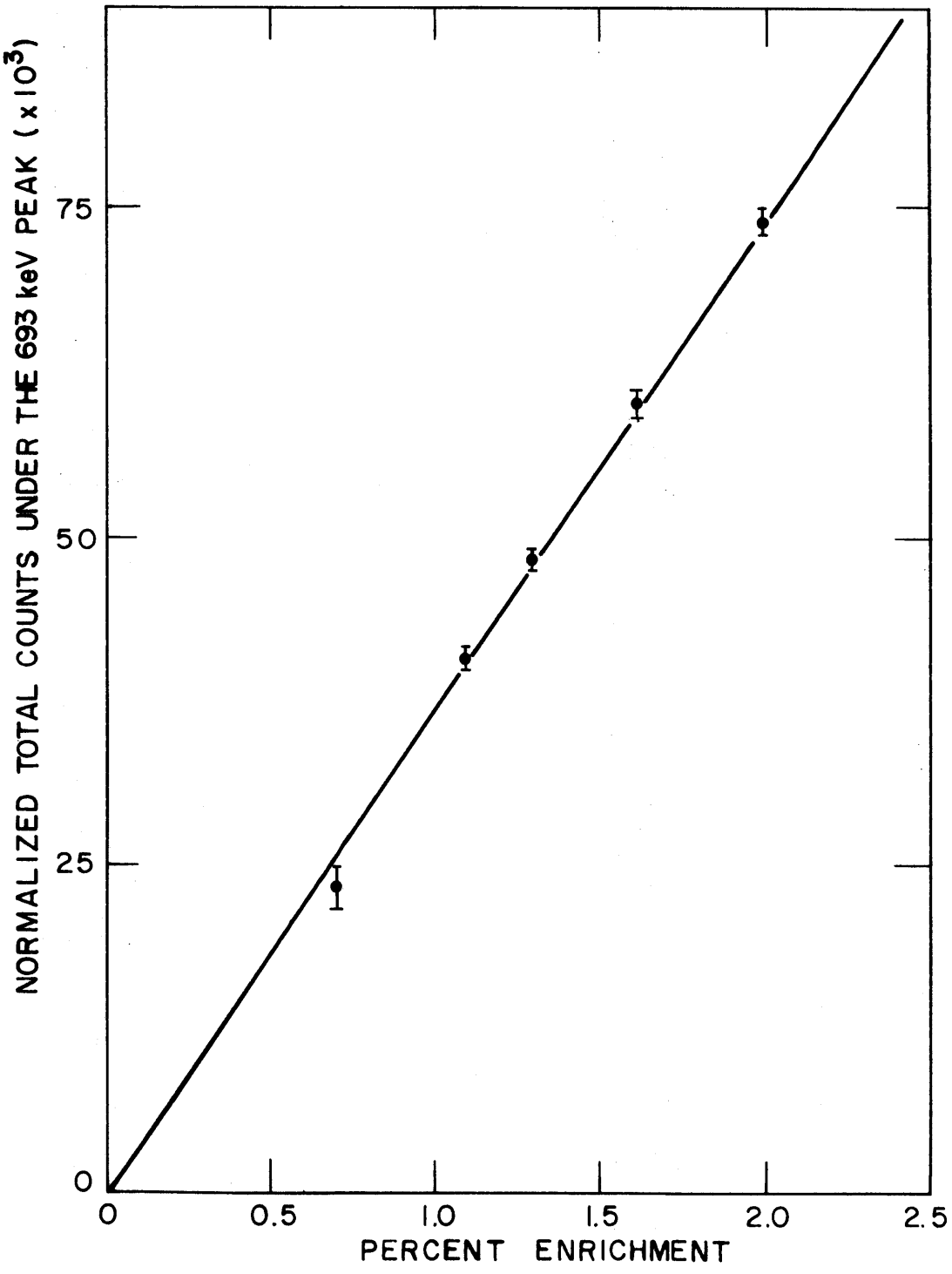

FIG. 3.18 RELATION OF THE MEASURED FISSION NEUTRON YIELD TO THE FUEL ENRICHMENT

could provide information on the neutronic behavior of a fuel rod by means of external measurements would be valuable. The emission of capture and fission gammas and fission neutrons by a fuel element during irradiation in an exponential facility suggested this study of the potential applicability of gamma-ray spectroscopy to this problem.

A method of measuring two parameters for the fuel rods with the experimental configuration shown in Fig. 3.14 is proposed, which if performed for the fuel rod inserted in an exponential facility would yield the parameter η and the initial conversion ratio, C.

For the experimental configuration shown in Fig. 3.14, C was measured using prompt gammas taken in the triple coincidence mode. The results are shown in Table 3.9.

TABLE 3.9

The Relative Initial Conversion Ratio

	C Relative to 1.61% Enriched Fuel Rod	
Fuel Rod	Measured	Calculated*
2%	0.806 ± 0.106	0.802
1.3%	1.180 ± 0.102	1.242
1.1%	1.551 ± 0.103	1.471

*Calculated from $(N_5^S/N_5^X)(N_8^X/N_8^S)$, where the values of N were taken from the data given by the fuel fabricator: this assumes all microscopic nuclide cross sections are identical for the rods irradiated.

The fission neutron yield parameter, η, is defined as the ratio of the rate at which fission neutrons are produced to the rate at which neutrons are absorbed in the uranium of the fuel rod. The parameter η can be decomposed according to the expression,

$$\frac{1}{\eta} = \frac{1}{\eta_5} + \frac{1}{\eta_8} ,$$

where η_5 is the ratio of the rate at which total fission neutrons are produced in the fuel to the rate at which neutrons are absorbed in U^{235}, and η_8 is the ratio of the rate at which total fission neutrons

are produced in the fuel rod to the rate at which neutrons are absorbed in U^{238}. The results are shown in Tables 3.10 and 3.11.

TABLE 3.10

The Relative Values of η_5

	η_5 Relative to 1.61% Enriched Fuel Rod	
Fuel Rod	Measured	Calculated*
2%	1.019 ± 0.063	1.00
1.3%	0.974 ± 0.070	1.00
1.1%	1.030 ± 0.075	1.00

*Calculated by assuming the same ν and α_{25} for all the rods.

TABLE 3.11

The Relative Values of η_8

	η_8 Relative to 1.61% Enriched Fuel Rod	
Fuel Rod	Measured	Calculated*
2%	1.264 ± 0.089	1.247
1.3%	0.820 ± 0.049	0.805
1.1%	0.657 ± 0.052	0.680

*Calculated from $(N_5^x/N_5^s)(N_8^s/N_8^x)$ where the values of N were taken from the data given by the fuel fabricator.

Based on the preceding results, further exploration of the applicability of using in-core gamma-ray spectroscopy is recommended in order to measure the fission neutron yield parameter and the initial conversion ratio for a single rod located at the center of an exponential facility. A plan view of the conceptual design of an in-core gamma spectrometer operating in the MITR exponential facility is presented in Fig. 3.19. An evacuated aluminum guide tube conducts the gamma beam from the fuel element to the Ge(Li) detector, which is contained together with the NaI crystals inside a "gun barrel" which serves as a gamma shield for the detecting system.

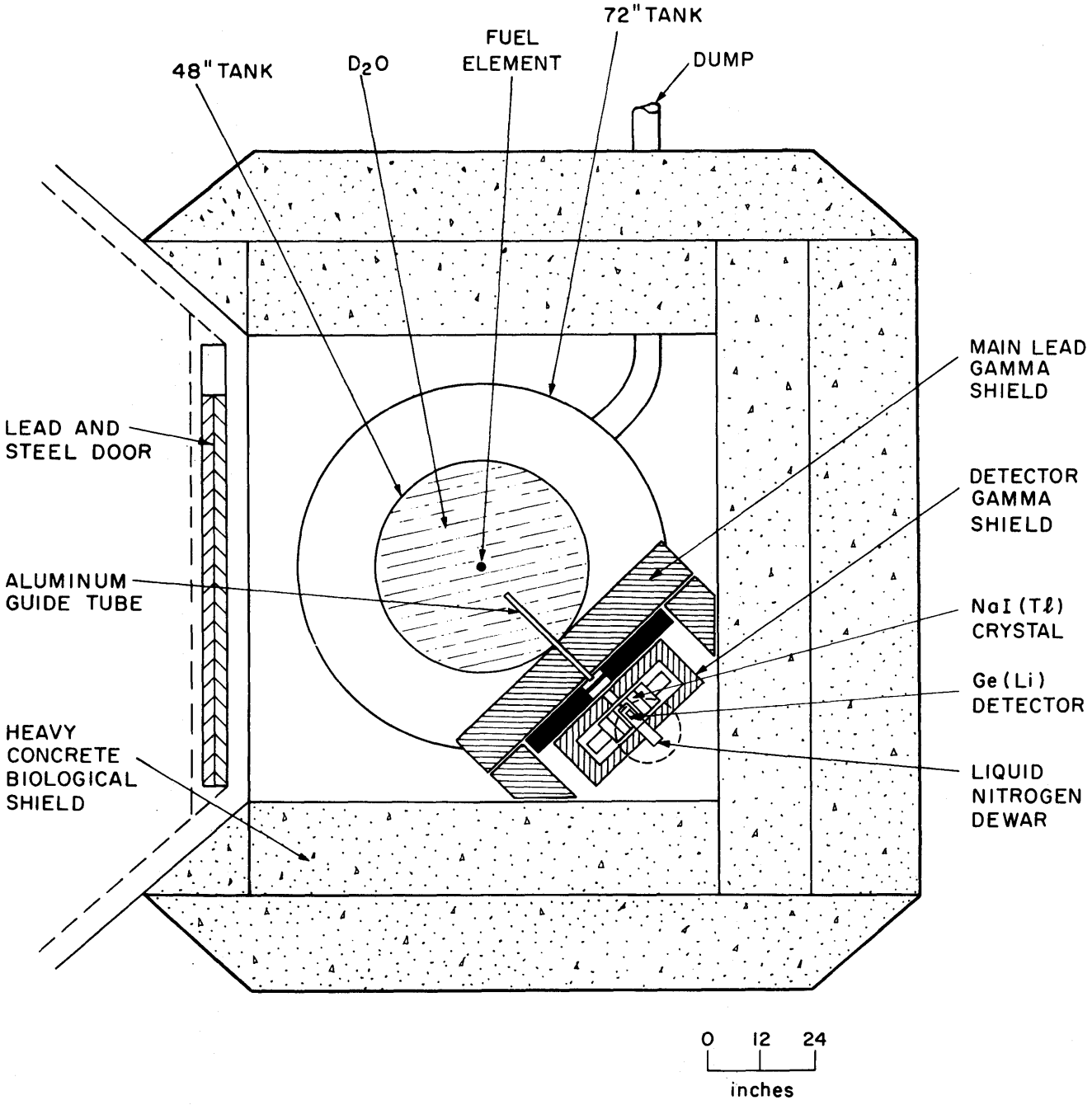

FIG. 3.19 PLAN VIEW OF THE PROPOSED GAMMA SPECTROMETER OPERATING IN THE M.I.T. EXPONENTIAL FACILITY

3.8 Conclusions and Recommendations

3.8.1 Conclusions

This present work was a study of the gamma rays emitted by the products of the interaction of thermal neutrons with the nuclei of U^{238}, Th^{232}, U^{235} and Pu^{239}, during and after the irradiation. The use of these gammas for fuel rod assay was also explored.

A method of assaying fuel rods containing a mixture of plutonium (about 0.25% of Pu^{239}) and uranium oxide (0.30% of U^{235}), based on the difference in the observable yield of the fission products I^{135} and Sr^{92}, was developed. This method required the use of a standard rod (1.30% of U^{235}) and a set of two calibrating foils, one containing only plutonium and another containing only uranium; an accuracy ranging from ± 6% to ± 10% was proven to be possible for determining the Pu and U content in a day of work.

The energies and intensities of the thermal neutron capture gamma rays for U^{238} and Th^{232} were determined. Compton suppression and triple coincidence modes of operation were used in low and high energy regions, respectively. A few new lines have been found for U^{238} in the energy region previously unexplored. In the case of Th^{232}, 66 lines were observed compared to the 7 lines reported in the literature.

The prompt gammas emitted by the highly excited fission products following the fission of U^{235} and Pu^{239} were resolved in the energy region above 1.4 MeV. For U^{235} fissions, 57 certain lines were found, and for Pu^{239}, 51 certain lines were recorded. Most of these gammas were present in both the spectra of U^{235} and Pu^{239}. It was concluded that the majority of these gammas are fission gammas emitted soon after the boil-off of the prompt neutrons, within 10^{-6} sec after the fission, by the de-excitation of the fission fragments. The number of prompt gammas per fission, above 1.4 MeV, was found to be 35% greater for U^{235} fissions than for Pu^{239} fissions. A few of these gammas might come from short-lived fission product decays; however, the transitions found in the spectrum of one fissile nucleus but not found in the spectrum of another were assigned tentatively as due to capture gammas (3 lines for U^{235} and 10 lines for Pu^{239}).

Fission gammas were used for assaying a plutonium-uranium oxide rod containing 0.25% of Pu^{239} and 0.30% of U^{235} in weight. An accuracy of ± 7% was obtained for the analysis of U^{238} content, and 10% to 20% accuracy was obtained for U^{235} and Pu^{235} compared to the manufacturing analysis.

It was found that Ge(Li) detectors can be used as energy threshold neutron detectors, and by operating as such they could be used to determine the relative fission neutron yield. With this method, the enrichment of uranium rods can be found with an accuracy of ± 1% to ± 2% in the range of 1% to 2% enrichment.

The feasibility of using prompt gammas for the measurement of the initial conversion ratio, C, and the neutron yield parameter, η, in an exponential facility was studied. The results obtained suggest strongly that an in-core gamma spectrometer operating in an exponential facility could yield these reactor physics parameters.

3.8.2 Recommendations

(1) It is suggested that future work investigate the possibility of using the Rh^{103}-La^{140} gamma rays instead of the I^{135}-Sr^{92} gamma rays. This new pair of fission products would be preferable because of their yield difference which is of the order of a factor of 10, compared to 2 for I^{135} and Sr^{92}. However, in this case a longer cooling time, on the order of a few days, would be required.

For quicker analysis, it is recommended that a study of the use of all prominent peaks of the short-lived fission product spectra, as obtained in this present work, be undertaken in order to improve the statistics of counting and consequently the accuracy of the present method. A careful analysis of the correction factors would be necessary.

It is suggested that the use of the present method for detecting nonuniform distribution of fissile elements in plutonium-uranium rods be investigated.

It is also recommended that the present method be investigated for use in analyzing burned fuel rods. However, a neutron flux of the order of 10^{10} n/cm^2-sec would be necessary for reirradiation and analysis of a typical burned fuel rod.

(2) It is recommended that a study of the energy level structure for Th^{233} be undertaken by complementing the data found in this work with a $Th^{232}(d,p)Th^{233}$ reaction study.

(3) It is recommended that the data of Pu^{239} prompt gammas be improved by using a sample containing a smaller amount of Pu^{239} than the present work in order to lower the count rate and so increase the resolution.

(4) The poor accuracy of the method of analysis of fuel rods using prompt gammas was due mainly to the low count rate, and consequently the poor statistics. It is recommended that this method be used with a more favorable geometrical arrangement, with a larger detection solid angle and a greater detector efficiency, in order to improve the statistics of counting.

(5) It is recommended that consideration be given to the use of Ge(Li) detectors as fission neutron detectors for the determination of Pu^{239} content of spent fuel. This method would require incident neutrons of two different energies in order to distinguish U^{235} from Pu^{239} by differences in the fission cross section as a function of energy.

(6) It is recommended that the feasibility study of an in-core gamma spectrometer be followed by actual construction of a spectrometer to operate in the MITR exponential facility.

Finally, it is recommended that the use of gamma-ray spectroscopy of fuel elements be extended to many still unexplored applications for the measurement of reactor physics parameters and that special consideration be given to the use of prompt gammas for measurements involving burned fuel rods.

3.9 References

(1) R.K. Sheline, W.N. Shelton, T. Udagawa, E.T. Turney and H.T. Motz, "Levels in U-239," Phys. Rev. 151, No. 3, 1011 (November 1966).

(2) B.P.K. Maier, "Bestimmung des (631) K=1/2, I=1/2 Zustendes im U-239," Zeits. fur Physik 184, 143 (1965).

(3) L.V. Groshev et al., Atlas of Gamma-Ray Spectra from Radiative Capture of Thermal Neutrons, English translation by J.B. Sykes, Pergamon Press, London (1959).

(4) L.V. Groshev et al., "Compendium of Thermal-Neutron-Capture Gamma-Ray Measurements, Part III for Z=68 to Z=94," Nucl. Data, Section A, Vol. 5, No. 3-4 (February 1969).

(5) R.C. Greenwood and J.H. Reed, "Prompt Gamma Rays from Radiative Capture of Thermal Neutrons," Report No. IITRI-1193-53.

(6) T.L. Harper and N.C. Rasmussen, "Determination of Thermal Neutron Capture Gamma Yields," MITNE-104, Vol. 1 (1969).

(7) C.E. Miner, "A Semiconductor Detector Cryostat," Nucl. Instr. and Meth. 55, 125 (1967).

(8) V.J. Orphan and N.C. Rasmussen, "Study of Thermal Neutron Capture Gamma Rays Using a Lithium-Drifted Germanium Spectrometer," Contract No. AF19(628)5551, MITNE-80, Department of Nuclear Engineering, M.I.T. (1965).

(9) R.S. Forsyth and N. Ronquist, "Burnup Determination by High Resolution Gamma Spectroscopy: Spectra from Slightly Irradiated Uranium and Plutonium Between 400-830 keV," AE-241 (August 1966).

(10) N.P. Bauman et al., Lattice Experiments with Simulated Burned Fuel for D_2O Power Reactors," DP-1122 (February 1968).

(11) F.C. Maienschein et al., "Gamma Rays Associated with Fission," Proc. Intern. Conf. Peaceful Uses of Atomic Energy, 2nd, Geneva, 15, 366 (1958).

(12) J.N. Hamawi and N.C. Rasmussen, "Investigation of Elemental Analysis Using Neutron-Capture Gamma-Ray Spectra," MITNE-107, U.S. Bureau of Mines Contract No. H0180895 (1969).

4. APPLICATION OF THE SINGLE-ELEMENT METHOD TO H_2O-MODERATED SYSTEMS

M. S. Kazimi and L. L. Izzo

4.1 Introduction

The work reported in this chapter is concerned with the application of heterogeneous reactor theory to light water moderated systems. The theoretical and experimental evaluations of the fuel element characterization parameters Γ, η and A are treated.

Expressions for the extrapolation of single-element values to full lattice values are presented, and the effect of the moderating medium on the characterization parameters is shown to be either negligible or easily evaluated.

Finally, attempts to carry out single-element experiments in an H_2O-moderated exponential facility are described and the inherent limitations on this approach are discussed.

More detailed descriptions of the results described in the following sections of this chapter are contained in references (1) and (2).

4.2 Theoretical Considerations

Theoretical analysis enters into the single-element method in two important areas: in the extraction of the fuel element characterization parameters Γ, η and A from experimentally measured quantities, and in the extrapolation of single-element values of Γ, η and A to values appropriate for lattices made up of an array of fuel elements. Seth's work, reported in Chapter 2 and reference (3), exemplifies both types of analysis in the case of D_2O-moderated systems.

The work reported in this chapter was also concerned with both of these areas. However, concurrent experimental investigations, summarized in section 4.3, soon indicated that analysis of experimental data from H_2O exponential experiments would require a much more sophisticated level of analysis than that required for D_2O-moderated cases. In particular, the lack of axial spectral equilibrium

and the strong transport effects on the radial flux peak essentially eliminated the feasibility of using the analytic model developed for D_2O without extensive modification. Consideration of the various options available for resolution of this problem led to the focusing of emphasis on interrelating parameter values for the same fuel element in different moderators. This conclusion was based on the judgment that experiments should be performed in a medium offering the highest precision and most easily interpretable data and then be corrected to obtain values appropriate for other moderators.

Thus this section will deal primarily with theoretical aspects related to the demonstration of the applicability of heterogeneous reactor theory to H_2O systems, the relation between single-element and lattice parameters in H_2O and the effect of moderator properties on the fuel element characterization parameters.

A small but growing body of pertinent reports in the literature provided the base for the present work. The work by Seth (3) on D_2O-moderated systems has already been mentioned. His work was preceded at M.I.T. by that of Pilat (4). Hamilton (5) evaluated the potential applicability of the single-element method for the evaluation of the heterogeneous parameters in light water systems. Klahr et al. (6) indicated that with properly chosen diffusion and slowing-down kernels the source/sink formulation may be applied. Finally, Donovan (7) and Higgins (8) investigated the relation of the heterogeneous parameters to in-rod foil activation data and the determination of kernel parameters, respectively.

4.2.1 The Thermal Constant Γ

The parameter Γ is defined as the ratio of the asymptotic neutron flux at the surface of the fuel element to the number of thermal neutrons absorbed per unit length of the element. By asymptotic flux is meant the value of the flux which would exist if the fuel element were shrunk to a line sink and the transport transient neglected, making diffusion theory applicable. It can be related to the thermal utilization, f, by the following simple expression:

$$\Gamma = \frac{1}{(\Sigma_a V)_M}\left(\frac{1}{f} - 1 - G\right), \tag{4.1}$$

where $(\Sigma_a V)_M$ is the product of the average thermal neutron absorption cross section and moderator area (volume per unit length) in the unit cell, while G is the so-called excess absorption, which is adequately estimated in the present case by:

$$G = \frac{V_c}{4\pi L_M}\left\{\frac{v}{2} - \frac{3}{2} - \frac{\ln v}{1-v}\right\}, \tag{4.2}$$

in which V_c is the unit cell area, L_M is the moderator diffusion length and v is the volume fraction fuel in the unit cell.

Equations 4.1 and 4.2 were used to determine Γ from experimental data reported in reference (9). Table 4.1 shows the results of this computation for a variety of fuel elements and for several fuel-to-moderator volume ratios, V_F/V_M. It is clear that the inferred Γ values are constant, independent of the lattice spacing. This result is similar to that obtained for the behavior of this parameter in graphite- and D_2O-moderated systems. Figure 4.1 shows a plot of these data together with a theoretically estimated value, determined as discussed below.

Application of asymptotic diffusion theory and collision probability theory allows derivation of the following simple theoretical expression for Γ (1):

$$\Gamma = \frac{1}{(\Sigma_a V)_F}\left\{1 + \frac{1}{3}\left[1 + \frac{4}{3}(\Sigma_s R)_F\right](\Sigma_A R)_F\right\} + \Delta\Gamma,$$

$$\Delta\Gamma = \frac{I(c_F) - I(c_M)}{2\pi R_F}, \tag{4.3}$$

where

R = fuel element radius,

c = number of secondaries per collision = $\Sigma_s/(\Sigma_s+\Sigma_A)$,

I(c) = a function tabulated by Pomraning and Clark (10).

Table 4.2 lists the values of Γ calculated using Eqs. 4.3 for the fuel rods of Table 4.1. As can be seen by comparing these two sets of results and the plots of Fig. 4.1, the agreement between theory and

TABLE 4.1

The Thermal Constant, Γ, Determined from Experimental Values of the Thermal Utilization Factor, f_c

Fuel Description	$\frac{V_F}{V_M}$ *	$\frac{\phi_M}{\phi_F}$ **	f_c **	f_Γ *	Γ (cm^{-1}) *
Metal, 0.6-in. dia., 1.3% U-25	0.823	1.39	0.918 ± 0.004	0.922	1.41 ± 0.06
	0.618	1.45	0.890 ± 0.004	0.894	1.38 ± 0.06
	0.410	1.49	0.843 ± 0.003	0.847	1.41 ± 0.04
Metal, 0.6-in. dia., 1.15% U-25	0.618	1.45	0.881 ± 0.004	0.885	1.52 ± 0.07
	0.410	1.45	0.835 ± 0.005	0.839	1.48 ± 0.08
UO_2 (7.53 g/cm^3), 0.6-in. dia., 1.3% U-25	1.150	1.09	0.873 ± 0.004	0.885	3.31 ± 0.15
	0.880	1.14	0.837 ± 0.005	0.850	3.36 ± 0.19
	0.702	1.16	0.805 ± 0.005	0.815	3.27 ± 0.18
UO_2 (7.53 g/cm^3), 0.384-in. dia., 1.3% U-25	0.988	1.10	0.836 ± 0.004	0.887	8.10 ± 0.37
	0.795	1.10	0.807 ± 0.004	0.861	8.06 ± 0.36
UO_2 (10.53 g/cm^3), 0.384-in. dia., 1.3% U-25	0.982	1.10	0.874 ± 0.004	0.887	6.01 ± 0.27
	0.772	1.13	0.848 ± 0.004	0.861	5.95 ± 0.27
	0.384	1.13	0.804 ± 0.004	0.822	5.95 ± 0.27

*This work, includes clad as part of fuel element.

**From ref. (9), clad not considered part of fuel.

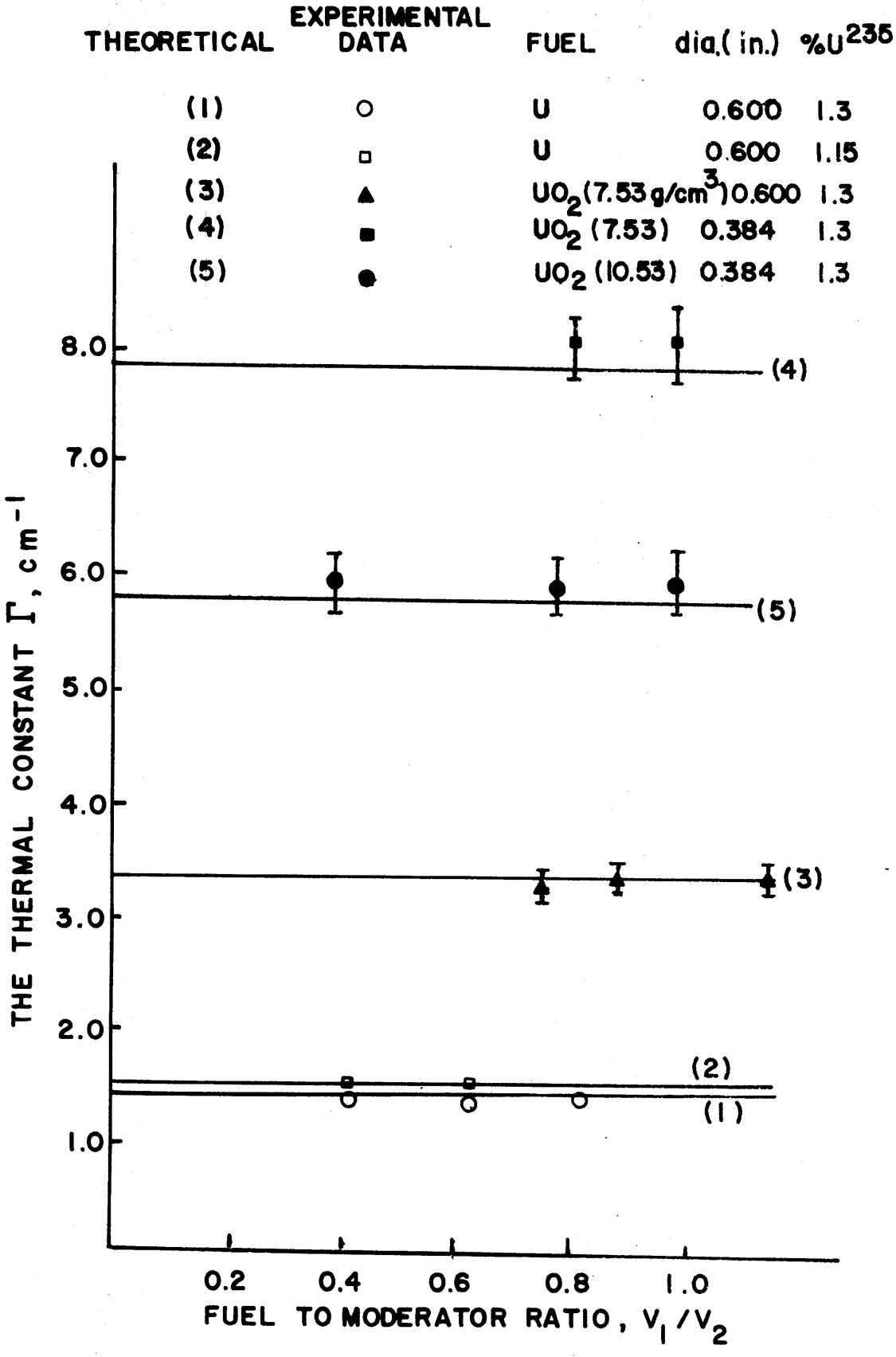

FIG. 4.1 THE PARAMETER Γ FOR U AND UO_2 RODS IN H_2O

experiment is excellent and within the experimental error in all cases. Note that Eqs. 4.3 contain no dependence on lattice spacing, so that the theory also predicts that Γ is indeed a constant.

TABLE 4.2
Theoretical Values for Γ

Case	Rod Description	Γ^o (cm^{-1})	$\Delta\Gamma$ (cm^{-1})	Γ (cm^{-1})
1	0.6-inch diameter, metal, 1.3% U-25	1.2756	0.1837	1.4593
2	0.6-inch diameter, metal, 1.15% U-25	1.368	0.1775	1.5455
3	0.6-inch diameter, UO_2, 1.3% U-25, 7.53% g/cm^3	3.212	0.1623	3.3643
4	0.384-inch diameter, UO_2, 1.3% U-25, 7.53 g/cm^3	7.620	0.2400	7.8600
5	0.384-inch diameter, UO_2, 1.3% U-25, 10.53 g/cm^3	5.553	0.2378	5.7908

Note: Γ^o is first term on right-hand side of Eq. 4.3: $\Gamma = \Gamma^o + \Delta\Gamma$.

Equations 4.3 are also useful for predicting the effect of moderator properties on Γ. Since $\Delta\Gamma$ is the only term containing moderator properties, we have directly:

$$\Gamma_{H_2O} - \Gamma_{D_2O} = \frac{-\{I(H_2O) - I(D_2O)\}}{2\pi R_F} . \qquad (4.4)$$

Since, from reference (10), $I(H_2O) \approx 0.0950$ and $I(D_2O) \approx 0.0020$, a typical 1-cm-diameter fuel pin would have a value of Γ which differs only by about 0.03 cm^{-1} between the two moderators. This is considerably less than the experimental uncertainties in Γ reported in Table 4.1.

Only a few data are available for the same fuel in different moderators. Table 4.3 shows the one comparison which could be made. As can be seen, the values of Γ for nearly identical fuel rods in H_2O and D_2O are the same within expected experimental uncertainties and furthermore are in equally good agreement with the theoretical values predicted by Eqs. 4.3.

In view of the above results, it was concluded that the behavior of the thermal constant, Γ, was sufficiently well understood for H_2O lattices and, in fact, that no essential difference in this parameter occurs due to the selection of either moderator type or lattice spacing. In this regard, it is indeed a powerful fuel characterization parameter.

4.2.2 The Fast Neutron Yield Parameter η

In this work, η is defined as the net number of fast neutrons produced per thermal neutron absorbed in the fuel element. It includes the effects of both epithermal and fast fission, which vary with lattice spacing and which therefore make η a function of lattice spacing as well as fuel rod properties. Thus we are concerned with the extrapolation of measured single-element values, η_{SE}, to full lattice values, η_L. Donovan (7) has extensively discussed various definitions of η and their relation to experimentally measurable quantities.

Using kernel summation methods described by Seth (3) and Higgins (8) and paralleling their treatment of D_2O lattices, one obtains:

$$\eta_L = \eta_{SE}\left(1 + F_e\, e^{-B^2\tau} + F_f\, e^{-B^2\lambda^2/3}\right), \tag{4.5}$$

where the fast and epithermal factors, F_f and F_e, are given by:

$$F_e = \nu_e N RI_{ef}\left\{\frac{V_F}{V_M} - \frac{V_F V_M}{4\pi(V_F+V_M)\tau}\right\},$$

$$F_f = (\nu-1-\alpha)_f N\sigma_{ff}\left\{\frac{V_F\lambda}{V_F+V_M} + \frac{\pi R}{4}\sqrt{\frac{3V_F}{V_F+V_M}} + \frac{\pi}{16}\frac{V_F}{\lambda}\right\} e^{-\frac{\pi}{2}\frac{R}{\lambda}\sqrt{\frac{3(V_F+V_M)}{V_F}}}. \tag{4.6}$$

TABLE 4.3

Values of Γ for 0.75-Inch-Diameter Fuel Rod in H_2O and D_2O

Moderator	Fuel Diameter (Inch)	Enrichment	V_F/V_{CELL}	f	Γ^* (cm^{-1})	Γ^{**} (cm^{-1})
99.75% D_2O	0.75	0.947%	0.0816	0.9935	1.39	1.400
H_2O	0.75	1.027%	0.259	0.819	1.34	1.383

*Value of Γ determined from experimental value of f.

**Value of Γ calculated from Eqs. 4.3.

The parameters appearing in these equations are defined as follows:

V_F, V_M = fuel, moderator cross-sectional area (volume per unit length), respectively,

RI_{ef} = resonance integral for epithermal fission of U^{235},

ν_e = neutrons per epithermal fission of U^{235},

τ = effective age to epithermal fission,

λ = mean free path for fast neutrons,

σ_{ff} = fission cross sections of U^{238} for fast neutrons,

R = fuel rod radius,

$(\nu-1-\alpha)_f$ = net fast neutron yield for U^{238} fast absorption.

Figure 4.2 shows the variation of η_L with the fuel-to-moderator volume ratio, together with η values inferred from experimental data for a number of lattices. As can be seen, the agreement is good, substantiating the conclusion that, given accurate values of η_{SE}, extrapolation to lattice values is as easily and as accurately carried out in H_2O systems as was shown previously by Seth et al. (3) for D_2O systems.

The second major item of interest with regard to η is the relation among single-element values measured in different moderators. This can be shown to be (1), (7):

$$\frac{\eta_{SE1}}{\eta_{SE2}} = \frac{\left(1 + \delta^{25}_{SE1}\right)\left(1 + \beta\, \delta^{28}_{SE1}\right)}{\left(1 + \delta^{25}_{SE2}\right)\left(1 + \beta\, \delta^{28}_{SE2}\right)}, \tag{4.7}$$

where

δ^{28}_{SE} = ratio of fissions in U^{238} to those in U^{235}, for the single-element experiment,

δ^{25}_{SE} = ratio of epithermal to thermal fissions in U^{235}, for the single-element experiment,

$$\beta = \left(\frac{\nu^{28} - 1 - \alpha^{28}}{\nu^{25}}\right).$$

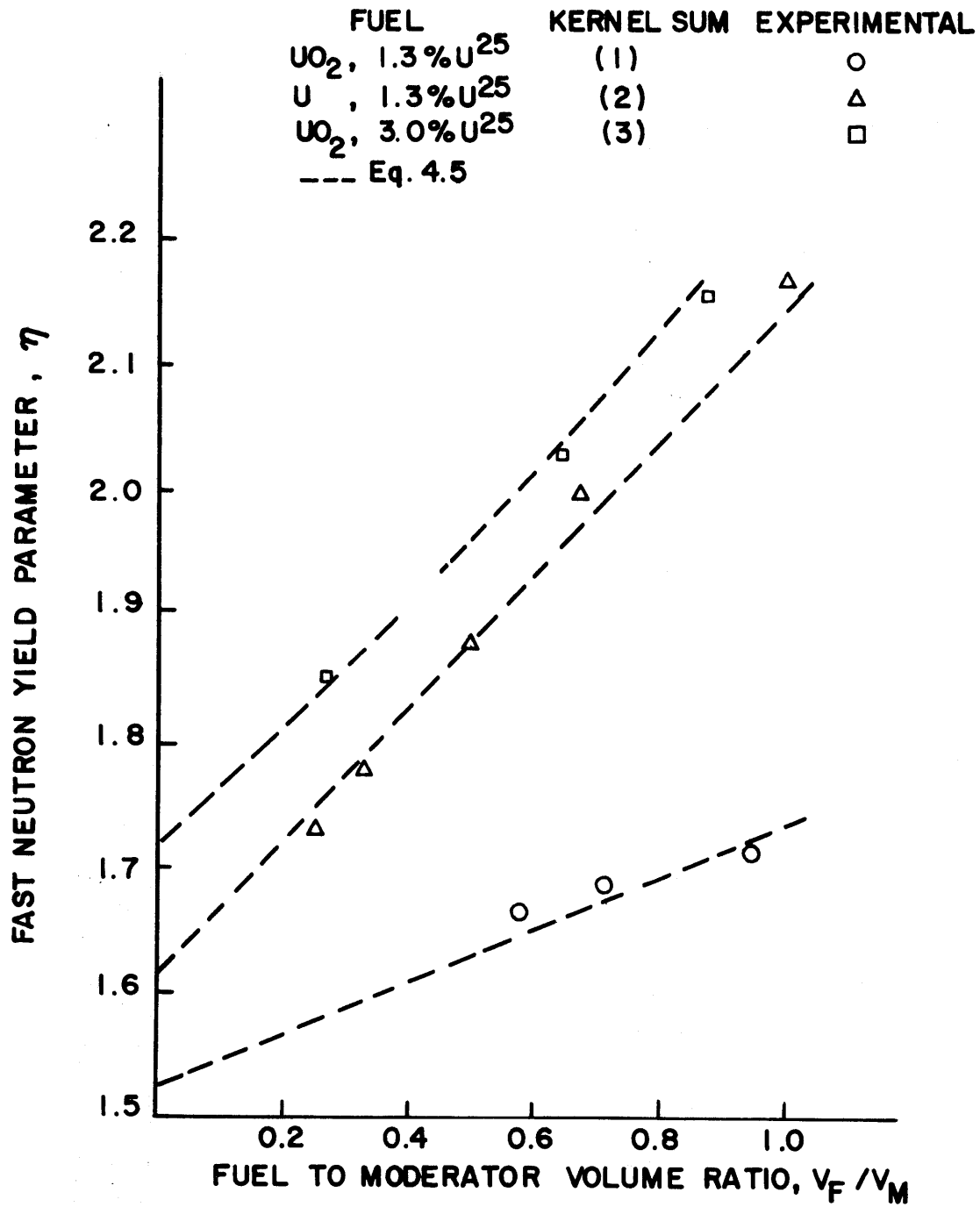

FIG. 4.2 VARIATION OF η WITH V_F / V_M IN H_2O LATTICES

Since δ_{SE}^{28} and δ_{SE}^{25} are typically in the neighborhood of 0.02 or less for representative UO_2 fuel rods and are also weak functions of moderator characteristics, it follows directly that η_{SE} is also a very weak function of moderator properties, certainly varying less than the obtainable experimental precision of approximately ± 1% or ± 2% to which η_{SE} can be determined in moderators such as D_2O or graphite.

Thus, like Γ, η can also be measured in the most convenient moderator and its value in any other moderator inferred directly.

4.2.3 The Epithermal Absorption Parameter A

The parameter A is defined as the epithermal neutron absorption per unit slowing-down density at the fuel element surface.

In this work, two important differences between H_2O and D_2O systems were identified which required modification of the prior treatments of resonance absorption in terms of the characterization parameter A. First, a clear distinction must be made between moderator and total unit cell volumes, since the fuel volume is no longer negligible. Secondly, the close spacing requires that the effect of Dancoff shadowing be included.

Analytic treatment of these added effects, again paralleling the work reported previously for D_2O, yielded the following prescriptions for estimation of lattice values for A from single-element values:

$$A_L = A_{SE}\left\{1 - \Delta\left(\frac{1}{E}\right) - \Delta(D)\right\}, \tag{4.8}$$

$$\Delta\left(\frac{1}{E}\right) = \frac{V_F}{V_M}\frac{N^{28}\,RI^{28}}{\Sigma_{SM}(1+\chi)}\left\{\chi^2\,\frac{m}{2} + \frac{n}{2} + \frac{mn}{m+2}\,2\chi\right\},$$

$$\Delta(D) = \frac{1 - (a+b\sqrt{\delta S/M})/(a+b\sqrt{S/M}}{1+\chi},$$

where

$$\chi = \frac{N^{25}\,RI_{\alpha}^{25}}{N^{28}\,RI^{28}}.$$

In Eq. 4.8, the $\Delta(1/E)$ term accounts for the fact that resonance absorption depletes the slowing-down flux, resulting in a non-1/E

functional behavior for $\phi(E)$; and the $\Delta(D)$ term accounts for Dancoff shadowing, where a and b are constants in the usual semi-empirical relation for the resonance integral of U^{238} rods and the Dancoff factor δ (usually defined in the literature as (1-c)) can be evaluated using Bell's prescription (11). The parameters m and n are the slopes of the ln RI vs. ln E correlations for U^{235} and U^{238}, respectively.

In addition to permitting calculation of lattice values from single-element data, Eq. 4.8 allows the calculation of theoretical values of the parameter A if we take

$$A_{SE} = \frac{V_F \cdot N \cdot RI}{\xi \Sigma_{SM}} . \tag{4.9}$$

Figure 4.3 shows a plot of lattice values of A calculated using Eqs. 4.8 and 4.9 together with values of A calculated from experimental values of the integral parameters ρ^{28} and δ^{25} and the thermal utilization, f, according to the relation:

$$\frac{1}{A} = \frac{1}{V_M}\left\{ 1 + \frac{1}{f} \frac{\left(\Sigma_a^{28}/\Sigma_f^{25}\right)_{SC} + 1 + \alpha_{SC}^{25}}{\rho^{28}\left(\Sigma_a^{28}/\Sigma_f^{25}\right)_{SC} + \delta^{25}\left(1+\alpha_{EC}^{25}\right)} \right\}, \tag{4.10}$$

where $\left(\Sigma_a^{28}/\Sigma_f^{25}\right)_{SC}$ is the ratio of captures in U^{238} to fissions on U^{235} for neutrons below cadmium cutoff, and α_{SC}^{25} and α_{EC}^{25} are the sub- and epicadmium capture-to-fission ratios for U^{235}.

The agreement between theory and experiment shown in Fig. 4.3 is good, particularly for the lower enrichment fuel. This also suggests that even better agreement for higher enriched fuel can be obtained if self-shielding and Dancoff shadowing of U^{235} are considered.

It is important to note that as the fuel-to-moderator ratio, V_F/V_M, increases, the value of A decreases, similar to its behavior in D_2O lattices. Previous workers (5, 6) had reported that A increased for H_2O, but this anomalous behavior is due to their use of the cell volume, V_c, in place of the moderator volume, V_M, in some of the relationships used to define and evaluate A. We again conclude that the epithermal absorption parameter is an equally valid concept for description of epithermal absorption in H_2O-moderated systems as

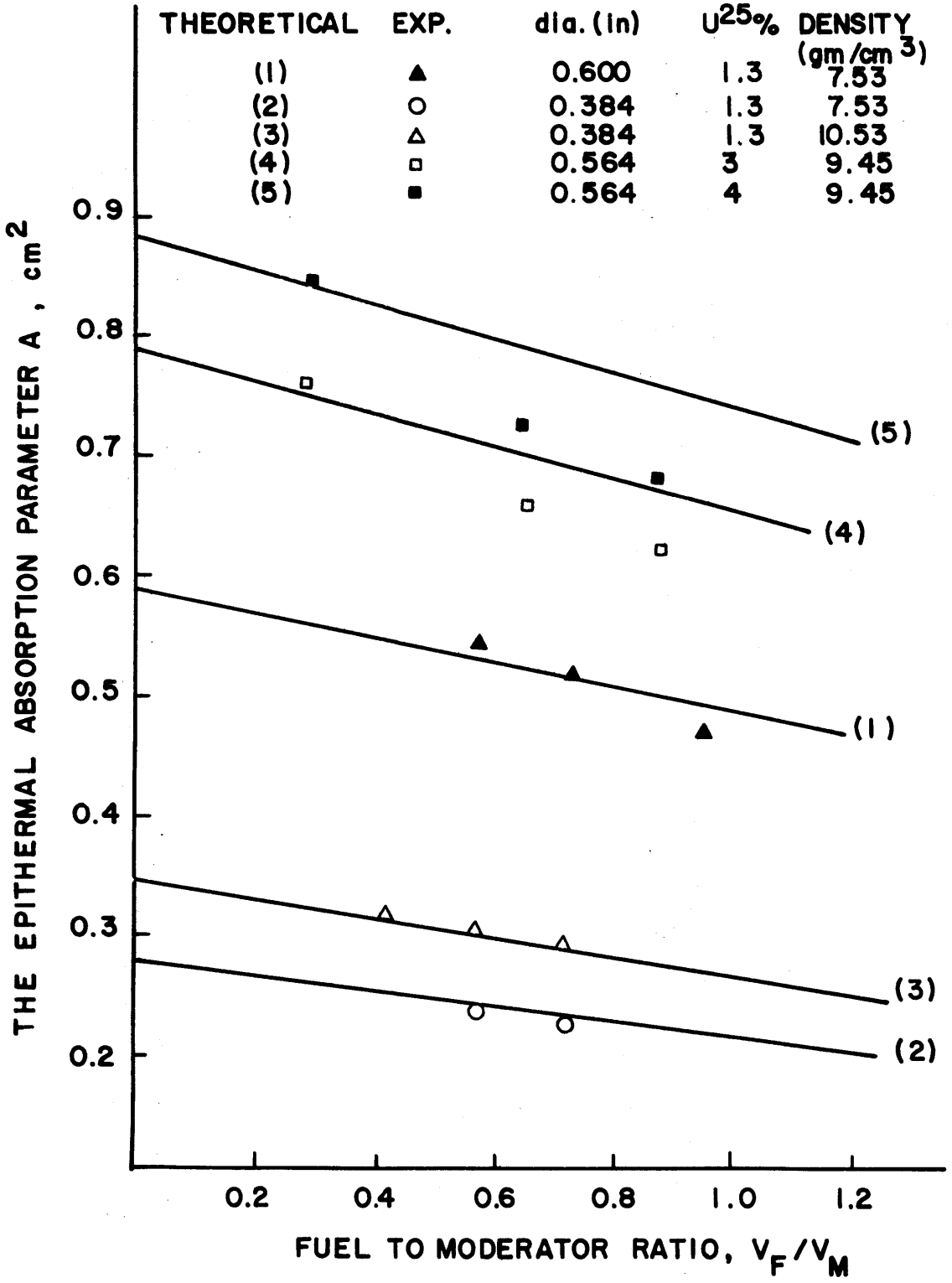

FIG. 4.3 THE PARAMETER A FOR UO_2 RODS IN H_2O LATTICES

previously demonstrated for D_2O-moderated systems.

Finally, Eq. 4.9 shows that single-element results in different moderators are simply related:

$$\frac{A_{SE1}}{A_{SE2}} = \frac{(\xi \Sigma_{SM})_1}{(\xi \Sigma_{SM})_2} . \tag{4.11}$$

Equation 4.11 predicts that A_{SE} in H_2O would be approximately 0.13 times that in D_2O and 0.04 times that in graphite. Although direct experimental confirmation of this simple prescription is lacking, we should be able to place a high degree of reliance upon this relation in view of the extensive work which has been done with the effect of moderator properties on the effective resonance integral.

4.3 Experimental Investigations

Single-rod exponential experiments were attempted on two UO_2 fuel rods in H_2O moderator: one an unirradiated element and the other a fuel pin which had previously been irradiated to 20,000 MWD/T burnup in the Dresden BWR. Table 4.4 lists some of the pertinent parameters for the fuel rods in question.

TABLE 4.4

Fuel Elements Studied in H_2O Moderator

Quantity	Primary Standard	Unirradiated 1.3% UO_2 Rod	Irradiated* Dresden Pin
Fuel Type	U-Metal	UO_2	$UO_2 + PuO_2$
Density (g/cc)	18.9	10.1	--
Diameter (in.)	1.01	0.491	0.38
Enrichment: Wt. % U-235	0.71	1.3	0.935 0.398 ($Pu^{239} + Pu^{241}$) 0.177 ($Pu^{240} + Pu^{242}$)
Cladding Type	A1	A1	Zircaloy-2
Thickness (in.)	0.014	0.030	0.022
Burnup	0	0	20,200 MWD/TU

*GE/AEC designation A4, removed from the Dresden-I BWR on 1/13/67.

4.3.1 Experimental Procedures

The experimental procedures, with the exceptions noted below, were identical to those previously developed for, and successfully applied to, D_2O-moderated systems at M.I.T., as described in Chapter 2 of this report and reference (3). The exponential tank employed was again the facility driven by the M.I.T. reactor, with the D_2O moderator replaced by distilled demineralized H_2O. The following four quantities were measured in the moderator surrounding the fuel element: the cadmium ratio of gold foils, the radial distance to the thermal flux peak, the axial buckling (or exponential relaxation length) and the ratio of cadmium-covered gold-to-molybdenum foil activities irradiated on the fuel surface.

One important difference between experiments carried out in H_2O and D_2O is the rapid exponential attenuation in the former: for the MITR facility, the measured axial exponential attenuation coefficients for thermal neutron are $\gamma_{H2O} \cong 0.27\ cm^{-1}$ and $\gamma_{D2O} \cong 0.05\ cm^{-1}$. This had several important consequences for the execution of experiments in H_2O:

(a) The flux attenuation was so rapid that statistically useful data could only be obtained in the bottom 16 inches of the tank even though irradiation times were increased to 48 hours, and a well-type scintillation detector was used to achieve a fivefold increase in count rate.

(b) Better horizontal alignment of foil holders was required to avoid errors due to flux tilt, which could otherwise give rise to unacceptable errors in the radial traverses carried out to locate the radial flux peak.

(c) Better vertical alignment of foil packets was required to measure the axial variation of the cadmium ratio since the bare and cadmium-covered foils must either be interspersed axially on the same holder or placed at equivalent heights on adjacent holders.

Despite these problems in experimental technique, it was possible to obtain usable data for all foil activations required as input to the single-element method of analysis, although in all instances

the precision was inferior to that achievable in D_2O.

No special innovations in technique over those described by Seth were introduced, although tests were run using both lucite and aluminum foil holders because it was thought that moderator displacement effects might be more important in H_2O: no effects were in fact observed for the present experiments.

The crux of the experimental difficulties encountered is illustrated in Fig. 4.4, which shows the results of the bare and cadmium-covered axial foil traverses for the 1.3% enriched UO_2 fuel rod. Similar results were obtained for the Dresden fuel pin and for the reference fuel rod, a 1-inch-diameter, natural uranium metal rod. Note that while both epicadmium and subcadmium neutrons are reasonably well described by exponentials, the slopes differ and thus the cadmium ratio varies with height. Since all of the theoretical foundation permitting interpretation of single-element experiments is based upon achievement of axial spectral equilibrium, this factor precluded meaningful interpretation of the data to extract the parameters Γ and η. Tests were carried out to show that this anomaly was not influenced by the choice of foil size, foil holder material or the radial position at which the axial traverse was measured.

Since determination of the parameter A is carried out independently of the other parameters, it was possible to measure this quantity.

4.3.2 Determination of A

The procedure employed for the determination of the epithermal absorption parameter, A, was identical to that developed for D_2O-moderated systems. As described in Chapter 2 of this report, the procedure involves measurement of the ratio of activities induced in cadmium-covered gold and molybdenum foils irradiated on the fuel element surface, comparison with a standard rod, and use of multigroup calculations (i.e., the ANISN program) to generate normalization and calibration curves.

Figure 4.5 shows the ANISN-generated curve of the foil activity ratio versus the parameter A. It indicates a value of A determined from the experimental ratio, Fe = 1.637 ± 0.025, using the normalization factor, C = 0.383 ± 0.010, determined by measurements on the

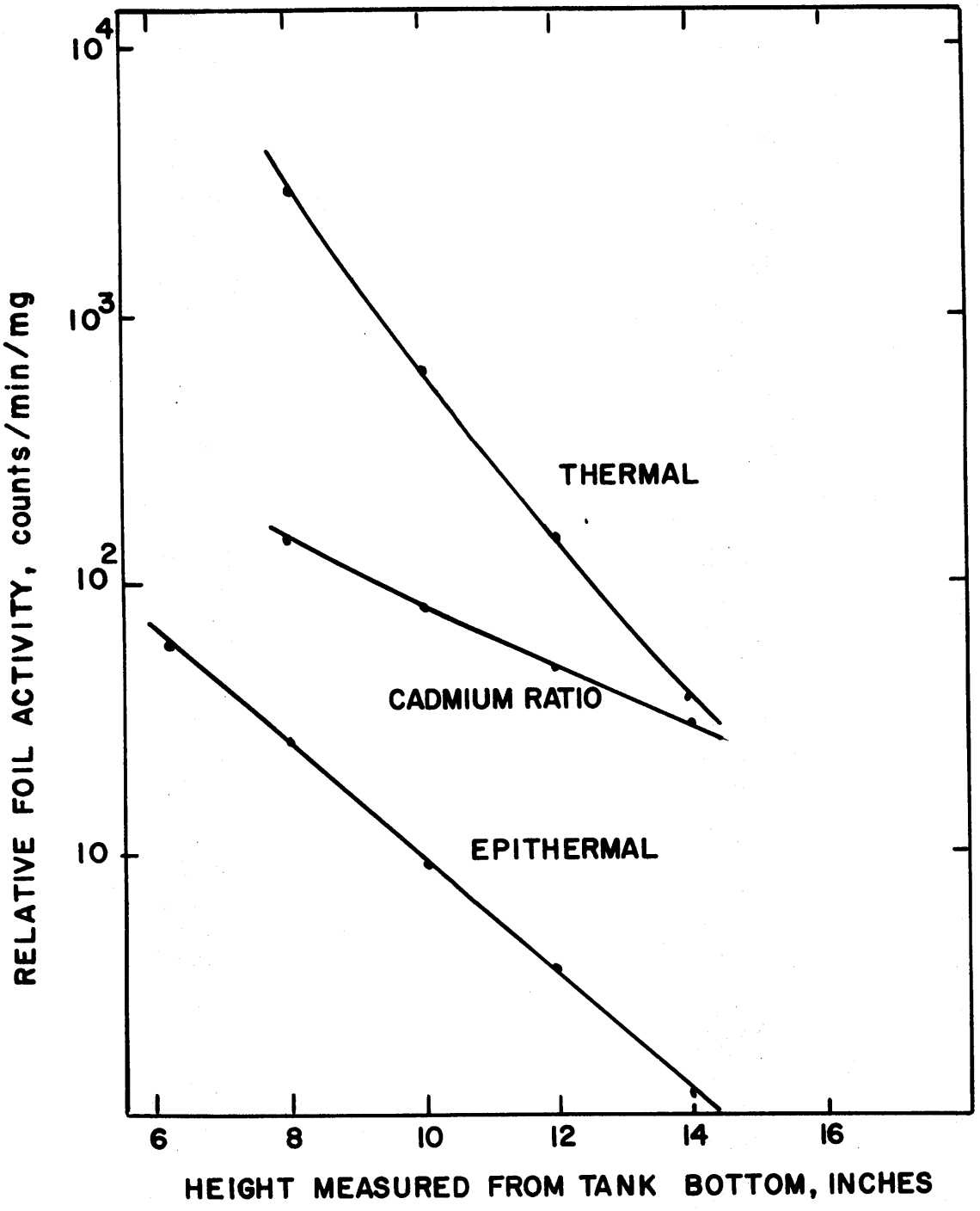

FIG. 4.4 AXIAL FLUX DISTRIBUTION FOR 1.3% UO_2 FUEL ROD

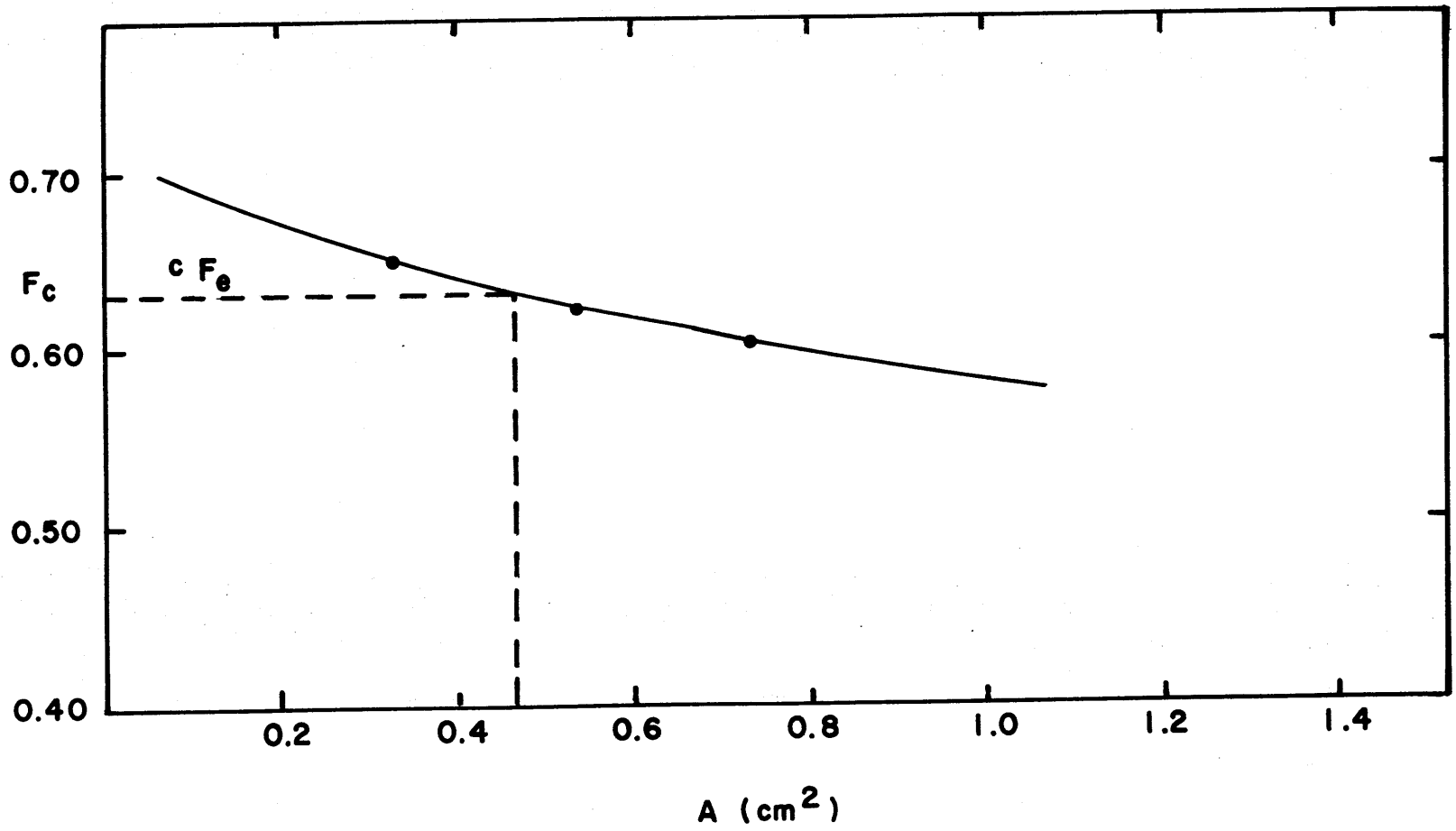

FIG. 4.5 A PLOT OF F_c VERSUS A FOR THE 1.3% ROD

1-inch-diameter, natural uranium reference rod; the value of A inferred in this manner for the 1.3% enriched fuel rod is:

$$A = 0.48 \pm 0.12 \text{ cm}^2,$$

which is in good agreement with the theoretical value of 0.46 cm^2 (1). This figure also demonstrates an important inherent limitation on epithermal absorption parameter measurements in H_2O. As can be seen, small errors in the foil ratio give rise to large errors in A: a ± 2% uncertainty in F, which is a reasonable expectation from foil activation experiments, gives rise to a corresponding ± 25% uncertainty in A. This is to be contrasted to the situation for D_2O moderator where a comparable error in F leads to ± 8% uncertainty in A (3). Thus, even if all other anomalies are resolved, considerably greater precision will be required for experiments using H_2O moderator.

Applying corrections for non-1/E flux and Dancoff shadowing, as discussed in section 4.2 of this chapter, values of A appropriate for two representative lattices composed of 1.3% enriched fuel rods were computed from the single-element result. The lattice spacings were chosen to correspond to systems of very similar fuel studied experimentally by Klein (9), from which results were readily interpolable for comparison with the present data.

Table 4.5 shows the values of A and the resonance escape probability, p, computed from A, for the single-element results extrapolated to full lattice values and for the (interpolated) Klein data. While the single-element method A-values are 15% lower than the corresponding lattice values, p is only 4% higher because A is proportional to (1-p).

TABLE 4.5. Comparison of Epithermal Parameters for Lattices of 1.3% Enriched Fuel

V_f/V_m	A_k (cm^2)	A_L (cm^2)	p_k	p_L
1.40	0.469	0.416	0.726	0.757
1.76	0.486	0.421	0.776	0.804

V_f/V_m = fuel to moderator volume ratio in unit cell of lattice.

p_k, A_k = "measured" values from foil activation experiments reported by Klein et al. (9).

p_L, A_L = lattice values calculated from measured single-element value of A = 0.480 cm^2.

4.3.3 Other Experimental Problems

One other important problem encountered in the interpretation of light water single rod experiments involves determination of the diffusion-theoretic radial flux peak. In heavy water systems, transport effects on peak location are negligible (3), but this is not the case with H_2O. Since the measurement naturally contains the transport effect, it is necessary to correct the data to obtain a value consistent with the use of a diffusion kernel treatment of thermal neutron behavior. The method employed in this research involved use of the ANISN code in both the diffusion and S_8 options to obtain a correction factor directly in terms of the ratio of diffusion to experimental distances. Thus, for example, for the 1.3% enriched fuel the ANISN calculations gave an 11% increase in the distance to the peak.

A second difficulty which complicated interpretation of the experimental data involved the determination of the perturbed radial buckling, α^2. In D_2O-moderated experiments it was possible to infer this quantity from the simple expression $\alpha^2 = \gamma^2 - L_o^{-2}$, where γ^2 is the measured axial buckling and L_o^{-2} is the moderator diffusion area. In D_2O, $L_o^{-2} \ll \gamma^2$, but in H_2O these two quantities are of comparable magnitude and their difference is comparable to the uncertainty in each quantity. Thus, application of this prescription led to negative values of α^2, in contradiction to the obvious convex radial flux profile. This problem was avoided by iterative adjustment of the radial buckling value until the calculated and measured radial flux profiles gave the same location for the radial flux peak. This procedure was possible because in the single-element method the problem is overdetermined: four quantities are measured, but only three fuel characterization parameters are inferred.

Finally, on the positive side of the ledger, note should be taken of the fact that no particular difficulty was encountered in handling the highly radioactive Dresden fuel pin. The transfer flask used by Agarwala in the research described in Chapter 5 proved adequate for moving the fuel to and from the exponential facility; and when in the exponential tank, the moderator provided sufficient shielding to permit experimenters access for the short time spans required for foil packet

insertion and retrieval. The only condescension made to the special nature of the fuel was the use of a special foil holder to place the gold and molybdenum foils used in the A measurement up against the fuel rod, rather than to tape the foil packet to a rod as was done for the much less radioactive fuel elements previously studied.

4.3.4 Sensitivity Studies

As part of the feasibility investigation into single rod experiments in H_2O, a sensitivity study was carried out. In this study the variation of the three heterogeneous parameters Γ, η and A was calculated as a function of variation in several experimentally measured quantities: x (distance to the radial thermal flux peak), γ (axial relaxation coefficient), R (the cadmium ratio of gold), α (square root of the radial buckling), F (gold to molybdenum foil activity ratio). The computer code THINK, written by Seth (3), was used to generate the required functional variations.

Figures 4.6 through 4.8 show the results for a representative single rod experiment in H_2O, while Figs. 4.9 through 4.11 show comparable results for Seth's experiments in D_2O. These studies show that while Γ and η are only slightly more sensitive to errors in the experimental data, in the H_2O case A is a factor of three more sensitive to errors in the gold-molybdenum activity ratio. Thus, the ultimate problem in H_2O experiments would appear to lie in development of a more sophisticated method for analysis of the data to obtain Γ and η; while for A, the problem is basically one of achieving significantly better precision in the experimental measurements.

4.4 Conclusions

The investigations described in this chapter have substantially strengthened the conclusion that heterogeneous reactor theory can be successfully applied to H_2O-moderated lattices. Anomalous variation of the characterization parameters compared to their behavior in other moderators, such as D_2O and graphite, has been shown not to occur if proper attention is paid to the fact that the volume fraction of fuel is large in H_2O-moderated unit cells.

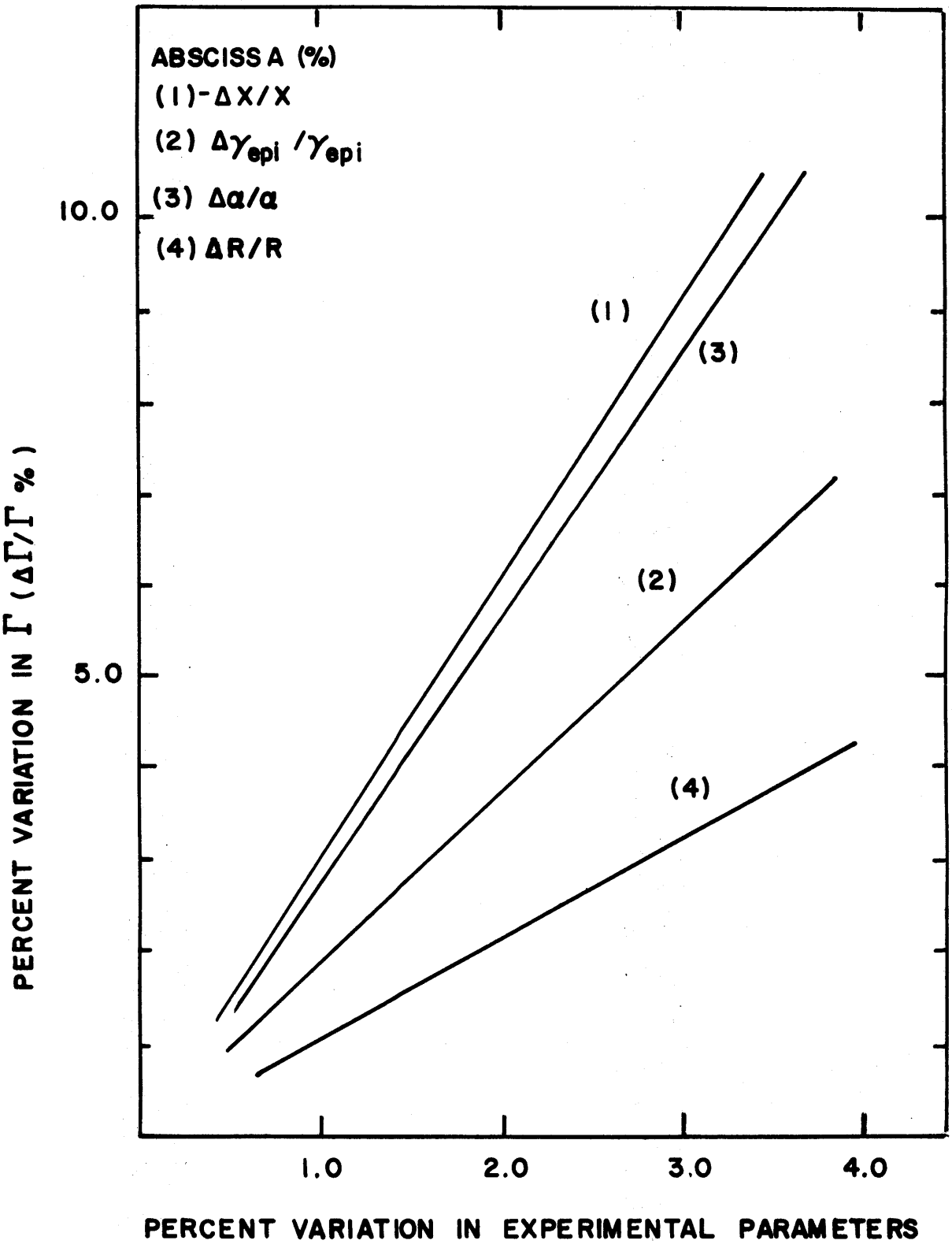

FIG. 4.6 SENSITIVITY OF Γ IN H_2O EXPERIMENTS

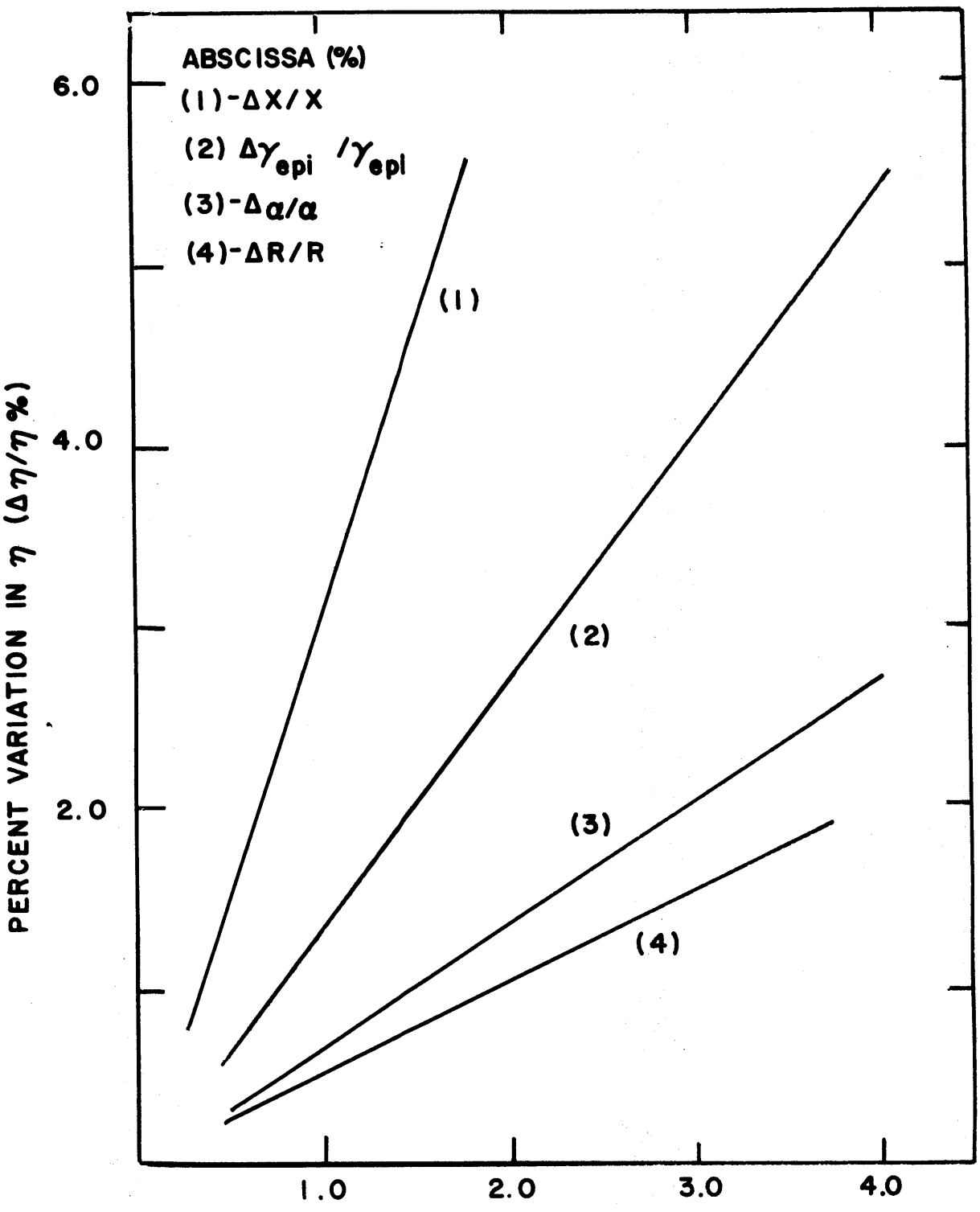

FIG. 4.7 SENSITIVITY OF η IN H_2O EXPERIMENTS

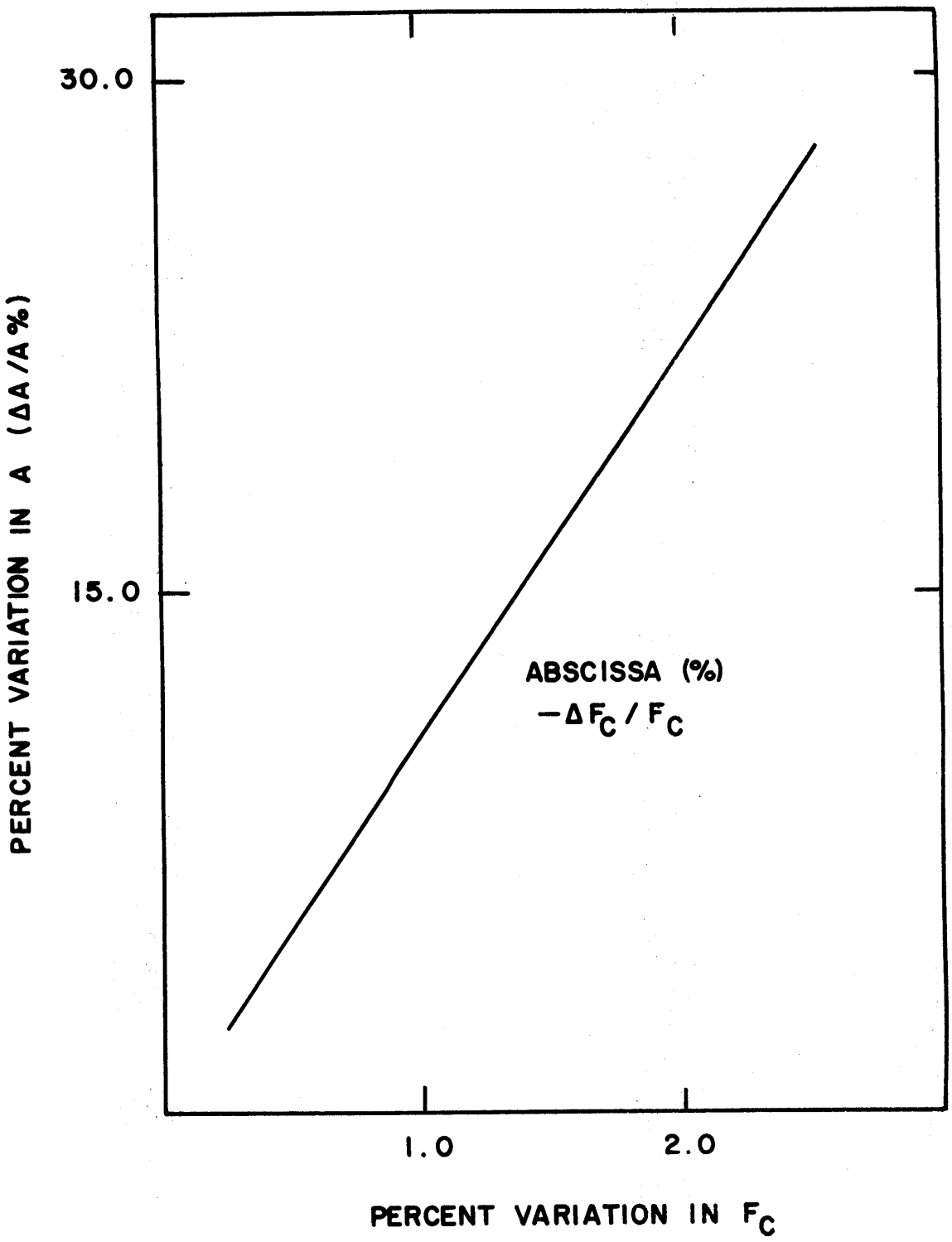

FIG. 4.8 SENSITIVITY OF A IN H_2O EXPERIMENTS

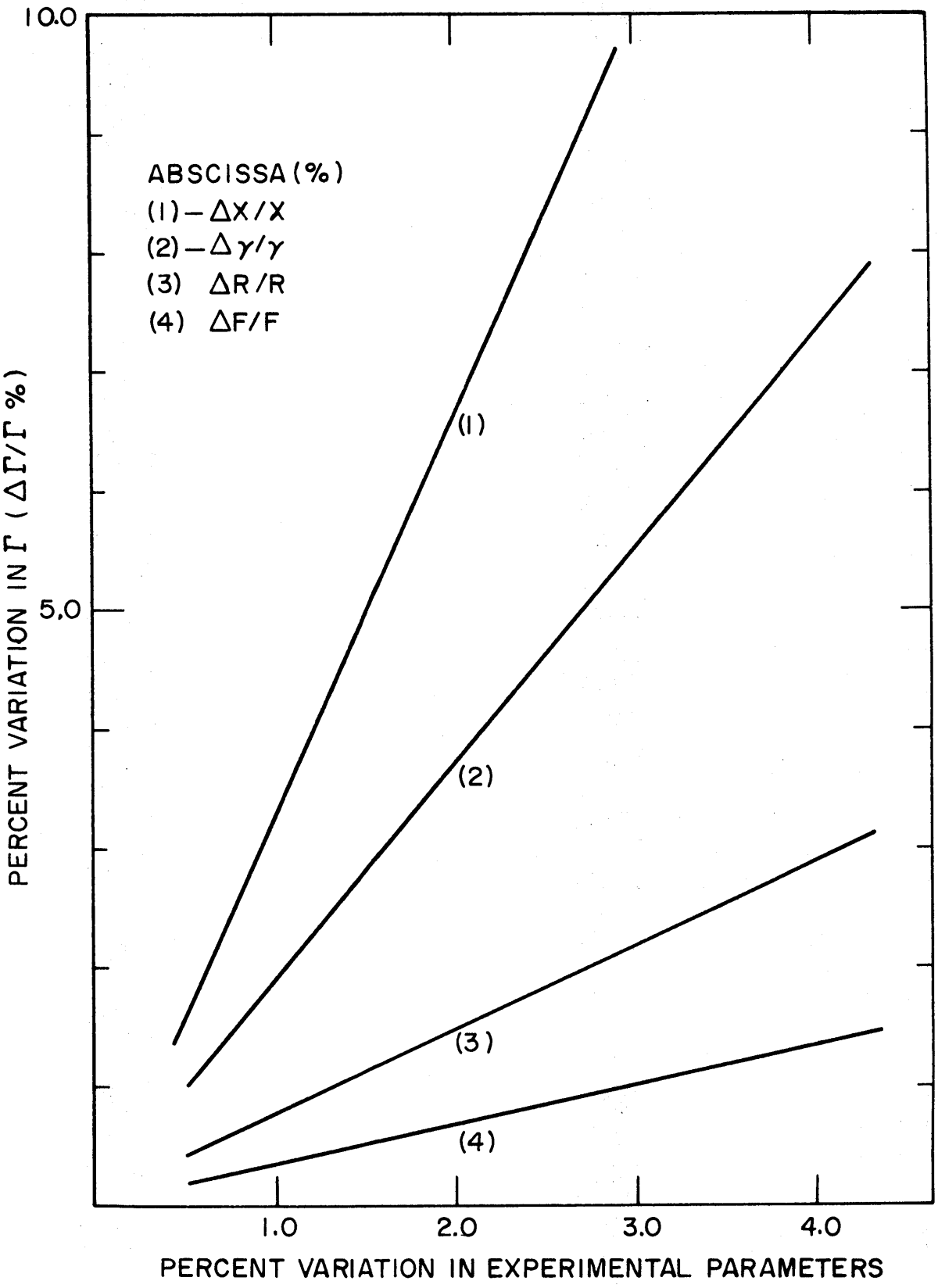

FIG. 4.9 SENSITIVITY OF Γ IN D_2O EXPERIMENTS

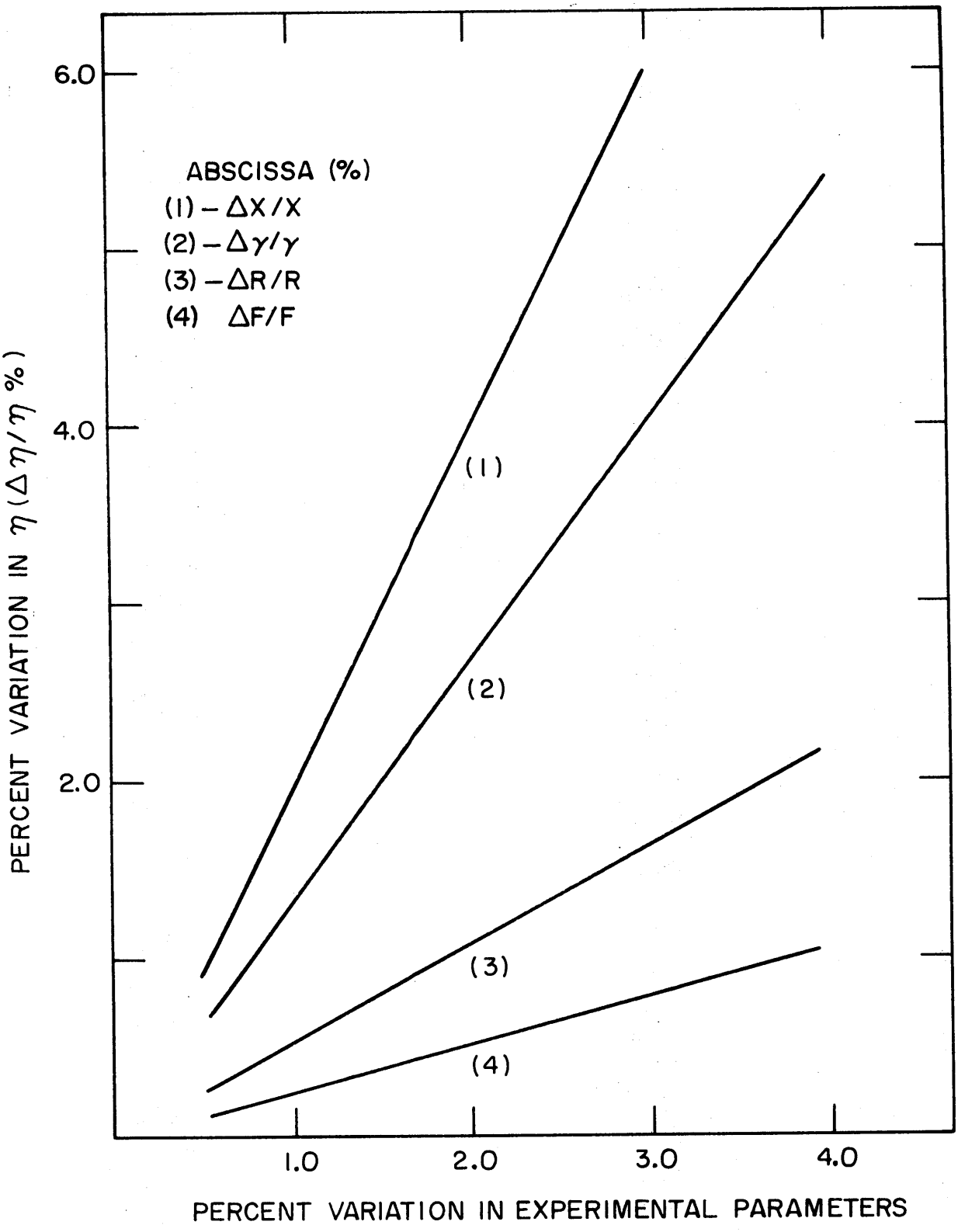

FIG. 4.10 SENSITIVITY OF η IN D_2O EXPERIMENTS

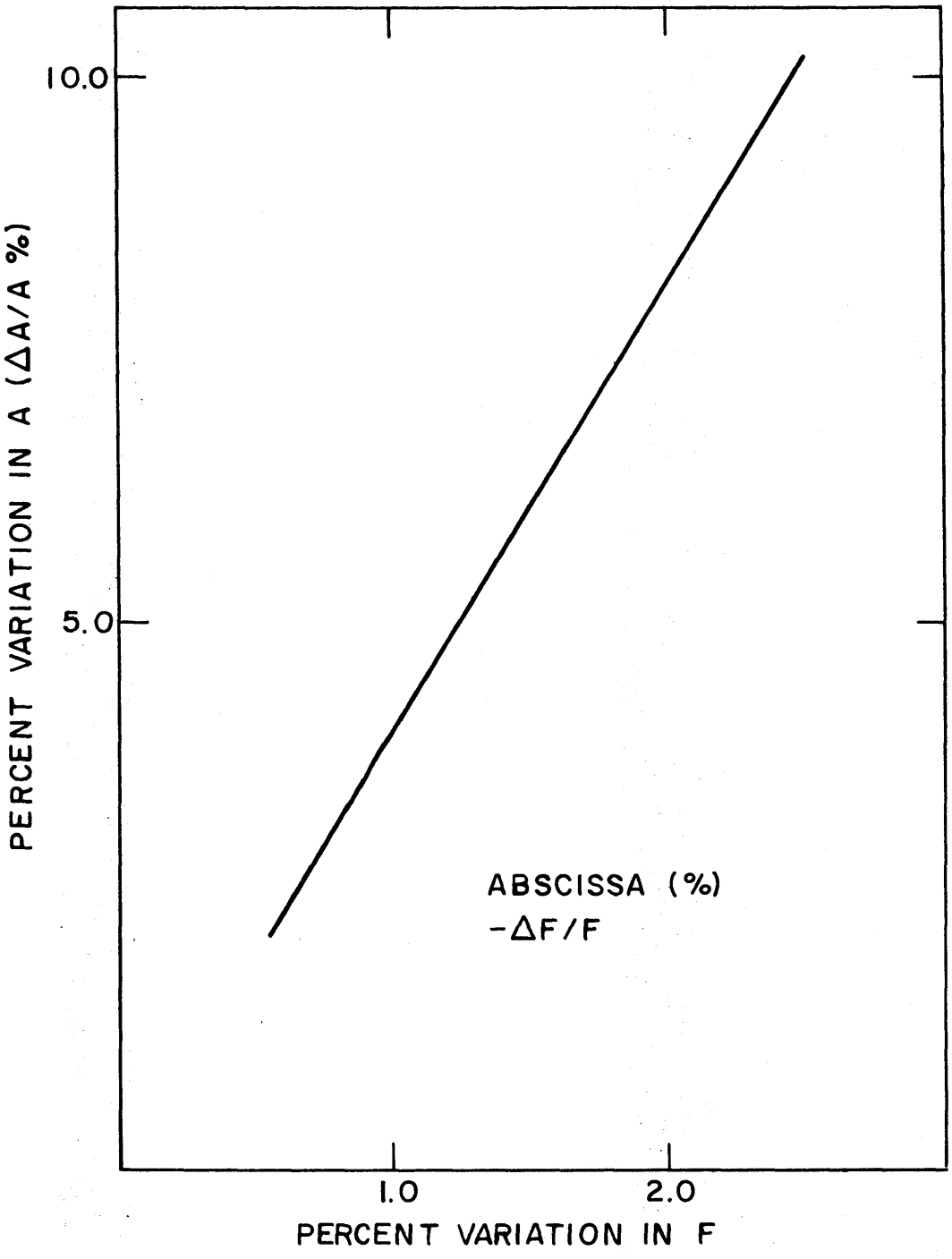

FIG. 4.11 SENSITIVITY OF A IN D_2O EXPERIMENTS

The relations necessary to link single-element and lattice parameter values have been derived and shown to give good agreement with available experimental data, closely following the trends previously established for D_2O-moderated lattices.

Direct determination of the single-element parameters by exponential experiments in H_2O moderator was unsuccessfully attempted. The major problem encountered was the failure to achieve a region of axial spectral equilibrium. Although a more sophisticated technique for analysis of light water experiments might eventually be capable of resolving these difficulties, a second approach is considered to be more practicable based on the present theoretical analysis. It was found that the moderator properties had very little effect on the single-element values of Γ and η and that the effect of A was easily calculated. Thus, measurement of the characterization parameters in easily interpretable experiments using D_2O or graphite appears preferable, followed by calculation of the corresponding values appropriate to H_2O moderator.

4.5 References

(1) M.S. Kazimi, "Reactor Physics Considerations in the Evaluation of the Heterogeneous Parameters A, Γ and η in Light Water Lattices," S.M. Thesis, Massachusetts Institute of Technology, Department of Nuclear Engineering, October 1970.

(2) L.L. Izzo, "The Determination of H_2O Lattice Parameters from Single-Element Experiments," S.M. Thesis, M.I.T., Department of Nuclear Engineering, September 1970.

(3) S.S. Seth, M.J. Driscoll, I. Kaplan, T.J. Thompson and D.D. Lanning, "A Single-Element Method for Heterogeneous Nuclear Reactors," MIT-3944-3, MITNE-109, May 1970.

(4) E.E. Pilat, M.J. Driscoll, I. Kaplan and T.J. Thompson, "The Use of Experiments on a Single Fuel Element to Determine the Nuclear Parameters of Reactor Lattices," MIT-2344-10, MITNE-81, February 1967.

(5) G.T. Hamilton, "Application of the Single-Element Method to Light Water Lattices," S.M. Thesis, M.I.T., Department of Nuclear Engineering, June 1969.

(6) C.N. Klahr et al., "Test and Verification of Heterogeneous Calculation Methods," NYO-3194-1 (1964).

(7) R.E. Donovan, "Determination of the Heterogeneous Parameters Γ, A and η by Measurements on a Single Fuel Element," S.M. Thesis, M.I.T., Department of Nuclear Engineering, December 1967.

(8) M.J. Higgins, "Determination of Reactor Lattice Parameters Using Experimentally Measured Kernels," S.M. Thesis, Department of Nuclear Engineering, January 1968.

(9) D. Klein et al., "Measurements of Thermal Utilization, Resonance Escape Probability, and Fast Effect in Water-Moderated, Slightly Enriched Uranium and Uranium Oxide Lattices," Nucl. Sci. Eng., Vol. 3, No. 4, April 1958.

(10) G.C. Pomraning and M. Clark, Jr., "A New Asymptotic Diffusion Theory," Nucl. Sci. Eng., Vol. 17, No. 2, October 1963.

(11) G.J. Bell, "A Simple Treatment for Effective Resonance Absorption Cross Sections in Dense Lattices," Nucl. Sci. Eng., Vol. 5, No. 2, February 1959.

5. GAMMA SPECTROSCOPY OF PARTIALLY BURNED FUEL

V. K. Agarwala

5.1 Introduction

Nondestructive analysis has been made of fuel pins irradiated previously in the Dresden BWR to 20,000 MWD/MT (1). The properties of these fuel pins are summarized in Tables 5.1 through 5.4.

For this analysis, high resolution Ge(Li) gamma-ray spectroscopy was employed, using essentially the same apparatus as already described by Hukai in Chapter 3 of this report. The primary effort was focused on the use of long-lived fission product decay gammas to determine burnup level through extension of methods developed by Sovka (2), but work was also done on prompt capture and fission gammas and on short-lived fission product decay gammas following the procedures developed by Hukai for fresh fuel (3).

The results reported in this chapter will be concerned primarily with the processed data and their analysis, since the 4TH1 Irradiation Facility, which was used for all of this work, and associated detectors, electronics systems, and the data analysis program (GAMANL) have already been completely described elsewhere (3). Likewise, while the use of highly radioactive spent fuel required the development of remote handling and encapsulation procedures, the design of special tools and a shielded transfer flask, these followed rather straightforward precedent and the mechanical details are fully described in reference (1).

5.2 Burnup Analysis

In this phase of the work the use of decay gammas from long-lived fission products was evaluated for the determination of self-consistent values of burnup, fluence, flux and irradiation time. The method employed is an extension of that previously applied by Sovka to highly enriched MITR fuel (2). It is based upon analysis of representative radionuclides from each of three groups of fission products:

TABLE 5.1

Irradiation History of Fuel Pins

Reactor	VBWR*			DNPS**		
Fuel Pin	Date Charged	Date Discharged	In-Pile Residence Time (sec.)	Date Charged	Date Discharged	In-Pile Residence Time (sec.)
A4	1/11/61	12/9/63	0.92×10^8	6/9/64	1/13/67	0.82×10^8
A28	6/7/61	12/9/63	0.79×10^8	6/9/64	1/13/67	0.82×10^8

*VBWR = Vallecitos Boiling Water Reactor

**DNPS = Dresden-I Nuclear Power Station

TABLE 5.2

Pre-Irradiation Data for Fuel Pins

Fuel Pin	A4	A28
Total Length (in.)	40.73	40.72
Active Length (in.)	37.0	37.0
Clad (Zircaloy) (in.)	0.030	0.030
Rod Diameter (in.)	0.426	0.430
U^{235} Enrichment (%)	2.76	2.76
Weight UO_2 (gm.)	693.30	703.00
Weight U (gm.)	610.10	618.64
Weight U^{235} (gm.)	16.84	17.07

TABLE 5.3

Post-Irradiation Data After VBWR

Fuel Pin	A4	A28
Weight U (gm.)	603.63	610.92
Weight U^{235} (gm.)	12.31	11.75
Weight Pu (gm.)	1.98	2.31
Weight 49 + 41 (gm.)	1.73	1.98
Average BU (10^4 MWD/TU)	0.548	0.654

TABLE 5.4

Post-Irradiation Data After DNPS

Fuel Pin	A4	A28
Weight U (gm.)	594.57	602.37
Weight U^{235} (gm.)	5.70	5.44
Weight Pu (gm.)	3.51	3.75
Weight 49 + 41 (gm.)	2.42	2.47
Average BU (10^4 MWD/TU)	2.02	2.12
Percent Depletion	1.825	1.880
Percent U^{235}	0.935	0.880
Percent Pu	0.575	0.606
Percent 49 + 41	0.398	0.400
Percent Fission	2.545	2.622
Percent U	97.455	97.37

(a) Those produced directly from fission or by short half-life precursors: Cs^{137} and Ru + Rh^{106} in the present application.

(b) Those produced from other fission products by (n, γ) reactions: e.g., Cs^{134}.

(c) Those having negligible direct yield but which are also not in secular equilibrium with their precursors: Pr^{144} in the present case.

From these three categories the following activity ratios are constructed:

$$R_1 = \frac{\text{Type (a) activity}}{\text{Type (b) activity}} = \frac{\text{Activity of } Cs^{137}}{\text{Activity of } Cs^{134}}$$

$$R_2 = \frac{\text{Type (a) activity}}{\text{Type (a) activity}} = \frac{\text{Activity of } Cs^{137}}{\text{Activity of } Rh^{106}}$$

$$R_3 = \frac{\text{Type (a) activity}}{\text{Type (c) activity}} = \frac{\text{Activity of } Cs^{137}}{\text{Activity of } Pr^{144}}$$

A combination of experimental and analytical techniques is then pursued to determine burnup, fluence, flux and irradiation time. Experimental determination of R_1, R_2 and R_3 and calculation of the same ratios using some appropriate burnup model permit selection of a self-consistent set of irradiation parameters and end-of-life fuel composition.

5.3 Experimental Results

The gamma-ray spectra of the Dresden fuel pins (I and II in our notation which are, respectively, pins A-28 and A-4 in GE/AEC notation) were measured using the standard Ge(Li) system installed at the 4TH1 beam port. The electronics were employed in free mode operation, and counting live times of 160 minutes were used. The gamma beam was filtered by an 0.50- to 0.75-inch Pb attenuator to reduce low energy background. Figure I shows a typical multichannel spectrum for Pin I. The GAMANL code (4) was used to extract photopeak energies and intensities from the measured spectra. Table 5.5

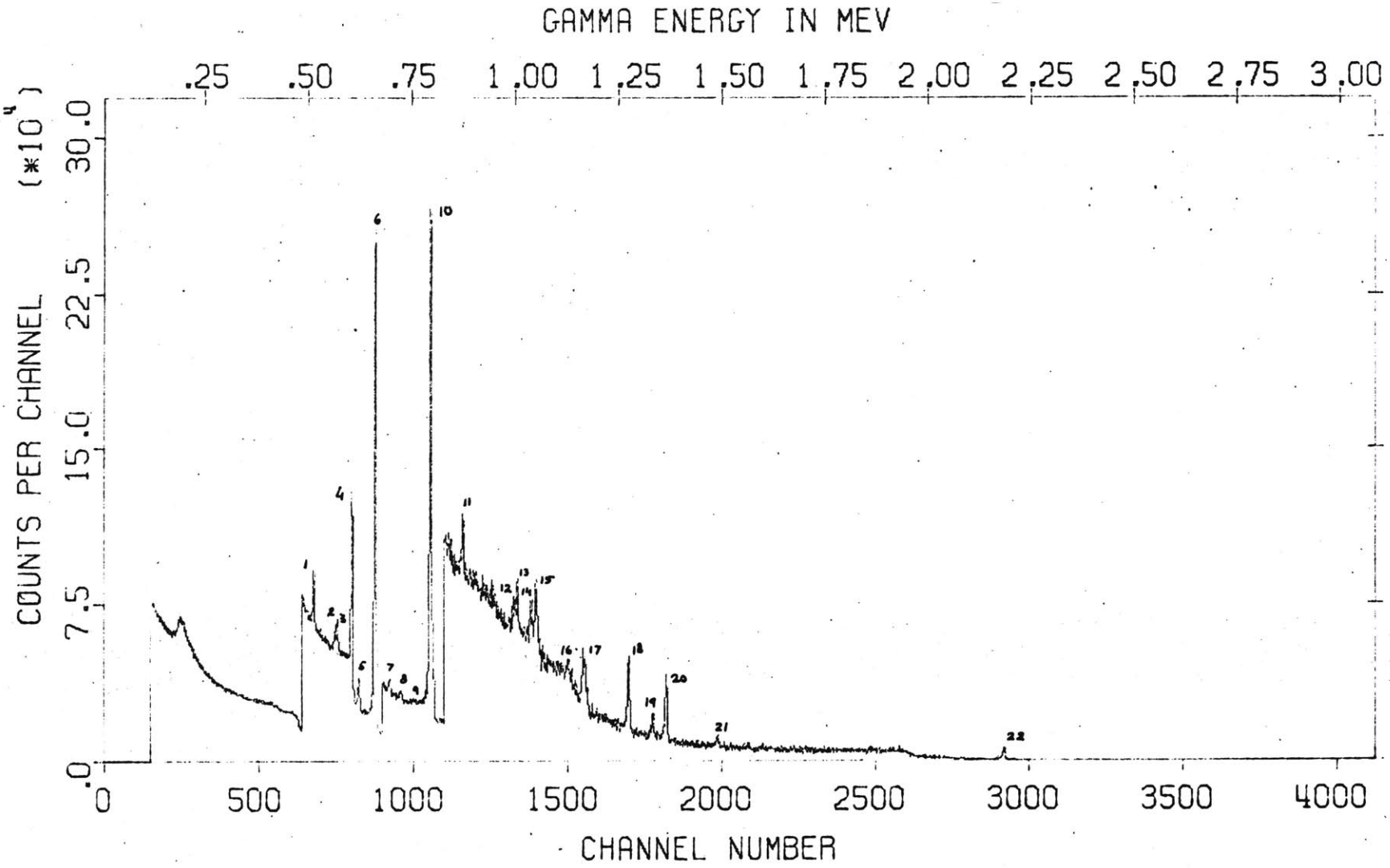

FIG - 5.1 The Long-Lived Fission Product Gamma-Ray Spectrum of Dresden Fuel Pin I Taken in Free Mode

lists the results of this analysis. The resulting data were corrected for decay since irradiation in Dresden, gamma yield per disintegration, counting system efficiency and gamma-ray attenuation to yield corrected activities (sample listed in Table 5.6 for fuel Pin I) from which the ratios R_1, R_2 and R_3 shown in Table 5.7 were then computed.

5.4 Theoretical Analysis

The essential idea behind the subject burnup method is to compare the experimental fission product activity ratios with comparable calculated ratios to find a set of compatible flux, time, fluence and burnup parameters. It is clear that a wide range of possible analytic models exists, having various levels of sophistication. In the present work a simple one-group method was used: effective one-group cross sections were determined for the core constituents using a scheme developed by Malec (5), and these in turn were used in the differential equations governing nuclide concentration during burnup (6). Solution of these equations for continuous irradiation under constant flux then gave a set of fuel nuclide concentrations (hence burnup) and various fission product radionuclide concentrations versus time.

Figures 5.2 through 5.4 show the calculated fission product ratios versus fluence for various fluxes. These functional relationships are solved simultaneously for the fluence ($\phi\tau$), flux (ϕ) and time (τ). Although a computer program was devised to solve these relations through an iterative procedure, the following graphical procedure can also be employed, and is worth description because of the added insight which it can provide. The experimental value of the appropriate fission product activity ratio, R, is used to enter the figure at an appropriate value on the vertical axis. The dotted lines in Figs. 5.2, 5.3 and 5.4 trace out typical values and their intersections with the function curves. These intersections can be used to plot a new family of fluence vs. flux curves: a sample is presented in Fig. 5.5. The common intersection of these latter curves defines a compatible set of ϕ and τ values. As can be seen from Fig. 5.5, the combined effect of experimental error and analytical oversimplification leads to a non-coincident set of intersections in this over-determined problem. The

TABLE 5.5

Gamma-Ray Peaks Extracted from the Long-Lived Fission Product Gamma-Ray Spectra of the Dresden Fuel Pins

Peak Number	Pin I		Pin II		Fission Product
	Energy (KeV)	Counts	Energy (KeV)	Counts	
1	512.2	25876 ± 3.1%	512.4	30740 ± 2.8%	Rh-106
2	563.2	9964 ± 7.4%	563.0	12010 ± 6.6%	Cs-134
3	569.1	15941 ± 4.8%	570.0	23264 ± 3.5%	Cs-134
4	605.0	104883 ± 1.0%	605.0	152895 ± 0.7%	Cs-134
5	622.3	16440 ± 3.7%	621.8	24884 ± 2.6%	Rh-106
6	662.0	289978 ± 0.5%	661.9	522114 ± 0.3%	Cs-137
7	697.8	4084 ± 10.1%	697.0	5297 ± 8.1%	Pr-144
8	723.4	2054 ± 18.7%	723.0	4126 ± 9.9%	Zr-95
9	---	---	757.9	1481 ± 26.4%	Zr-95
10	796.0	122317 ± 0.8%	796.0	220105 ± 0.5%	Cs-134
11	874.0	2316 ± 13.8%	873.0	4219 ± 8.2%	?
12	996.0	1066 ± 25.3%	995.8	2838 ± 11.0%	?
13	1005.7	2027 ± 14.1%	1004.6	4619 ± 7.1%	?
14	1038.8	1644 ± 16.4%	1038.6	3843 ± 8.1%	Cs-134
15	1050.6	2436 ± 11.6%	1049.5	6995 ± 4.8%	Rh-106
16	1128.6	---	1128.0	---	?
17	1166.7	3143 ± 12.0%	1165.5	6836 ± 4.1%	?
18	1274.7	2414 ± 11.4%	1272.7	8794 ± 3.1%	?
19	1330.8	1109 ± 21.0%	1331.0	1390 ± 11.8%	?
20	1366.4	2045 ± 17.7%	1363.2	8467 ± 3.0%	Cs-134
21	---	---	1486.8	1458 ± 9.6%	Pr-144
22	2182.0	---	2181.2	1739 ± 14.2%	Pr-144

TABLE 5.6

Corrected Fission Product Activity for Pin I

Correction for	[a]Rh-106 / [b](γ-513)	Cs-134 (γ-605)	Rh-106 (γ-624)	Cs-137 (γ-662)	Pr-144 (γ-697)	Cs-134 (γ-796)
Attenuation (1/2" Pb)	0.1327	0.1968	0.2097	0.2321	0.2496	0.2992
Efficiency ($\times 10^5$)	0.0210± 5%	0.0158± 5%	0.0150± 5%	0.0135± 5%	0.122± 5%	0.0100± 5%
Cooling[c]	0.1186± 3%	0.3546± 7%	0.1186± 3%	0.9314± 0.8%	0.0650±0.4%	0.3546± 7%
γ/Disintegration[d]	0.205± 0%	0.98 ± 2%	0.105 ± 5%	0.92 ± 3%	0.0160± 2%	0.95 ± 5%
Total Correction Factor	0.677±5.8%	10.805± 8.8%	0.3917± 7.7%	26.849±5.9%	0.0317± 5.4%	10.079±9.9%
Relative Intensity ($\times 10^9$) ($\times 10^{-4}$)	2.5876±3.1%	10.4883±1.0%	1.6440±3.7%	28.998±0.5%	0.4084±10.1%	12.2317±0.8%
Corrected Activity ($\times 10^{-13}$)	3.822 ±6.6%	0.971± 8.9%	4.197± 8.5%	1.080± 5.9%	12.895±11.4%	1.240± 10%

[a]Radionuclides responsible for observed fission product gammas.

[b]Energies of gamma ray from radionuclides in (a), keV.

[c]Correction for a cooling period of 0.969×10^8 sec.

[d]Obtained from "Nuclear Data Sheets."

TABLE 5.7

Experimental Value of Ratios R_1, R_2 and R_3 for Dresden Fuel Pins

Fuel Pin	R_1			R_2			R_3
	(γ-605)	(γ-796)	Average	(γ-513)	(γ-624)	Average	
I	1.11 ± 0.12	0.87 ± 0.10	0.99 ± 0.16	0.283 ± 0.025	0.257 ± 0.026	0.27 ± 0.036	0.084 ± 0.010
II	1.23 ± 0.13	1.03 ± 0.12	1.13 ± 0.18	0.306 ± 0.027	0.274 ± 0.027	0.29 ± 0.038	0.111 ± 0.013

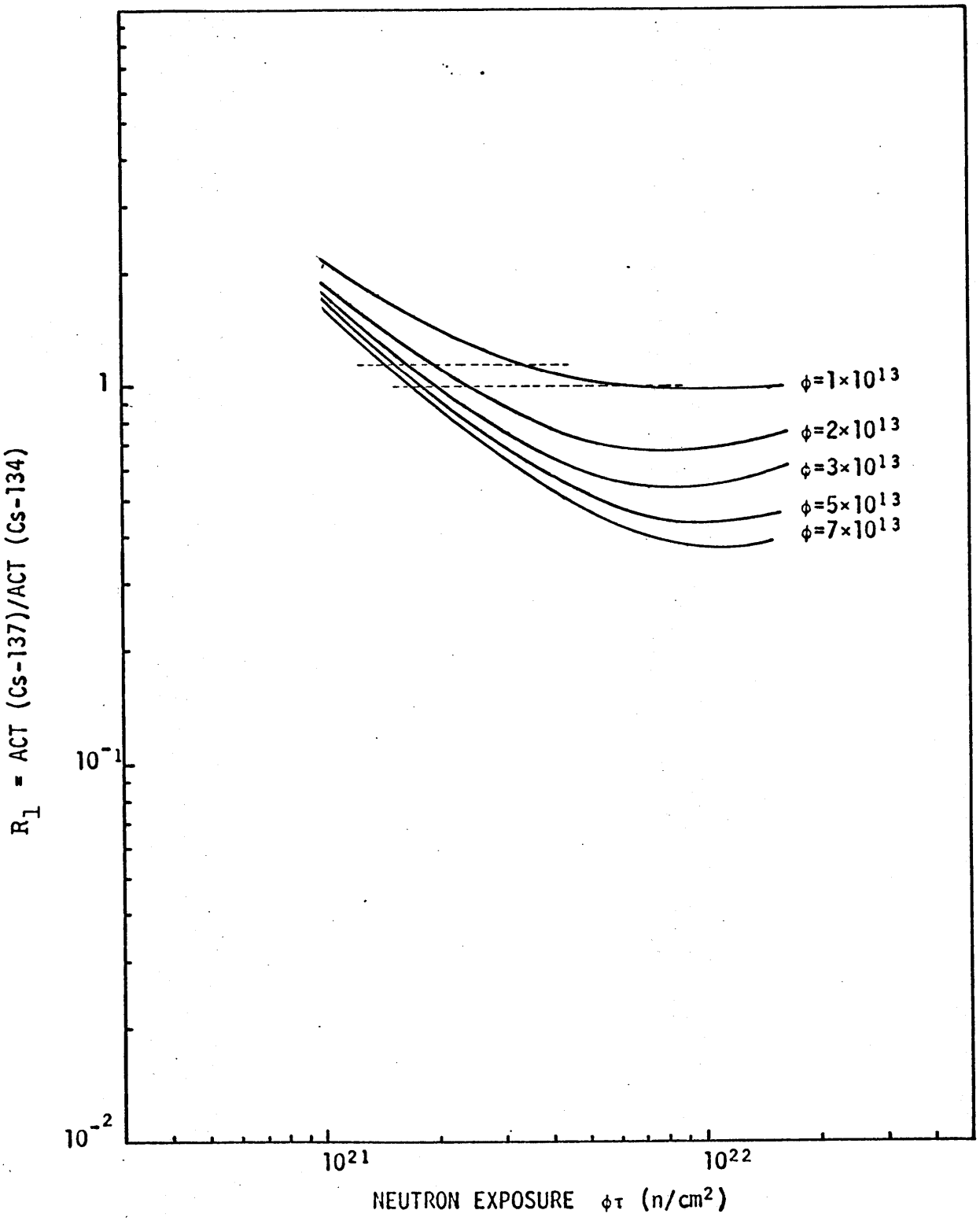

FIG - 5.2 Ratio of Cs-137 to Cs-134 Activities vs. Neutron Exposure for the Dresden Fuel at Various Fluxes

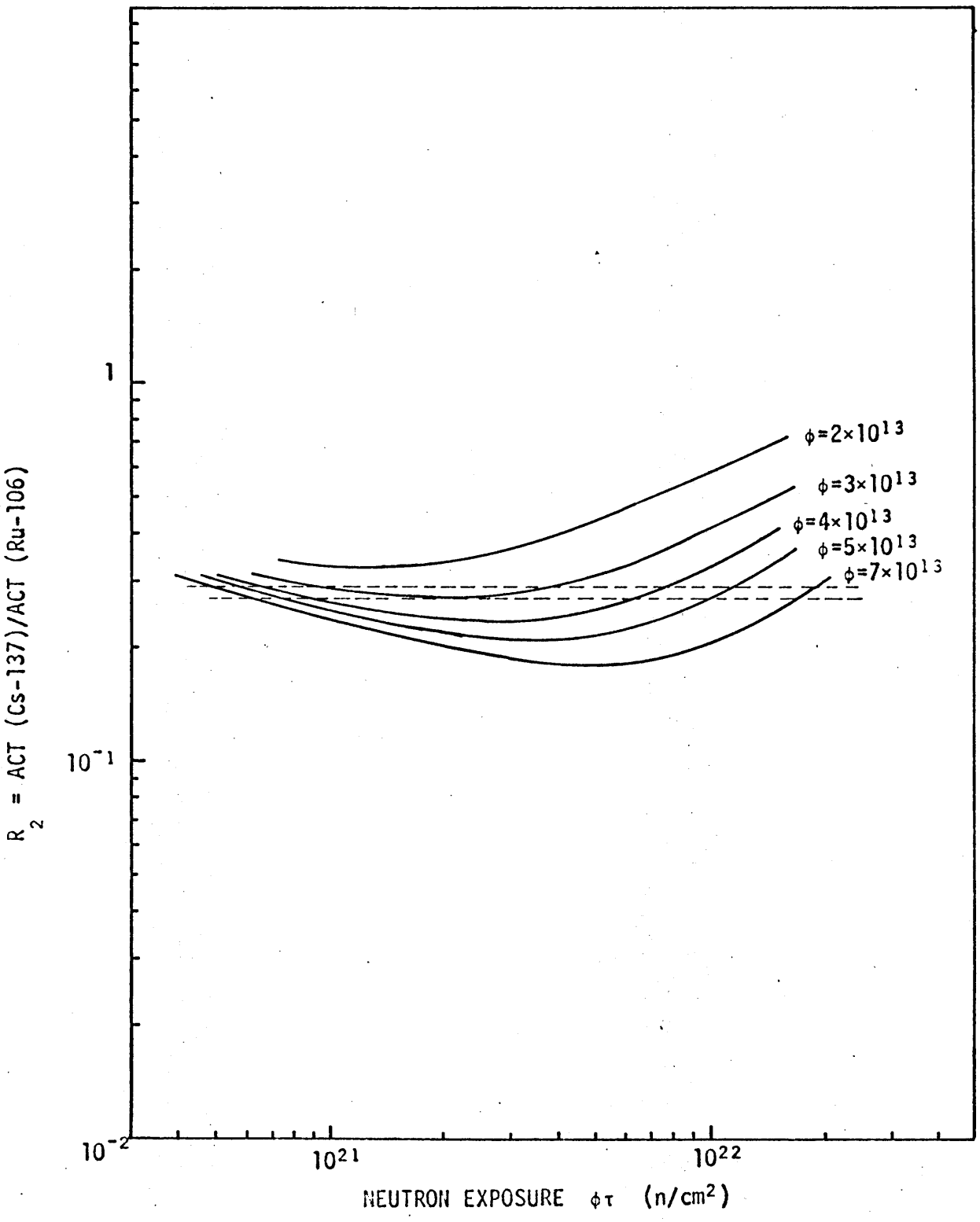

FIG - 5.3 Ratio of Cs-137 to Ru-106 Activities vs. Neutron Exposure for the Dresden Fuel at Various Fluxes

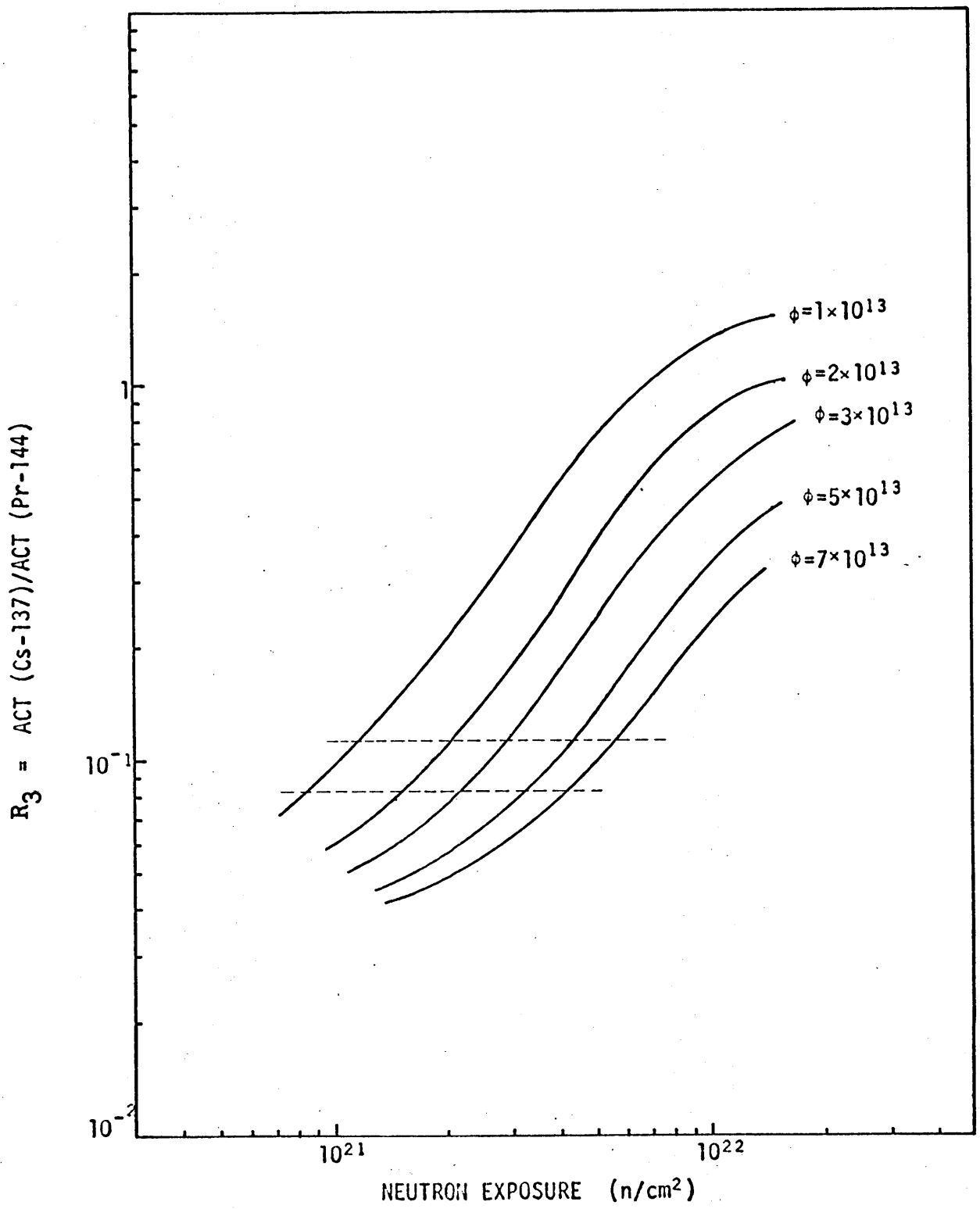

FIG - 5.4 Ratio of Cs-137 to Pr-144 Activities vs. Neutron Exposure For the Dresden Fuel at Various Fluxes

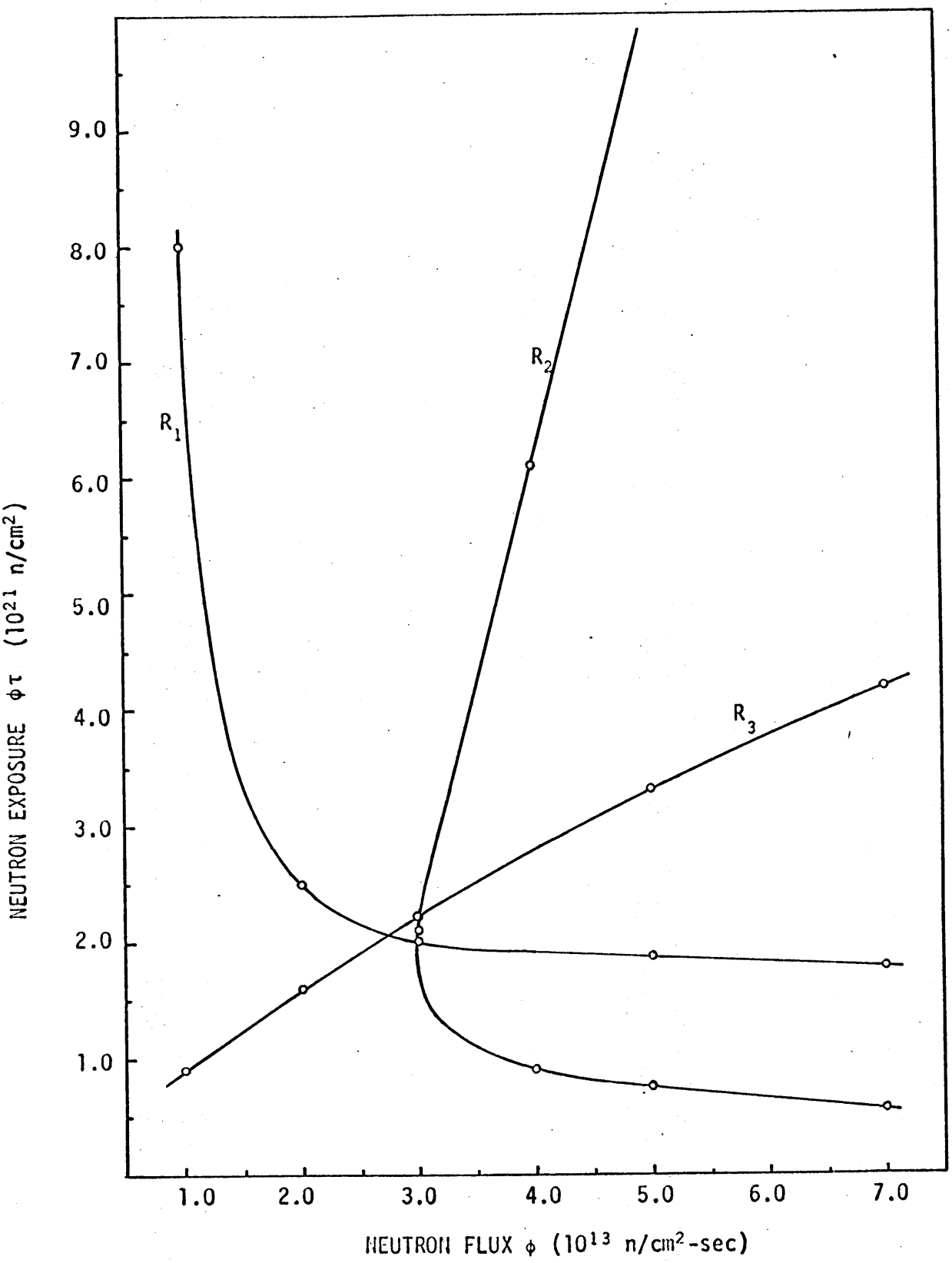

FIG - 5.5 Curves of Neutron Exposure vs. Neutron Flux for Activity Ratios R_1, R_2 and R_3 for Dresden Fuel Pin I

results are, however, in good agreement and define a set of values within a tolerable error bound.

Table 5.8 summarizes the results obtained in this manner for the two Dresden fuel pins. The quoted uncertainties are standard deviations estimated from two independent determinations. It should be noted that the flux and time quoted are effective values, which require further interpretation before comparison with other data. The "flux," for example, is an effective one-group value whose magnitude depends upon the prescription used to define the one-group cross sections. Thus it is more meaningful to extract from the total flux the thermal flux component. Similarly, the "time" quoted is an effective full-power value which must be corrected for plant capacity factor. Table 5.9 presents the results so interpreted. As can be seen, they are in good agreement with the nominal results quoted for the fuel pins by the supplier. In particular, the data of primary interest – burnup – is within the quoted uncertainty of the analysis.

5.5 Discussion

The results of the burnup characterization confirm the validity of the present approach for validating burnup history and for assaying burnup level. Some obvious improvements could clearly improve this approach still further:

(1) Conducting the experiment within a few months to one year of the end of irradiation, rather than over three years as in the present case. This would improve the statistical accuracy of the experimental data, particularly for Pr^{144}, and lead to more accurate experimental activity ratios.

(2) Using more sophisticated computer programs such as LEOPARD (7) and CINDER (8) for the burnup calculations required to generate theoretical values of the activity ratios.

(3) Using more gamma rays for each fission product, and more fission products, in the analysis.

(4) Obtaining better nuclear data on key constituents, such as the (n, γ) cross section Cs^{133}, and on the half lives of all fission products used in the analysis.

TABLE 5.8

Calculated Irradiation Data for Dresden Fuel Pins I and II

	Pin I	Pin II
Average "one-group" flux, ϕ (n/cm^2-sec)	2.855×10^{13}	1.887×10^{13}
Total neutron exposure, $\phi\tau$ (n/cm^2)	2.076×10^{21}	1.979×10^{21}
Total irradiation time, τ (sec)	0.727×10^{8}	1.048×10^{8}
Burnup due to fission in U^{235} (MWD/MTU)	13,899 ± 12%	13,525 ± 11%
Burnup due to fission in Pu^{239} (MWD/MTU)	2,948 ± 36%	2,729 ± 31%
Burnup due to fission in U^{238} (MWD/MTU)	1,766 ± 23%	1,683 ± 21%
Total Burnup (MWD/MTU)	18,613 ± 17%	17,937 ± 15%

TABLE 5.9

Comparison of Neutron Flux, Irradiation Time and Burnup of Dresden Fuel Pins Evaluated in the Present Work with Independently Obtained Data

	Present Work		Independently Obtained Values (1)	
	Pin I	Pin II	Pin A28	Pin A4
Thermal Flux, ϕ (10^{13} n/cm^2-sec)	2.4 ± 0.1	1.9 ± 0.3	2.0	2.0
Irradiation Time, τ (10^8 sec)	0.71 ± 0.04	0.87 ± 0.15	0.81	0.77
Burnup (MWD/MTU)	18,613 ± 17%	17,937 ± 15%	21,200[a]	20,200[a]

[a] Burnup values reported by GE.

In short, by proper assessment, long-lived fission product activities can provide useful information on the burnup status of spent fuel by nondestructive means using state-of-the-art equipment and procedures.

5.6 Prompt Gammas and Those from Short-Lived Fission Products

A second objective of the present work was the application and evaluation of the methods described by Hukai in Chapter 3 and reference (3) for assay of the spent fuel.

The apparatus and procedure developed by Hukai for fresh fuel were used without modification for the Dresden fuel pins. In both the prompt and decay spectra it was found that the photopeaks and background observed were primarily due to the long-lived fission products and not to the desired radionuclides. It was possible, however, to identify the known strongest peaks in the spectra (due to U^{235}, U^{238} and I^{135}) and from these data to compute that successful application of the subject methods could unquestionably be achieved if the neutron flux during the re-irradiation could be increased from the value of 4×10^8 n/cm^2 sec used in this work to about 5×10^9 n/cm^2 sec. Although this could be achieved at the MITR, it would require design and construction of new facilities and experimental setups, and it was therefore decided not to carry this aspect of the work beyond establishment of feasibility through to a demonstration application.

5.7 References

(1) V.K. Agarwala, "Study of Fission Product and Prompt Gamma Rays from Irradiated Dresden Fuel," S.M. Thesis, M.I.T. Nuclear Engineering Department, January 1971.

(2) J.A. Sovka and N.C. Rasmussen, "Nondestructive Analysis of Irradiated MITR Fuel by Gamma-Ray Spectroscopy," AFCRL-65-787, MITNE-94, October 1965.

(3) Y. Hukai, N.C. Rasmussen and M.J. Driscoll, "Some Applications of Ge(Li) Gamma-Ray Spectroscopy to Fuel Element Assay," MIT-3944-5, MITNE-113, April 1970.

(4) T. Harper, T. Inouye and N.C. Rasmussen, "GAMANL – A Computer Program Applying Fourier Transforms to the Analysis of Gamma Spectral Data," MIT-3944-2, MITNE-97, August 1968.

(5) W.F. Malec, "A Simple Physics Model for PWR Core Calculations," S.M. Thesis, M.I.T., Department of Nuclear Engineering, August 1970.

(6) M. Benedict and T.H. Pigford, Nuclear Chemical Engineering, McGraw-Hill Book Company, Inc., 1957.

(7) R.F. Barry, "LEOPARD – A Spectrum-Dependent Non-Spatial Depletion Code for the IBM-7094," WCAP-3269-26 (Revised August 1968).

(8) T.R. England, "CINDER – A One Point Depletion and Fission Product Program," WAPD-TM-334 (Revised June 1964).

6. SUMMARY AND CONCLUSIONS

The conclusions spelled out in the preceding chapters of this report and in the various progress and topical reports issued during the coarse of the project (see Appendix A) are dispersed in location, and overly specific in nature. Therefore, in this chapter an attempt will be made to recapitulate and generalize concerning overall project objectives and accomplishments.

6.1 Introduction

The conviction that an experimentally based version of heterogeneous reactor theory could serve as the basis for a useful reactor physics tool evolved during the Heavy Water Lattice Project at M.I.T. (1). This came about as a result of work carried out at M.I.T. and elsewhere, as referenced in Appendix B. The progress achieved at M.I.T. in this predecessor to the present project is summarized in the topical report by Pilat et al. (2).

Although published work on the theoretical foundation of the heterogeneous method can be traced back as far as 1952, it was not until 1956 that attempts to use single rod experiments to measure fuel characterization parameters were recorded. In recent years the analytical apparatus has been considerably expanded, particularly through development of versions compatible with numerical methods, which in turn has led to the programming of a number of production codes (e.g., HERESY, HETERO, MICRETE). This work was carried out mainly by reactor physicists concerned with D_2O-moderated reactors. The general consensus is that heterogeneous theory can provide a valid and useful description of the neutronic behavior of heavy water moderated reactors. While the analytical and numerical methods development in this area has evolved to the point where useful design tools have been made available to the reactor physicist in the form of production codes, the experimental aspects of the heterogeneous method have received only sporadic attention.

6.2 Review and Evaluation

Previous work on the experimental heterogeneous method had shown that the heterogeneous fuel characterization parameters Γ, η and A could be related to the experimental integral parameters δ_{28}, δ_{25}, and ρ_{28}, which are measured inside a fuel rod using foil techniques (1). This method was not pursued further in the present study, however, because one objective established at the outset was the use of measurements external to the rod, in view of projected applications to fuel types containing both plutonium and fission products, with the attendant contamination hazard if measurements inside the fuel were required.

Thus the first important point established in the present research was the feasibility of devising an experimental heterogeneous method using only external measurements. While satisfactory, the methods which were developed do not decouple the parameter measurements. Specifically, Γ and η are extracted from the data only through solution of a set of coupled equations. With the exception of the Γ determination, the measurements are not absolute in nature, requiring use of a known standard for comparison. Successful application of these methods to clustered fuel rods in D_2O is described in Chapter 2 of this report.

Attention was next devoted to the feasibility of extending the single element or experimental heterogeneous method to H_2O-moderated systems. Analysis indicated that this extension was theoretically possible. While experiments in light water proved to be impracticable, analysis again showed one way around this difficulty, namely the relative simplicity of converting between parameter values in different moderators. Thus, barring the development of alternative experimental techniques in H_2O, the preferable approach appears to be extrapolation of results to H_2O from experimental measurements in a more amenable moderator such as D_2O or graphite.

Parallel to the work devoted to measurement of the heterogeneous parameters, research was conducted into methods for characterization of the composition of test fuel elements. Again, because of the desirability of being able to deal with fuel containing plutonium and

fission products, nondestructive methods, based on high resolution gamma-ray spectroscopy using solid state Ge(Li) detectors, were pursued. Work on fresh fuel is described in Chapter 3 of this report, while measurements using fuel burned up to a level of 20,000 MWD/T are summarized in Chapter 5. It was found that fissile and fertile compositions could be established using methods based on the analysis of prompt or fission product decay gammas. It was also shown that analysis of long-lived fission products in the partially burned fuel could establish burnup level.

6.3 Recommendations

Although recommendations concerning future work might be considered somewhat out of place in a report representing the conclusion of a project, there are several reasons motivating inclusion of this section in the present case. For one, reorientation of AEC priorities in regard to support of thermal reactor physics research occurred during the course of the project, resulting in a reduction in scope in its latter stages, and termination before exhaustive exploitation of the research potential of the topic. Secondly, interest in, and work on, this topic is still alive in the reactor community, as evidenced by the fact that a "Conference on the Analysis of Few Rod Experiments in Reactor Physics" was held in Ispra, Italy in May 1969.

In the area of methods development, one major need is for a method for determination of the epithermal absorption parameter, A, without reliance upon use of multigroup calculations for generation of calibration and normalization curves. One obvious approach would involve the use of reference standard elements geometrically similar to the unknown.

One advance in the theoretical realm worth seeking is a simple relation between the actual and asymptotic surface fluxes on a fuel element. This would permit use of surface current and flux measurements, or traverses near the rod, for determination of the thermal constant Γ. This would also have the considerable advantage of decoupling the Γ and η measurements.

More work is recommended on light water applications, which did not receive as complete an evaluation as those in heavy water in the present work. Development of an alternative experimental approach to the single rod exponential experiment in H_2O will be necessary unless moderator effects are accounted for analytically as suggested in Chapter 4 of this report. In general, more comparisons between the results of heterogeneous calculations and parameters measured on complete lattices, such as the material buckling, are called for in the area of light water lattices.

Finally, although the feasibility of basing the heterogeneous treatment on experimentally measured characterization parameters, rather than on calculated ones, has been established in the present work, it will only be through continued application and evolutionary improvements that this tool can become an established part of reactor physics methods. In its present state of development it can already be of direct use in D_2O-moderated applications. Because of this, and because such experiments can be implemented at a low incremental cost, it would appear that the single element method can best be further developed as part of an on-going research program on heavy water reactors.

6.4 References

(1) Heavy Water Lattice Project Final Report, MIT-2344-12, MITNE-86, September 30, 1967.

(2) E.E. Pilat et al., "The Use of Experiments on Single Fuel Elements to Determine the Nuclear Parameters of Reactor Lattices," MIT-2344-10, MITNE-81, February 1967.

Appendix A

BIBLIOGRAPHY OF REACTOR PHYSICS PROJECT PUBLICATIONS

In this appendix are tabulated all publications directly associated with work performed in the M.I.T. Reactor Physics Project. Sc. D. theses are listed first, followed by S.M. and other theses and then by other publications.

1. Doctoral Theses on M.I.T. Reactor Physics Project

(Also see item 3 for corresponding technical reports.)

Hukai, Yoshiyuti
Some Applications of Ge(Li) Gamma-Ray Spectroscopy to Fuel Element Assay, Ph.D. Thesis, M.I.T. Nuclear Engineering Department, April 1970.
(Thesis Supervisors: N.C. Rasmussen and M.J. Driscoll)

Seth, Shivaji S.
A Single-Element Method for Heterogeneous Nuclear Reactors, Sc.D. Thesis, M.I.T. Nuclear Engineering Department, May 1970.
(Thesis Supervisors: I. Kaplan and M.J. Driscoll)

2. Other Theses on M.I.T. Reactor Physics Project

Agarwala, Vinay K.
Study of Fission Product and Prompt γ-Rays from Irradiated Dresden Fuel, S.M. Thesis, M.I.T. Nuclear Engineering Department, December 1970 (est.).
(Thesis Supervisors: M.J. Driscoll and N.C. Rasmussen)

Hamilton, George T.
Application of the Single-Element Method to Light Water Lattices, S.M. Thesis, M.I.T. Nuclear Engineering Department, June 1969.
(Thesis Supervisor: M.J. Driscoll)

Izzo, Lawrence L.
The Determination of H_2O Lattice Parameters from Single-Element Experiments, S.M. Thesis, M.I.T. Nuclear Engineering Department, September 1970.
(Thesis Supervisors: M.J. Driscoll and D.D. Lanning)

Kazimi, Mujid S.
Reactor Physics Considerations in the Evaluation of the Heterogeneous Parameters A, Γ and η in Light Water Lattices, S.M. Thesis, M.I.T. Nuclear Engineering Department, November 1970.
(Thesis Supervisor: M.J. Driscoll)

Kelley, Thomas J.
Nondestructive Analysis of Irradiated Reactor Fuel by Gamma-Ray Spectroscopy, Naval Engineer and M.S. in Nuclear Engineering, June 1969.
(Thesis Supervisor: M.J. Driscoll)

Leung, Timothy C.
Measurement of η Using Foil Activation Technique, S.M. Thesis, M.I.T. Nuclear Engineering Department, May 1969.
(Thesis Supervisor: M.J. Driscoll)

McFarland, Emerson L.
Experimental Determination of the Epithermal Absorption Parameter, A, S.M. Thesis, M.I.T. Nuclear Engineering Department, November 1969.
(Thesis Supervisor: M.J. Driscoll)

Sicilian, James M.
The Feasibility of Gamma-Ray Spectroscopy in an Exponential Facility, B.S. Thesis, M.I.T. Department of Physics, June 1969.
(Thesis Supervisor: M.J. Driscoll)

3. Reactor Physics Project Publications

M.J. Driscoll and T.J. Thompson
Reactor Physics Project Progress Report, MIT-3944-1, MITNE-96, September 30, 1968.

T.L. Harper, T. Inoue and N.C. Rasmussen
GAMANL, A Computer Program Applying Fourier Transforms to the Analysis of Gamma Spectral Data, MIT-3944-2, MITNE-97, August 1968.

S.S. Seth, M.J. Driscoll, I. Kaplan, T.J. Thompson and D.D. Lanning
A Single-Element Method for Heterogeneous Nuclear Reactors, MIT-3944-3, MITNE-109, May 1970.

M.J. Driscoll, I. Kaplan and D.D. Lanning
Reactor Physics Project Progress Report No. 2, MIT-3944-4, MITNE-111, September 30, 1969.

Y. Hukai, N.C. Rasmussen and M.J. Driscoll
Some Applications of Ge(Li) Gamma-Ray Spectroscopy to Fuel Element Assay, MIT-3944-5, MITNE-113, April 1970.

M.J. Driscoll, I. Kaplan, D.D. Lanning and N.C. Rasmussen
Reactor Physics Project Final Report, MIT-3944-6, MITNE-117, September 30, 1970.

S.S. Seth, M.J. Driscoll, T.J. Thompson and I. Kaplan
Development and Application of Single-Element Methods, Trans. Am. Nucl. Soc., Vol. 13, No. 1, June 1970.

Appendix B

BIBLIOGRAPHY OF PUBLICATIONS ON HETEROGENEOUS REACTOR THEORY

This bibliography contains a selection of references which deal with various aspects of heterogeneous reactor theory and single fuel element neutronics. It is not meant to be exhaustive in scope but merely to indicate the sources which proved most influential upon, and useful to, the research effort described in this report. A brief comment is included on each reference.

Special mention should be made of the major topical meeting held on this subject, described in Nuclear Science Abstracts (24 : 36002) as follows:

> Proceedings of the Conference on Analysis of Few Rod Experiments in Reactor Physics, JRC, Ispra, Italy, May 12-14, 1969, S. Tassan (ed.), EUR-4470, March 1970.
>
> A review of the status of development of few rod experimental programs for fast and thermal reactors is presented. Significant features of the experimental techniques are described. Theoretical models for the interpretation of the experiments and comparison of results obtained under similar conditions in different laboratories are presented. Trends for future developments in few rod experiment programs are predicted.

1. Barden, S.E. et al., "Some Methods for Calculating Nuclear Parameters for Heterogeneous Systems," Proc. Intern. Conf. Peaceful Uses At. Energy, Geneva, P/272 (1958). Application of heterogeneous method to finite arrays of rectangular shape.

2. Bernard, E.A. and R.B. Perez, Determination of Heterogeneous Parameters by the Neutron Wave Technique," Trans. Am. Nucl. Soc., 12, No. 1, 663 (1969). Measurement of the thermal constant in a single-element experiment; analysis by age-diffusion theory.

3. Blaesser, G., "An Application of Heterogeneous Reactor Theory to Substitution Experiments," P/42/52, IAEA Symposium, Amsterdam (1963). The method avoids many difficulties which are typical of homogenized treatment as, for example, determination of coupling constants.

4. Corno, S.E., "Interpretazione Teorica delle Esperienze di Moltiplicazione Neutronica su un Solo Elemento di Combustible," Energia Nucleare, 10, 11 (1963). A highly theoretical application of small source theory to the problem of a single rod in an exponential pile. (Series of three articles.)

5. Corno, S.E., "Theory of Pulsed Neutron Experiments in Highly Heterogeneous Multiplying Media," in Pulsed Neutron Research, Vol. II, IAEA, Vienna (1965). A theory of pulsed neutron experiments applicable to a single fuel element.

6. Donovan, R., "Measurement of Heterogeneous Parameters," MIT-2344-12 (1967). Calculations based on measurements on a single element using foil techniques.

7. Durrani, S., E. Etherington and J. Ford, "Determinations of Reactor Lattice Parameters from Measurements on a Single Fuel Element Channel," APC/TN 1054. Another application of the method in (30) below.

8. Estabrook, F.B., "Single Rod Exponential Experiments," NAA-SR-925, P13. Reports other data on some experiments as in (14).

9. Feinberg, S.M., "Heterogeneous Methods for Calculating Reactors," Proc. Intern. Conf. Peaceful Uses At. Energy, Geneva, P/669 (1955). One of the original and basic theoretical papers on heterogeneous methods.

10. Galanin, A.D., "The Thermal Coefficient in a Heterogeneous Reactor," and "Critical Size of Heterogeneous Reactors with Small Number of Rods," loc. cit. 8, P/666 and P/663. Two of the original and basic theoretical papers on heterogeneous methods.

11. Graves, W.E. et al., "A Comparison of Heterogeneous Nuclear Reactor Lattice Theory with Experiment," Nucl. Sci. Eng., 31, 57 (1968). Comparison is made for thermal neutron densities and critical geometric bucklings.

12. Hamilton, G.T., "Application of the Single Element Method to Light Water Lattices," MIT-3944-4 (1969). Data on H_2O-moderated lattices shown to be interpretable in terms of heterogeneous reactor theory.

13. Hassit, A., "Methods of Calculation of Heterogeneous Reactors," Progress in Nuclear Energy, Series I, Vol. II, P271 (1958). Describes the "mesh method" of solving the two group diffusion theory equations within the moderator region of the heterogeneous system using finite difference equations.

14. Heinzman, O.W. and S.W. Kash, "Intracell Flux Distributions for an Extensive Series of Heavy Water, Uranium Rod Lattices," NAA-SR-1548 (1956). Reports radial flux traverses about 1-inch-diameter single rods.

15. Higgins, M.J., "Fuel Rod Interaction Kernels," MIT-2344-12 (1967). Describes experimental determination of the rod interaction kernels and methods that can use these kernels to predict integral parameters for entire lattices.

16. Horning, W.A., "Small Source Model of a Thermal Pile," HW-24282 (1952). An early attempt at an analysis that could be used to relate theory and experiment.

17. Jonsson, A., "Heterogeneous Calculation of Fast Fission," AE-42 (1961). An exact calculation of the collision probabilities is included.

18. Jonsson, A. and G. Naslund, "Heterogeneous Two Group Diffusion Theory for a Finite Cylindrical Reactor," AE-57 (1961). Describes the basis for the computer code HETERO.

19. Jonsson, A., G. Naslund et al., "Theory of Application of Heterogeneous Methods for D_2O Reactor Calculations," Proc. Intern. Conf. Peaceful Uses At. Energy, Geneva, P/683 (1964). Extension of heterogeneous methods to finite cylindrical systems.

20. Klahr, C.N. et al., "Heterogeneous Calculation Methods," NYO-2680 (1961). A final report on small source reactor physics calculations using the HERESY code.

21. Lanning, D.D., "Heterogeneous Reactor Critical Conditions Using Small Source Theory," TID-7532, Part I (1957). The application of heterogeneous analysis using age theory, to reactors containing control rods.

22. Meetz, K., "Exact Treatment of Heterogeneous Core Structures," loc. cit. 1, P/968. A theoretical paper which develops a mathematical formalism for such problems.

23. Papay, L.T., "Fast Neutron Fission Effect for Single Slightly Enriched Uranium Rods in Air and Heavy Water," MIT-2344-4 (1965). Describes the determination of δ_{28} for small diameter single rods.

24. Pershagen, B., G. Anderson and I. Carlvik, "Calculation of Lattice Parameters for Uranium Rod Clusters in Heavy Water and Correlation with Experiments," loc. cit. 1, P/151. An example of the application of the Poisson summation in heterogeneous lattices.

25. Pilat, E.E. et al., "The Use of Experiments on Single Fuel Elements to Determine the Nuclear Parameters of Reactor Lattices," MIT-2344-10 (1967). Combines experiments on a single element with a theory which describes a lattice of such elements.

26. Rodeback, G.W., C.H. Skeen and J.W. Zink, "Single Element Measurements," Trans. Amer. Nucl. Soc., 2, 1 (1959). A preliminary report on (30).

27. Saji, G. and A. Axford, "Space-Time Kinetics for Heterogeneous Reactor Models," Nucl. Sci. Eng., 35, 319 (1969). A new theoretical formalism of the space-time kinetics is developed for heterogeneous reactor models.

28. Seth, S.S., "Measurement of Integral Parameters," MIT-2344-9 (1966) and MIT-2344-12 (1967). Reports include techniques to obtain single element integral parameters.

29. Stewart, J.D. et al., "MICRETE: A G-20 Program for Calculating Finite Lattices by the Microscopic Discrete Theory," AECL 2547 (1966). Description of the program MICRETE for solving 2D reactor lattice problem using heterogeneous theory.

30. Zink, J. and G. Rodeback, "The Determination of Lattice Parameters by Means of Measurements on a Single Fuel Element," NAA-SR-5392 (1960). Actual experiments on a single fuel rod are used to infer parameters of graphite uranium lattices, with best results in the thermal energy region. Also reported in Nucl. Sci. Eng., 9, 16 (1961).